

UNESCO-IHE INSTITUTE FOR WATER EDUCATION



Numerical Modelling with Graded Sediments for 2D Morphological changes for Pilot Project Meers (Common Meuse)

Beston I. Sharef

MSc Thesis (WSE-HERBD-06.01)
Feb. - 2006

Numerical Modelling with Graded Sediments for 2D Morphological changes for Pilot Project Meers (Common Meuse)

Master of Science Thesis
by
Beston I. Sharef

Supervisors
Ir. G. J. Klaassen (UNESCO-IHE)
Dr. E. Mosselman (Delft Hydraulics)

Examination committee
Prof. J. A. Roelvink (UNESCO-IHE), Chairman
Ir. G. J. Klaassen (UNESCO-IHE)
Dr. E. Mosselman (WL/Delft Hydraulics)

This research is done for the partial fulfilment of requirements for the Master of Science degree at the UNESCO-IHE Institute for Water Education, Delft, the Netherlands

Delft
February - 2006

The findings, interpretations and conclusions expressed in this study do neither necessarily reflect the views of the UNESCO-IHE Institute for Water Education, nor of the individual members of the MSc committee, nor of their respective employers

Abstract

The Meuse River is the only major gravel bed river in the Netherlands, and it is considered as a very complicated river in terms of its morphology due to the steep slopes and the strongly graded bed material, which is armoured during all but the highest floods. The Common Meuse River - the part of the river where (over a length of about 90 km) it forms the border between Belgium and The Netherlands - is not navigable. Because of this, it provides a good opportunity for re-naturalization. Recently a plan has been approved to re-naturalize the river, and to combine this with flood protection and gravel mining over the whole length of the gravel bed part of the Meuse River.

The Pilot Project Meers is the first project where the planned measures are implemented over a number of kilometres and it was started around 2001. Within the framework of this pilot project, the floodplain level was lowered by gravel mining in the inner bend of the river near Meers over a substantial area. After some major floods in the period 2002 – 2003 it was observed that the river had responded quickly to these interventions. Substantial deposits of gravel had formed in the main channel at the beginning of the excavated area, some erosion along the outer (Belgium bank) side of the river had occurred, whereas finer particles had deposited on the floodplain away from the main channel.

In order to see whether it would be possible to simulate the observed phenomena it was decided to apply the modelling package Delft3D with the graded sediment option. The underlying idea was that this would allow for a better understanding of the observed phenomena. Subsequently this improved understanding can be used to prevent unfavourable developments in the future. This is in particular relevant as the Common Meuse project will continue for other bends along the gravel bed reach. Numerical modelling of sediment transport pattern is generally recognized as a valuable tool for understanding and predicting morphological developments, and it is important to find out whether or not this model can be used (i) for reproducing these complex phenomena with high flow velocities due to the steep slopes, the strong spiral flow and the graded sediment and (ii) for the future design of floodplain lowering without subsequent unexpected and serious consequences.

After some initial simulations with the model with different inflow hydrographs and input parameters, the numerical model – even though it was not properly calibrated on all relevant phenomena - was able to reproduce most of the phenomena observed after the 2002-2003 floods, including the sedimentation in the inner bend and the erosion in the outer bend, at least in a qualitative way. The result shows that probably the implemented Pilot Project Meers is the major cause of the observed problems.

Here it can be concluded that the observed phenomena could have been prevented or reduced by taking some measures in the main channel such as protecting the channel bed upstream of the excavated area with some large sediment particles (large gravels or boulders), to prevent that the armour layer would have failed. Delft3D can be used to obtain more precise and accurate results, but for that purpose a better calibration and verification of the model with field measurements is needed. Furthermore some development of the package is probably still needed to better represent the real situation.

Keywords: Numerical modelling, morphological development, graded sediment, armouring, Meuse River

Acknowledgements

After one and a half year study, which was full of exciting new learning experiences, albeit far away from my beloved family, I have succeeded to complete my M.Eng. courses and to finalize the M.Sc. thesis study at UNESCO – IHE and WL | Delft Hydraulics. Here, I would like to take the opportunity to express my sincere appreciation and deep gratitude to those who assisted me in my work and supported me in one way or another during this period.

I like to express my great respect and gratitude to my supervisors Ir. G. J. Klaassen – UNESCO-IHE and Dr. E. Mosselman – WL | Delft Hydraulics and Prof. J.A. Roelving-UNESCO-IHE (chairman) for their kind supervision, excellent guidance, continuous encouragement and valuable advices and suggestions during all stages of my study. They were always very helpful for discussion about research. Prof. J.A. Roelving is acknowledged for chairing the MSc awarding committee.

I like to express my sincere thanks and appreciation to Dr. Bert Jagers and Dr. Mohammed Yossef of WL | Delft Hydraulics for their cooperation during my study and help in using Delft^{3D} software. I also like to express my sincere thanks and gratitude to Dr. Saskia van Bures of WL | Delft Hydraulics for her sincere and continuous help during my work at Delft Hydraulics. Many thanks to Dr Martin Baptist - TU Delft for his kind helping in visiting Meers location and providing valuable references.

I would like to extend my thanks to all people in particular to Mr. Udo Boot and Mr. Henk Verkerk who helped in collecting and providing data and support that made it possible to work on the Meuse River at the Meers location.

I would like to thank all my friends from Iraq, for helping me in different way to finish this study in a relatively short time and to return early to my home country and family which I missed so much.

I also like to thank the Student Affairs department and other staff of IHE for their support and help concerning my living and studying in deep. I like to thank all of my friends from the HERBD (Hydraulic Engineering and River Basin Development) specialization, who have given me such a nice memory and made my life so colourful.

I am grateful to Ministry of Water resources – Central Government with cooperation of US Army Corps of Engineering for providing a fellowship and other financial support for my M.Eng. courses and MSc thesis study.

Also I am grateful to Ministry of Agricultural and Irrigation – Regional Governments (Kurdistan) for sending me abroad to do this study, I will never forget that, and I will do my best in developing my beloved country.

Most importantly, I wish to extend my profound gratitude to my beloved wife and daughter, my mother, brothers, sisters and other relatives who all supported me wholeheartedly for their moral support during my long stay away from them.

Beston I. Sharef
Delft, The Netherlands

Table of Contents

Abstract.....	i
Acknowledgements	iii
List of symbols	xi
1. Introduction	1
1.1. General	1
1.2. Problem description.....	2
1.3. Research questions	4
1.4. Objective of the study.....	5
1.5. Study approach	5
1.6. Report Structure.....	5
2. Literature study	7
2.1. Introduction	7
2.2. Graded sediment transport.....	7
2.2.1 Introduction	7
2.2.2 Size fraction transport formula.....	7
2.2.3 Hiding / Exposure.....	12
2.2.4 Size selective sorting.....	15
2.2.5 Armouring	15
2.2.6 Initiation of Particle Motion.....	16
2.2.7 Bed load sediment sorting	20
2.3. Governing equations in Delft3D	20
2.3.1 Introduction	20
2.3.2 Hydrodynamic equations.....	20
2.3.3 Depth-averaged flow	21
2.3.4 Secondary flow (feature available in σ -grid only)	22
2.3.5 Effect of secondary flow on depth-averaged momentum equations	24
2.4. Transport equations	25
2.4.1 Introduction	25
2.4.2 Bed-load sediment transport of non-cohesive sediment	25
2.4.3 Sediment transport components per fraction.....	26
2.5. Active Layer-approach for erosion and deposition of fractions.....	27
3. The Meuse River	29
3.1. Introduction	29
3.2. The Meuse and the Meuse Valley together	29
3.3. Hydrological conditions	30
3.4. Gravel-sand content of the sediments.....	30
3.5. Sediment transport rates and measurements.....	30
3.6. Bed level and bed slope.....	32
3.7. Characteristics of the river bed.....	34
3.8. About Maaswerken.....	35
3.9. Socio – economic functions of the Meuse.....	37
3.10. Natural and human interventions in the river bed morphology.....	37
3.11. Data availability.....	38

ξ. Model Description.....	ξ 1
ξ.1. Introduction	ξ 1
ξ.2. Model Setup.....	ξ 1
ξ.2.1 Selecting boundaries of the model	ξ 1
ξ.2.2 Grid generation.....	ξ 2
ξ.2.3 Selection of time step (Δt)	ξ 3
ξ.2.4 Initial conditions.....	ξ 6
ξ.2.5 Roughness files (Chézy coefficient).....	ξ 9
ξ.2.6 Observation points and cross-sections.....	ο 0
ο. Model Calibration and Verification.....	ο 3
ο.1. Introduction	ο 3
ο.2. Effect of main channel roughness on the water level (Chézy coefficient).....	ο 4
ο.3. Model verification (hydrodynamic).....	ο 5
ο.4. Selection of morphological factor (MORFAC).....	ο 8
ο.4.1 Introduction	ο 8
ο.4.2 Hydrodynamic and morphological time of 10 days (10 days hydrograph and morphological factor 1)	ο 9
ο.4.3 Hydrodynamic time of 20 days and morphological time of 10 days (20 days hydrograph and morphological factor ξ).....	6 2
ο.4.4 Hydrodynamic time of 120 days and morphological time of 10 days (120 days hydrograph and morphological factor λ).....	6 4
ϒ. Model applications and analysis of results	ϒ 3
ϒ.1. Introduction	ϒ 3
ϒ.2. Without project situation study	ϒ 4
ϒ.2.1 Introduction	ϒ 4
ϒ.2.2 Case WOP ^ϒ : Using 60 days Constructed hydrograph	ϒ 4
ϒ.3. With project situation study.....	ϒ 6
ϒ.3.1 Introduction	ϒ 6
ϒ.3.2 Case WP ^ϒ : Using 60 days morphological study	8 0
ϒ.4. Comparison between the without and the with project situations.....	8 0
ϒ.5. Comparison between with project situation (according to Delft ^ϒ D simulation) and field measurements	9 0
ϒ.6. Bed material sorting	9 9
ϒ. Discussion	1 0 3
ϒ.1. General	1 0 3
ϒ.2. Model setup	1 0 4
ϒ.3. Comparison between uniform and graded sediment simulations.....	1 0 5
ϒ.4. Model calibration and verification:	1 0 6
ϒ.5. Impact of the Pilot Project Meers.....	1 0 8
ϒ.6. Comparison of results of simulations with field observations	1 0 8
ϒ.7. Proposed future data collection	1 0 9
ϒ.8. Preventive and remedial measures	1 1 0
ϒ.9. Future studies.....	1 1 1
λ. Conclusions and Recommendations.....	1 1 3
λ.1. Conclusions	1 1 3
λ.2. Recommendations	1 1 4

References: 117

List of tables

Table 3.1: Relevant publications concerning sediment transport data Grensmaas Source: Mer Project Grensmaas..... 32

Table 3.2: Grain size distribution of the bed composition for each of top layer and two sub-layers..... 40

Table 3.3: *Overview of cases studied*..... 43

Table 4.1: Necessary data to be collected for the study at different time intervals 110

Table 4.2: Possible preventive and/or remedial measures for the Pilot Project Meers..... 111

List of Figures

Figure 1.1a: *Meers bend at 1997 before the project* 2

Figure 1.1a: Project and problem location (Meers bend – Meuse River)..... 3

Figure 2.1: Definition of exposure and height of bed material (Weming et al., 2000)..... 12

Figure 2.2: Velocity distribution and particle motion in steep rough channel 18

Figure 2.3: Critical particle densimetric Froude numbers for initiation of particle motion 18

Figure 2.4: *Secondary flow definition in Delft 3D model* 22

Figure 2.5: *vertical distribution for a river bend* 23

Figure 2.6: The bed-layer schematization after Ribberink (1987), where sub-script i is associated to sediment size fraction \hat{i} 28

Figure 3.1: Gravel and sand content along the Meuse River..... 31

Figure 3.2: *Meuse River*..... 33

Figure 3.3: Variation of the D_{50} in the bed material along the Meuse River. 34

Figure 3.4: *Trend of the thalweg elevation along the Meuse River.*..... 35

Figure 3.5: *Meuse River at Meers (planned excavations)* 36

Figure 3.6: *Meuse River at Meers* 36

Figure 3.7: 2002-2003 hydrograph 39

Figure 3.8: *Rating curve for the Meuse River at km 38* 39

Figure 3.9: Grain size distribution of the bed composition for each of top layer and two sub-layers.____ 40

Figure 4.1: *Water level for different time steps* 44

Figure 4.5: Secondary flow intensity for different time steps _____	40
Figure 4.6: Depth averaged velocity for different time steps _____	40
Figure 4.7: Value of Currant number for morphological model _____	46
Figure 4.8: Bathymetry of 1994 used in Delft 3D model _____	47
Figure 4.9: 3D weirs schematisation in the floodplain used in Delft 3D model _____	48
Figure 4.10: Sample hydrograph for upstream boundary condition used in Delft 3D model _____	48
Figure 5.1: Effect of Chézy value on water level _____	54
Figure 5.2: defining input files in to Delft 3D _____	56
Figure 5.3: Simple schematisation of river section _____	56
Figure 5.4: cross-section in case of selecting max _____	56
Figure 5.5: cross-section in case of selecting min _____	57
Figure 5.6: cross-section in case of selecting mean _____	57
Figure 5.7: Sensitivity analysis for water level in Delft 3D _____	57
Figure 5.8: Verification of water level in Delft 3D _____	58
Figure 5.9: Normal peak hydrograph of 2002-2003 floods. _____	60
Figure 5.10: Cumulative erosion and deposition for 10 days hydrograph and morph. factor 1. _____	61
Figure 5.11: Cumulative erosion and deposition in the main channel for 10 days hydrograph and morph. factor 1. _____	61
Figure 5.12: Squeezed hydrograph of 2002-2003 floods by factor 4. _____	62
Figure 5.13: Cumulative erosion and deposition for 20 days hydrograph and morph. factor 4. _____	63
Figure 5.14: Cumulative erosion and deposition in the main channel for 20 days hydrograph and morph. factor 4. _____	63
Figure 5.15: Squeezed hydrograph of 2002-2003 floods by factor 8. _____	64
Figure 5.16: Cumulative erosion & deposition for 10 days hydrograph and morph. factor 8. _____	65
Figure 5.17: Cumulative erosion and deposition in the main channel for 10 days hydrograph and morph. factor 8. _____	65
Figure 5.18: Normal and squeezed hydrograph of 2002-2003 floods. _____	66
Figure 5.19: Cumulative erosion and sedimentation along longitudinal profile first line from the left bank (zero value is located at km 24.0 of the river). _____	67
Figure 5.20: Cumulative erosion and sedimentation along longitudinal profile second line from the left bank (zero value is located at km 24.0 of the river). _____	67
Figure 5.21: Cumulative erosion and sedimentation along longitudinal profile third line from the left bank (zero value is located at km 24.0 of the river). _____	68

Figure 6.22: Cumulative erosion and sedimentation along longitudinal profile fourth line from the left bank (zero value is located at km 24.0 of the river)..	68
Figure 6.23: Cumulative erosion and sedimentation along longitudinal profile final line at right bank (zero value is located at km 24.0 of the river).	69
Figure 6.24: Time dependent cumulative erosion and sedimentation at point where sedimentation had taken place (Without project situation).	70
Figure 6.25: Time dependent cumulative erosion and sedimentation at point where erosion had taken place (Without project situation).	70
Figure 6.26: Time dependent cumulative erosion and sedimentation at point where sedimentation had taken place (With project situation).	71
Figure 6.27: Time dependent cumulative erosion and sedimentation at point where erosion had taken place (With project situation).	72
Figure 6.28: Selected peaks from 2002-2003 hydrograph.	75
Figure 6.29: Selected peaks from 2002-2003 hydrograph.	75
Figure 6.30: Cumulative erosion and sedimentation for 60 days morphological study (squeezed real hydrograph).	76
Figure 6.31a: River cross-section	78
Figure 6.32: Expected 3D morphological changes after the project implementation for river with bends	79
Figure 6.33: Cumulative erosion and sedimentation study in the main channel for 60 days hydrograph.	80
Figure 6.34: Bed topography for the without project case (interest location).	81
Figure 6.35: Bed topography for the with project case (interest location).	81
Figure 6.36: Difference of bed topography for with project and without project cases (interest location).	82
Figure 6.37: Velocity vector for the situation of with project for the case 6.33.	83
Figure 6.38: Velocity vector for the situation of with project for the case 6.33 (zoomed area).	83
Figure 6.39: Cumulative erosion and sedimentation at outer bend (Belgium bank) for a point (19, 120).	84
Figure 6.40a: Cumulative erosion and sedimentation at upstream of the project at point (23, 109).	85
Figure 6.40b: Cumulative erosion and sedimentation location of the project at point (23, 117).	85
Figure 6.41a: Cumulative erosion and sedimentation downstream of the project at point (21, 144).	86
Figure 6.42a: Width averaged bed level along longitudinal profile of the river at the end of simulation ($Q \approx 0.0 \text{ m}^3 / \text{s}$) (zero value is located at km 24.0 of the river).	87
Figure 6.42b: Width averaged water level along longitudinal profile of the river at the end of simulation ($Q \approx 0.0 \text{ m}^3 / \text{s}$) (zero value is located at km 24.0 of the river).	88

Figure 6.14a: Width averaged water depth along longitudinal profile of the river at the end of simulation ($Q \approx 0.0 \text{ m}^3 / \text{s}$)(zero value is located at km 25.0 of the river).	88
Figure 6.15a: Width averaged velocity along longitudinal profile of the river at the end of simulation ($Q \approx 0.0 \text{ m}^3 / \text{s}$)(zero value is located at km 25.0 of the river).	89
Figure 6.20a: Width averaged bed shear stress along longitudinal profile of the river at the end of simulation ($Q \approx 0.0 \text{ m}^3 / \text{s}$)(zero value is located at km 25.0 of the river).	90
Figure 6.21: Bed shear stress along the river (Without project).	92
Figure 6.22: Bed shear stress along the river (With project).	92
Figure 6.23: Time varying bed shear stress at specific point (23,109) in the river for both of (with project) and (without project) cases.	93
Figure 6.24: Time varying bed shear stress at specific point (23,117) in the river for both of (with project) and (without project) cases.	93
Figure 6.25: Time varying bed shear stress at specific point (19,120) in the river for both of (with project) and (without project) cases.	94
Figure 6.26: Time varying bed shear stress at specific point (21,144) in the river for both of (with project) and (without project) cases.	94
Figure 6.27: Bed topography of the river reach from field measurements (WAQUA model input file).	96
Figure 6.28: Bed topography of the river reaches (Delft3D result of 60 days morphological time).	96
Figure 6.29: Bed topography of the river reaches for both Delft3D result and field measurements.	97
Figure 6.30: Bed level difference between 1998(before the project) and 2003 (after the flood) from field measurements.	97
Figure 6.31: Bed level difference between 1998(before the project) and 2003 (after the flood) Delft3D simulations (cases WOP3 and WP3).	98
Figure 6.32: Difference between bed level of the river reaches for both Delft3D result and field measurements.	98
Figure 6.33e: Percentage of fraction 0 (2mm – 110mm) in the longitudinal section of the river.	100
Figure 6.34: Arithmetic mean of bed material (transport layer) for the main channel and banks of the river for with project situation.	100
Figure 6.35: Arithmetic mean of bed material (transport layer) for the main channel and banks of the river for without project situation.	101
Figure 6.36: Cumulative erosion and sedimentation along the longitudinal profile of the river at centre of the main channel (zero value is located at km 25.0 of the river).	105

List of symbols

A_{sh} = Calibration coefficient generally taken equal to unity.

β_i = Direction of sediment transport for fraction i .

C_c^* = Dimensionless critical Chezy coefficient.

D_i = Characteristics grain sizes diameter of size fraction i .

D_{sh} = Coefficient determining the dependence of the Shields number on D_i or D_m

D^* = Dimensionless diameter of particles.

D_w = Thickness of the wake zone.

Δ = Relative density of sediment.

ξ_i = Hiding and exposure correction factor.

f_i' = Volumetric sediment transport (including pores) per unit width of size fraction i

f_b = Darcy-Weisbach friction factor at the bed.

ϕ = Friction angle of the bed particles.

κ = Von Karman constant.

K_c = Correction factor on the magnitude of the transport rate for the influence of bed slope.

K_{ld} = Ratio of the lift force to drag force on the grains.

μ = Ripple factor.

p_i = Probability (volume fraction) of size fraction i being present in a surface layer of the bed.

q_{in} = Local sources water per unit of volume (1/s).

q_{out} = Local sinks of water per unit of volume (1/s).

q_c = Critical unit discharge.

R^* = Reynolds number of the particles.

R_s^* = The effective radius of curvature.

s_i = Volumetric sediment transport (including pores) per unit width.

$s_{bxi}(x, y, t)$ and $s_{byi}(x, y, t)$ are the bed-load transport components per unit of width for fraction i .

τ_{*i}' = Dimensionless grain shear stress

τ_{c*} = Dimensionless critical bed shear stress (Shields).

τ_{*ei} = The effective non-dimensional shear stress

τ_{*ci} = The non-dimensional critical shear stress

τ_{*cm} = Critical non-dimensional shear stress (Shields value) for grain size D_m .

θ = Longitudinal angle of the bed channel.

u_* = Shear velocity.

U_c = Critical mean velocity

$|\bar{U}|$ = Magnitude of the depth-averaged horizontal velocity.

ν = Kinematics viscosity of the fluid

1. Introduction

1.1. General

This research is focussed on the numerical modelling of two dimensional morphological changes in the river with graded sediment and armoured layer. This is not an easy task, because both 2D morphological changes computation and graded sediment study are very complex in reality, which are not easy to reproduce them by simple calculations with some empirical relations. The combination of them, obviously becoming ever complex, needs a very powerful and well designed package to compute them.

Due to natural processes and human interference, river morphology will change. In order to understand and predict these changes the study of sediment transport is of great importance. Knowledge of the rate of total sediment transport for a given flow, fluid and sediment characteristics are essential in the study of alluvial streams. Most methods use the subdivision of the total sediment load into bed-load and suspended-load; this signifies the importance of the bed-load and suspended-load computations in the evaluation of total sediment transport.

Graded sediment is found everywhere within the natural environment, especially in rivers, and each of the grain sizes behave differently under the same flow conditions. Early research into sediment transport attempted to simplify the system by relating the sediment transport rate to specific attributes of the sediment, such as median grain diameter. However, this simplification can lead to significant underestimation of the transport rate, especially if a broad spectrum of grain sizes is available for transport. Accordingly, the grading of sediments should be taken into account in the modelling of sediment transport. By making a detailed analysis of the composition of the sediments, important information with regard to sediment transport processes can be obtained (Jervis, 2003).

The effect of the presence of one particle size on the transport rate of another size in the case of non-uniform sediment is supposed to be taken care of through several correction factors, initially introduced by Einstein (1950). Many checks on Einstein's methods using data for non-uniform sediments have shown that the agreement between the measured and computed total bed transport rate is not satisfactory (Swamee and Ojha, 1991).

Today, most of the models available to simulate river morphological problems are still primarily based on calculations for uniform sediment. These models cannot include the morphological processes that are related to the presence of the different grain sizes. At the same time little is known about the ability of non-uniform mathematical model and their sediment transport formulas to predict size-selective morphological processes.

In this particular study we will try to apply an advanced numerical model (Delft2D) which was developed by WL | Delft Hydraulics, for the simulation of morphological changes in the Meuse river. This river is the border between Belgium and the Netherlands. The comparison of the results with the real situation allows determining

the applicability of a such models for this kind of complex phenomena, especially when the graded sediment are present.

1.2. Problem description

The Meuse River (Maas River) is the second largest and the only gravel bed river in The Netherlands and it has an international basin that spreads over four countries. It enters The Netherlands in Southern Limburg near Maastricht from where it flows to the North forming the border with Belgium in the reach known as the Common Meuse. In this reach major nature restoration projects are planned (Helmer et al, 1991; Klaassen et al, 1999), which has generated substantial interest in the morphological phenomena occurring in this gravel bed river (Murillo and Klaassen, 2006).

In the period between 2000 and 2002, the Meuse River is subjected to a large number of interventions for the project developed by “De Maaswerken”. This project combines the aims for a more natural river, increased safety against flooding and gravel mining. Planned interventions will change the development of the river hopefully leading to a more desirable situation. Good prediction are needed in order to determine which interventions serve our needs best on the long-term. Lately this plan was started with a pilot project at specific location on the river called Meers.

Gravel mining from the river is an important element of the Meers pilot project in the common Meuse, because of the following result. Firstly, there will be profits from selling the gravel, and with this income other measures can be implemented. Secondly, the flood risk is reduced by widening the river and lowering the floodplain. Finally, the river becomes closer to natural-river by allowing more frequent flooding of the floodplains and the development of vegetation in the floodplain.

Figures 1.1a and 1.1b show the location of Meers before the project and after implementation of the gravel mining and floodplain lowering, respectively.



Figure 1.1a: *Meers bend at 1992 before the project*



Figure 1.1b: Meers bend at 2000 after the project

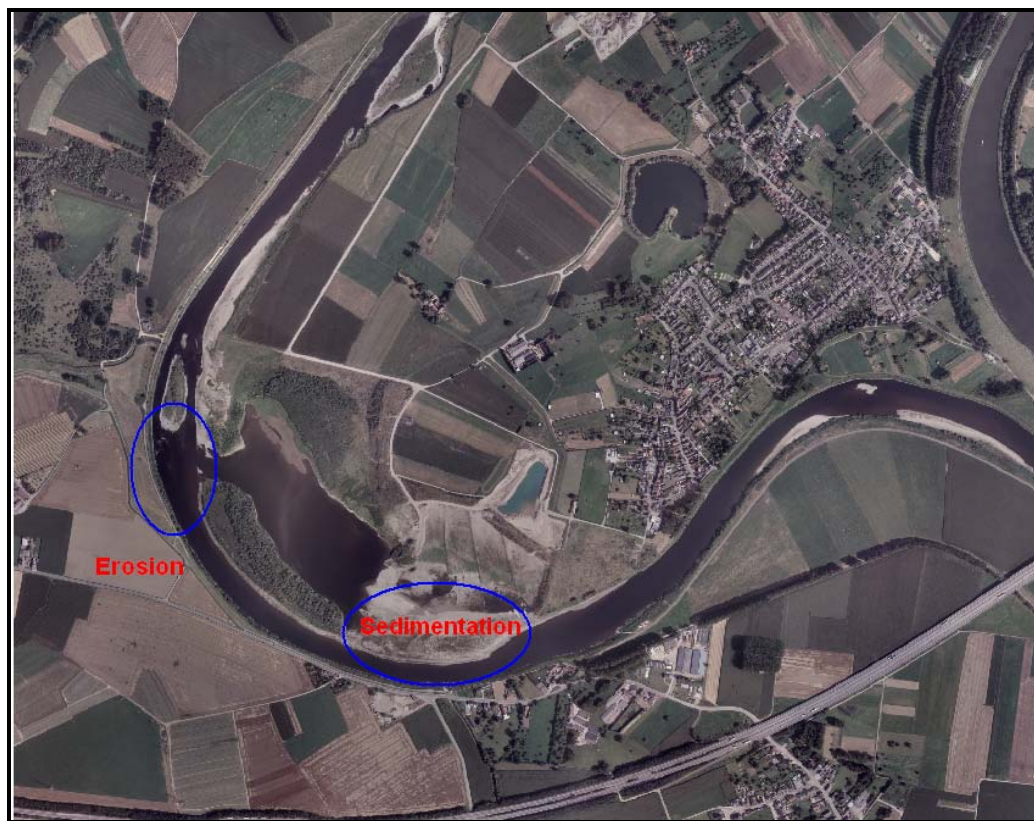


Figure 1.1a: Project and problem location (Meers bend – Meuse River)



Figure 1.7b: Photo of sedimentations in the Meers (taken on October-24-2009)

The effect of Pilot Project Meers was deposition of gravel in the main channel of the river as shown in the Figures 1.7a and 1.7b, deposition of sand in the floodplain near to the main channel forming a natural levee and, deposition of silt and clay in the floodplain area farther away from the main channel. Flow deviation by the gravel deposits has caused bank erosion along the opposite side of the river (outer bend in Belgium). That is a complex phenomenon difficult to predict by theoretical and empirical models and formulas, and the observed segregation of grain sizes indicates that transport processes of graded sediment are an important aspect that have to be taken into account.

1.3. Research questions

In consultation with WL | Delft Hydraulics and Public Works Department, Directorate Limburg, the following research questions were formulated.

- Can Delft2D package reproduce and predict the complex phenomena of graded sediment transport and morphological changes in the rivers?
- Can Delft2D package be used in designing the flood plain lowering in future or needs some improvement?

1.4. Objective of the study

The main objective of this study is answering the above questions about reproducing the situation by using a powerful software like DELFT2D, which has been developed by WL / Delft Hydraulics, to determine how good this package is in reproducing and predicting this type of complex phenomenon, to know the ability of avoiding these kind of problems of sedimentation and erosion when the other stages of the project will be implemented for other locations along Common Meuse and to have a better knowledge for future designing of flood plain lowering.

1.5. Study approach

The overall methodology for this study can be summarized as below:

- Problem definition and formulation approach.
- The literature study of two dimensional bed morphology, graded sediment and re-naturalization of Meuse River.
- Studying and understanding Delft2D package, and how it solves this kind of processes and problems.
- Specification of required data for the modelling and collecting them.
- Building, calibration and verification of the model for Pilot Project Meers.
- Application of the model for the cases of:
 - **Without project study:** In this part of the study we will focus on the condition of the river without the project, and what is the estimation result if this project was not implemented in the Meuse River.
 - **With project study:** In the second part of this report we will try to reproduce the phenomena in the Meuse River.
- Interpretation of obtained results and suggestion for further study.
- Report writing and presentation of the results.

1.6. Report Structure

In this section we will briefly outline the structure of report, how and where the results are presented and discussed.

In chapter 2 a summary is given of the relevant literatures important to consider them in this report, especially related to graded sediment, flow in bends, the effect of secondary flow on morphology and sediment direction, and some explanation about how Delft2D solve this types of problems and some governing equations. Chapter 3 some background and information about the Meuse River will present. The model descriptions and model setup will be the main topic of Chapter 4. Chapter 5 deals with the calibration and verification of the model essential for preparing a good model application.

Chapter 6 is the most essential part of the study that contains the most relevant results for the study cases and the comparison between with and without cases. Also the comparison between the result of the model and the existing situation will present also in this chapter. Other results are presented in a number of appendices. General discussion about the model and the results obtained is presented in chapter 7. The overall conclusions of the study and the model and general and specific recommendations are given in Chapter 8.

2. Literature study

2.1. Introduction

In this section some important aspects will be explained that studied by other researchers, for the purpose of having a good idea and clear insight about the issues that better to be taken into consideration in the prediction of 2D morphological changes with the graded sediment.

2.2. Graded sediment transport

2.2.1 Introduction

The earliest studies on the behaviour of non-uniform sediment were aimed at the development of an important empirical component of a morphological model, namely a transport formula. A basic principle, which is generally applied for non-uniform sediment, is the division of the sediment mixture into size fractions and the calculation of the transport rate of each size fraction separately. A characteristic phenomenon, the hiding or sheltering of the finer sizes, was specifically studied by Einstein & Ning Chien (1953) and later modelled theoretically by Egiazaroff (1960). Since then, many transport formula, originally developed for uniform sediment, have been adapted for use per size fraction.

Hirano (1970) was the first to apply transport relationship per size fraction in a larger mathematical model for the simultaneous computation of the bed level erosion and armouring. More recently Thomas (1977), Deigraad (1980), Bettess & White (1981) and Karim et al. (1983) developed and studied similar models. The basic principle of these models is the division of the riverbed into surface or transport layer, which is exposed to the flow, and non-moving bed. The grain size distribution of the transport layer material is used for the calculation of the size fraction transport. This composition can change through:

- A spatial gradient in size fraction transport
- Erosion of different sediment size from deeper layer (non-moving bed)

The thickness of the transport layer depends on the bed configuration, e.g. flat bed situation or bed forms, and is usually calculated with an empirical formula for the bed form height. Because the bed configuration is also of great importance for the bed roughness (bed resistance for the water motion), this empirical formula is often combined with the roughness predictor.

2.2.2 Size fraction transport formula

Generally, the transport formula for the bed load per size fraction is derived from an existing formula for uniform sediment. The simplest correction for the use per size fraction is a correction for availability of that size fraction i in the bed material given by:

$$s_i = p_i \times f_i' \dots\dots\dots 2.1$$

In which:

- s_i = Volumetric sediment transport (including pores) per unit width,
- p_i = Probability (volume fraction) of size fraction i being present in a surface layer of the bed,
- f_i' = Volumetric sediment transport (including pores) per unit width of size fraction i in the case of uniform sediment in identical hydraulic conditions.

This type of formula is considered too simple and extra corrections are thought to be necessary. Two types of corrections can be distinguished:

- 1. Correction of the effective bed shear stress τ' (grain shear), i.e. reducing its value for the finer fractions and increasing it for the coarser fractions,
 - 2. Correction of the critical bed shear stress τ_c , i.e. increasing its value for finer fractions and reducing it for coarser fractions.
- ‘Sheltering’ or ‘hiding’ of the smaller sizes in the lee of the larger sizes,
 - An increased exposure to the flow of the larger sizes.

Because in many transport formula the transport (s) is proportional to $\tau' - \tau_c$, these correction have a similar effect, viz. a reduction of the transport rate of the smaller sizes and an increase of the transport rate of the larger sizes.

A rough estimation of the necessary exposure correction is made below, using a totally different approach. Combining a bed load formula of the type of Meyer-Peter & Mueller (1948) with the correction formula (2.1), the following relationship is obtained:

$$s_i = p_i \times k \times (\Delta \cdot g \cdot D_i)'^{1/3} \times (\tau_i' - \tau_{c_i})^{2/3} \dots\dots\dots 2.2$$

In which according to Meyer- Peter & Mueller (MPM), $k = 13.3$ and $\tau_c = 0.045$.

Further:

- $\Delta = (\rho_s - \rho) / \rho_s$ Relative density of sediment
- D_i = Characteristic grain size diameter of size fraction i .

- $\tau_{*i}' = \tau' / (\rho_s - \rho) \cdot g \cdot D_i = \mu u_*'^2 / \Delta \cdot g \cdot D_i$ = Dimensionless grain shear stress..... 2.3
- $\mu = \tau' / \tau$ = Ripple factor
- u_*' = Friction velocity
- $\tau_{c_*} = \tau_c / (\rho_s - \rho) \cdot g \cdot D_i$ = Dimensionless critical bed shear stress (Shields)

Substituting equation 2.3 in equation 2.2 gives:

$$\frac{s_i}{p_i} = k \cdot (\Delta \cdot g)'^{1/3} \times \left(\frac{\mu u_*'^2}{\Delta \cdot g} - \tau_{c_*} \cdot D_i \right)^{2/3} \dots\dots\dots 2.4$$

The following assumptions are made:

- All size fractions are transported as bed load over dunes all of which have an equal shape, size and migration velocity (with $s = \bar{s}$ in the dunes troughs, $z = z_0$).
- The composition of the sediment mixture in the dunes can be used as bed material composition (p_i).

- For the average grain size

$$D_m = \sum_{i=1}^N p_i \cdot D_i$$

An exposure correction is necessary (N= number of fractions).

As the consequence of the first two assumptions, the dunes migrate as closed unit and the composition of the transported mixture $p_{iT} (= s_i / s)$ equal to the composition of the bed material p_i :

$$p_{iT} = \frac{s_i}{s} = p_i$$

Or:

$$\frac{s_i}{p_i} = s \dots\dots\dots 2.6$$

Comparison of equations 2.6 and 2.5 indicates that the right hand side of equation 2.5 should have the same value for all size fractions. This can be achieved with a correction factor for τ_{cs} .

This factor ξ_i should become equal to unity for $D_i = D_m$ (third assumption), or:

$$\xi_i \cdot \tau_{cs} \cdot D_i = \text{Constant} = \tau_{cs} \cdot D_m$$

Or:

$$\xi_i = \frac{D_m}{D_i} \dots\dots\dots 2.7$$

With this correction, all size fractions obtain the same critical bed shear stress (dimensional value).

A more theoretical approach to determining the exposure correction is followed by Egiazaroff (1960), who derives an expression for the critical bed shear stress for each fraction using the balance of forces acting on the individual grains in a flat bed situation; Egiazaroff 's expression can also be translated to a correction factor ξ_i for the critical bed shear stress:

$$\xi_i = \frac{\tau_{c_s}(\text{corrected})}{\tau_{c_s}} = \left\{ \frac{1 + \log \frac{D_i}{D_m}}{1 + \log \frac{D_i}{D_m}} \right\} \dots \dots \dots 2.7$$

According to Egiazaroff, the larger grain sizes, as part of a sediment mixture, experience a larger drag force than in the uniform case, because in the former case the point of application of this force lies at a higher level in a boundary layer of the flow. Egiazaroff verifies equation 2.7 using the experimental data of other researchers and find good agreement.

Ashida & Michiue (1973) use the result of Egiazaroff in combination with a transport formula of the MPM type. Based on a number of a laboratory experiments they present an empirical correction to equation 2.7 in the range $D_i / D_m < 0.5$ given by:

$$\xi_i = 0.8 \frac{D_m}{D_i} \dots \dots \dots 2.8$$

A part from the factor 0.8, this relationship is identical to equation 2.6, which, however, had totally different starting points.

The bed load formula of Einstein (1900) was one of the first formulas, which specifically focused of non-uniform sediment. Einstein introduces the hiding factor or sheltering coefficient ξ_i as correction factor for the bed shear stress. A general definition is:

$$\xi_i = \frac{\tau_{*i}}{\tau_{*i}(\text{corrected})} \dots \dots \dots 2.9$$

For the coarse sizes $\xi_i = 1$ and for the finer sizes $\xi_i > 1$ which results in a reduced transport rate of the finer sizes.

Einstein & Ning Chien (1953) present modified value for the hiding factor based on the series laboratory experiments with sediment mixtures. They also report the presence of surface segregation, i.e. the accumulation of coarse grains underneath the finer grains, which affects the effective shear stress acting on the grains and thus the hiding factor.

Day (1980) presents a large number of experimental data with sediment mixtures and proposes an exposure correction for the transport formula of Ackers & White (1973) based on these data. Day's correction factor for the mobility number (a kind of dimension less bed shear stress) in this formula can be translated into a sheltering coefficient for the effective bed shear stress:

$$\xi_i = \left\{ \frac{0.5 \xi}{(D_i / D_A)^{1/3}} + 0.7 \right\} \dots\dots\dots 2.10$$

In which D_A is that grain size in the mixture, which needs no correction; D_A is not necessarily equal to D_m or D_{50} , according to Day:

$$\frac{D_A}{D_{50}} = 1.7 \left(\frac{D_{\Delta z}}{D_{17}} \right)^{-0.78} \dots\dots\dots 2.11$$

Profitt & Sutherland (1983) also use the formula of Ackers & White (A&W) as the base for the size fraction transport formula. The following empirical relationship for the exposure correction is derived from a series of laboratory experiments:

$$\xi_i = \left\{ 0.3 \times 10^{-1} \log \left(\frac{D_i}{D_A} + 1 \right) \right\}^{-2} \quad \text{For } 0.7 \leq \frac{D_i}{D_A} < 3.7 \dots\dots\dots 2.12$$

$$\xi_i = 0.092 \quad \text{For } \frac{D_i}{D_A} > 3.7$$

Contrary to equation 2.11, D_A is not related to the gradation of the mixture but to the effective bed shear stress τ_{*c} . ($= u_*^2 / \Delta \cdot g \cdot D_{50}$).

Profitt & Sutherland also use the formula of Paintal (1971) in combination with the same experimental data; the following empirical exposure correction is the result:

$$\xi_i = 0.87 \left(\frac{D_i}{D_A} \right)^{-0.81} \quad \text{For } \frac{D_i}{D_A} < 0.7 \dots\dots\dots 2.13$$

$$\xi_i = \left(\frac{D_i}{D_A} \right)^{-0.51} \quad \text{For } 0.7 < \frac{D_i}{D_A} < 1.0$$

Another exposure correction of a recent date is that given by Misri et al. (1984) who find, on theoretical grounds, that:

$$\xi_i = \left(\frac{D_i}{D_A} \right)^{-1} \quad \text{For } \frac{D_i}{D_A} < 1.0 \dots\dots\dots 2.14$$

$$\xi_i = \left\{ \frac{1.49 \log(1.49)}{1.49 \log(1.49 D_i / D_A - 1.49)} \right\} \quad \text{For } \frac{D_i}{D_A} > 1.49$$

Misri verified equation 3.14, in combination with the transport formula of the type $s/\sqrt{\Delta \cdot g \cdot D^3} = f(\tau_*')$, using an extensive series of flume data. Especially in the finer part of the mixture, $\frac{D_i}{D_A} < 1.49$, the calculated sheltering coefficient is systematically too high (\approx factor 1.49); for the coarse sizes the agreement is good.

3.2.3 Hiding / Exposure

In graded sediment, the larger grains are more likely to be entrained than the uniform sediments of the equivalent sizes, as they are more exposed to the flow. However, the situation is reversed for smaller grain sizes, as they are more likely to be hidden between the larger grain sizes and less likely to be entrained in the flow. Based on this observation, it is important that the hiding and exposure effects are taken into account in the modelling of graded sediment transport. In the previous studies on graded sediment transport, a correction factor was used to modify uniform sediment transport formulas to non-uniform one (considering hiding and exposure).

Weming et al. (2000) developed a new hiding and exposure correction factor that can account for the influence of sediment particle size and also bed material gradation. In this factor the grain size of a fraction is compared with the grain sizes of the other fractions. It is assumed that the particles are distributed randomly on the bed. This leads to the assumption that the exposure height of a particle is normally distributed.

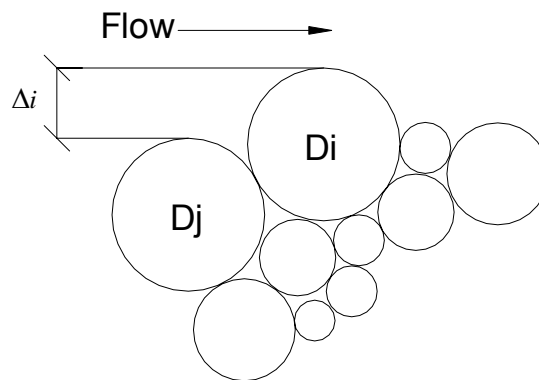


Figure 3.1: Definition of exposure and height of bed material (Weming et al., 2000)

As shown in the Figure above Weming et al. assumed that sediment particles are spheres with various diameters and defined the exposure height (Δ_i) for a particle with a size (D_i) as the elevation difference between the apexes of this particle and the upstream particle.

If $\Delta_i > 0$, the particle D_i is considered to be in an exposed state, and if $\Delta_i < 0$, in a hiding state. Since the sediment particles are distributed on the bed randomly, then Δ_i is a random variable, which is assumed to follow a uniform probability distribution, f . If the upstream particle is D_j , f can be expressed as:

$$f = \frac{1}{D_i + D_j} \Rightarrow \text{For } D_j \leq \Delta_i \leq D_i \dots\dots\dots 2.10$$

$$f = 0 \quad \text{Otherwise} \dots\dots\dots 2.11$$

The probability of particles D_j were staying in front of particle D_i were assumed by Weming et al. to be the percentage of particles D_j in the bed material P_{bj} . Therefore, the probability of particles D_i hidden and exposed by particle D_j can be obtained from equations below:

$$P_{hi,j} = P_{bj} \times \frac{D_j}{D_i + D_j} \quad \text{For hidden} \dots\dots\dots 2.12$$

$$P_{ei,j} = P_{bj} \times \frac{D_i}{D_i + D_j} \quad \text{For exposure} \dots\dots\dots 2.13$$

The total hidden and exposed probabilities of particle D_i can be obtained by summing the above two equations over all functions, respectively:

$$P_{hi} \sum_{j=1}^N P_{bj} \times \frac{D_j}{D_i + D_j} \dots\dots\dots 2.14$$

$$P_{ei} \sum_{j=1}^N P_{bj} \times \frac{D_i}{D_i + D_j} \dots\dots\dots 2.15$$

Where N is the total number of particle size fractions of graded sediment mixtures; P_{hi} and P_{ei} are the total hidden and exposed probabilities of particle D_i . When both probabilities are summed, they should equal to unity as expected. By applying the hiding and exposing probabilities, Weming et al. defines the hiding and exposure factor as:

$$\eta_i = \left(\frac{P_{ei}}{P_{hi}} \right)^m \dots\dots\dots 2.21$$

Where m is an empirical parameter.

Another factor suggested by Parker, (1992) for hiding function, according to him. The reason for this relates to the seminal work of Egiazaroff (1960), who derived a relation of from considerations of the forces acting on grains exposed on a bed containing a mixture of grain sizes. In Egiazaroff simple but cogent model, larger grains are harder to move because they are heavier. Larger grains are, on the other hand, easier to move because they tend to protrude more into the flow, so feeling a higher drag. (Hence the terminology “hiding,” in that the finer grains are sheltered from the full brunt of the flow by the protrusion of the coarser grains.) The net result of these two effects is a modest bias toward lesser mobility for coarser grains. The reduced mobility of coarser grains in a mixture turns out, however, to be much more subdued that what would be expected based on weight alone.

The dimensioned values of the critical (reference) boundary shear stresses based on skin friction (and surface content in the case of reference values) τ_{bsci} and τ_{bscg} (τ_{bssri} and τ_{bssrg}) associated with sizes D_i and D_g , respectively, are given from the relations

$$\tau_{bsci} = \rho R g D_i \tau_{sci}^* \quad , \quad \tau_{bscg} = \rho R g D_g \tau_{scg}^* \dots\dots\dots (2.22a,b, c, d)$$

$$\tau_{bssri} = \rho R g D_i \tau_{ssri}^* \quad , \quad \tau_{bssrg} = \rho R g D_g \tau_{ssrg}^*$$

$$\frac{\tau_{sci}^*}{\tau_{scg}^* (Re_{pg})} = F_{hc} \left(\frac{D_i}{D_g} \right) \quad , \quad \frac{\tau_{ssri}^*}{\tau_{ssrg}^* (Re_{pg})} = F_{hr} \left(\frac{D_i}{D_g} \right) \dots\dots\dots (2.23a,b)$$

Between equations (2.22) and (2.23) it is found that

$$\frac{\tau_{bsci}}{\tau_{bscg}} = F_{hc} \left(\frac{D_i}{D_g} \right) \equiv \frac{D_i}{D_g} F_{hc} \left(\frac{D_i}{D_g} \right) \dots\dots\dots 2.24$$

$$\frac{\tau_{bssri}}{\tau_{bssrg}} = F_{hr} \left(\frac{D_i}{D_g} \right) \equiv \frac{D_i}{D_g} F_{hr} \left(\frac{D_i}{D_g} \right) \dots\dots\dots 2.25$$

The above equations may be termed reduced hiding functions.

2.2.4 Size selective sorting

Due to the studies on sediment transport with uniform grain size, it is known that small grains are transported more easily than larger grains, e.g. Ferguson (1996) noticed that coarse grains are transported over shorter distances than fine grains in the same period of time. Gravity pulls the grain down to the riverbed and water flows exert forces sideward in downstream direction. The particle weight is affected more by change in grain diameter than the area on which the forces of the flow are exerted. This is due to the three-dimensional nature of the particle volume and the two-dimensional relationship of the side view with the grain diameter. Therefore, large grains stay immobile for higher flow velocities than fine sediments. As a result larger particles will be transported for shorter periods and travel over shorter distances.

2.2.5 Armouring

A phenomenon that is typical for gravel-bed rivers is armouring. It has a considerable effect on the sediment transport as the armour layer endures very high flow velocities without sediment being entrained. It is known that for some rivers the D_m -surface is 2 – 3 times larger than the D_m -subsurface (Andrews, 1984). This pattern is consistent with size selective transport. Due to large differences in mobility the fine sediments are entrained and surface coarsening will develop. This process will take place at low to moderate flow conditions.

Armouring of the channel bed by size selective entrainment is common whenever a pronounced imbalance between sediment supply and the transport capacity is maintained for any length of time. During low to moderate flows fine particles are transported and the coarse, less mobile ones stay behind on the riverbed. The resulting surface remains stable for all but the maximum discharges. Commonly they are called static or stable armour. The bed surface is broken when the coarsest material is entrained by the flow, thus allowing the underlying finer material to be transported. This leads to erosion gaps in the riverbed (Powell, 1998).

Amours can also exist in the presence of an upstream sediment supply and during flows that can move all size fractions. They are usually named as mobile amours. When the surface is broken, the underlying finer material is transported. As the flow decreases the coarse particles are deposited easier and form a new coarse layer on the riverbed. The remaining fine material for which the flow is still strong enough to transport will eventually be carried away.

2.2.1 Initiation of Particle Motion

In order to study the morphological changes in the river, a clear insight to sediment transport is required. The vital idea behind sediment transport is begin when the sediment start to move under a specified shear stress for each grain size which known as initiation of motion. And it is important to study this phenomenon.

The best-known and most widely used investigation on initiation of motion is that of Shields (1936). By considering the disturbing forces on particles to be restricted to shear stress, Shields found that the dimensionless critical shear stress, $\tau_c^* = \frac{\tau_c}{g.(s-1).D}$,

(τ_c = critical bed-shear stress) determines the initiation of motion of particles, and is a function of the Reynolds number of the particles, $R^* = \frac{u_* . D}{\nu}$ where u_* = the shear

velocity, and ν = the kinematic viscosity of the fluid. For $R^* > 100$, different researchers have obtained constant values of τ_c^* . Rouse (1937) found that τ_c^* is equal to 0.06, and Meyer-Peter and Mueller (1948) found it to be equal to 0.057. In any case, small rates of bed load transport can be measured at critical values of the Shields number; the reason being that sediment transport is a stochastic phenomenon.

The mean sediment transport for the so-called critical shear stress was found to be

$q_s^* = 1.0^{-1}$ (Taylor and Vanoni 1991), where $q_s^* = \frac{q_s}{u_{*c} . D}$ in which q_s is the sediment

discharge for unit width, and u_{*c} the critical shear velocity. Classical Shields plots (1936) give the dimensionless critical shear stress τ_c^* against critical Reynolds number of the

particles $R_c^* = \tau_c^{*1/2} . D^{*2/3}$ where $D^* = D \left[\frac{g(s-1)}{\nu^2} \right]^{1/3}$ is the dimensionless diameter of particles.

Wilcock (1993) found that the critical shear stress of individual fractions in unimodal and weakly bimodal sediment series exhibits little variation with grain size. Grain-size distributions other than bimodality seem to have little influence on critical shear stress of individual size fractions in sediment mixtures.

Chiew and Parker (1994) analyzed forces acting on sediment particles and found that the stream-wise bed slope has an important influence on the initiation of particle motion. The experimental data collapse into a single analytical curve showing the effect of the stream-wise slope on the threshold condition for sediment entrainment.

For $R_c^* > 1000$, a clear view of the multiple values of τ_c^* that a particle can show at the initiation of motion is presented in Figure 2.2 which shows an extrapolation of Shields diagram and a strong experimental evidence that for steep rough channels with large rugosities, there is not a constant critical stress. On the contrary, a single particle exhibits a wide range of critical shear stress variation. In the case of $D^* = 120$, τ_c^* varies between 0.02 and 0.06. Deviation from Shields constant value can be due to high-channel slopes up to $S = 0.2$, and relative rugosities up to $\frac{D}{d} = 0$.

To avoid the problem of having different shear stresses for the same particle diameter, Bathurst et al. (1987), whose study was based on the results previously obtained by Schoklitsch (1962) proposed a critical discharge for the initiation of motion q_c^* , given by:

$$q_c^* = \frac{q_c}{(g.D^3)^{1/3}} = 0.10.S^{-1/3} \dots\dots\dots 2.26$$

Where q_c = critical unit discharge. The equation above applies to uniform sediment for the slope range $0.05 < S < 0.10$. The concept of a critical discharge has shown good results when applied to channels and rivers of steep slope and large rugosities.

A third alternative to express critical conditions relates the moment produced by the force originated by the mean velocity on bed particles to the resistance moment of the particle due to gravity and other resistance forces.

Considering the existence close to the bed of a wake zone (Aguirre-Pe and Fuentes 1990) of constant velocity u_w , the critical conditions on the particle of diameter D , will be accurately established when a particle begins either to rotate or to move. The equilibrium condition for the moment due to drag and the moment due to weight can be given by

$$\frac{\rho.\delta_d.u_w^2.D^3}{(\rho_s - \rho)\delta_g.g.D^3.\cos\theta(\tan\phi - \tan\theta)} = 1 \dots\dots\dots 2.27$$

Where u_w = critical velocity in the wake; θ = longitudinal angle of the bed channel; ϕ = friction angle of the bed particles; and δ_d and δ_g factors that multiplied by D give the drag and gravity force arms in equilibrium conditions. Experimental data showed $\left(\frac{\delta_d}{\delta_g}\right)^{1/2} = 1.9$. They depend on the flow velocity near the bed and the shape of the particles. The velocity u is supposed to follow the Prandtl-von Karman (Figure 3) logarithmic law for $y \geq \beta.D$, where y is the vertical coordinate and $\beta = \frac{D_w}{D}$, D_w being the thickness of the wake zone.

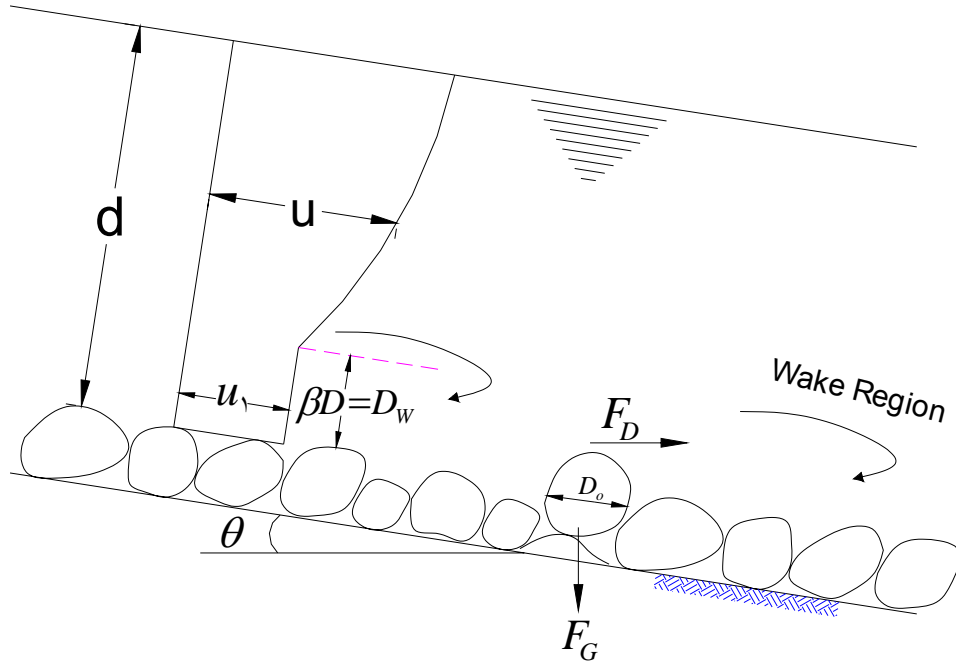


Figure 2.1: Velocity distribution and particle motion in steep rough channel

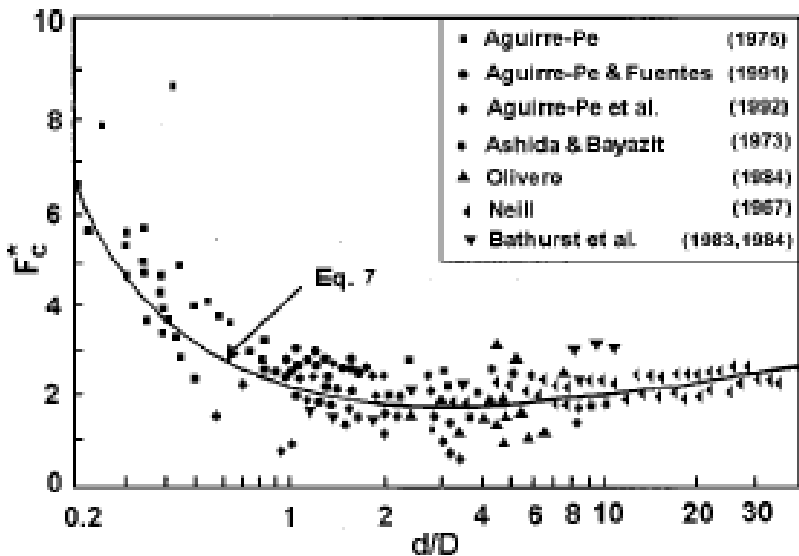


Figure 2.2: Critical particle densimetric Froude numbers for initiation of particle motion

Thus, by applying Aguirre-Pe and Fuentes' wake model (1991), the following equation is obtained for $y = \beta D$

$$\frac{u_{\lambda c}}{u_{*c}} = \frac{1}{k} \ln \frac{\beta D}{\alpha D} + B \dots \dots \dots 2.28$$

In which α = roughness coefficient; k = von Karman constant; $B = \lambda \cdot \rho$ at high Reynolds numbers of the particles, and u_{*c} can be expressed as $\frac{U_c}{C_c^*}$, C_c^* being the dimensionless critical Chezy coefficient. Substitution of equation (2.28) into equation (2.27) leads to

$$F_c^* = \frac{U_c}{[g(s-1)D \cdot \cos\theta(\tan\phi - \tan\theta)]^{1/2}} = \frac{\left(\frac{\delta_r}{\delta_s}\right)^{1/2}}{\frac{1}{k} \cdot \ln \frac{\beta}{\alpha} + B} C_c^* \dots\dots\dots 2.29$$

Where U_c = critical mean velocity, and C_c^* dimensionless critical Chezy coefficient obtained when the mean velocity and the mean bed shear velocity u_{*c} reach their critical values. For this condition, the following expression can be written $C_c^* = \frac{U_c}{u_{*c}}$.

The dimensionless critical Chezy coefficient expresses the minimum value of C^* which represents the dimensionless variable Chezy coefficient required to move particles at the flow bed. In equation (2.29), α and β depend on the shape, the relative size of the elements, and the flow conditions. These coefficients can be obtained experimentally. Mean experimental values were found to be $\alpha = 1.4$ and $\beta = 2.6$. According to Aguirre-Pe and Fuentes (1990), the dimensionless Chezy coefficient for macro-rough free surface flow, $C^* = \left(\frac{\lambda}{f_b}\right)^{1/2}$ (f_b = the Darcy-Weisbach friction factor at the bed), can be given by

$$C^* = 0.9 \cdot \text{Log}\left(\frac{d}{\alpha D}\right) + 6.0 + 2.0 \frac{\beta D}{d} \dots\dots\dots 2.30$$

Combining equation (2.29) and equation (2.30) for $C^* = C_c^*$ and giving the appropriate values to the remaining coefficients, it is found that

$$F_c^* = 0.9 + 0.0 \ln\left(\frac{d}{D}\right) + 1.2 \frac{D}{d} \dots\dots\dots 2.31$$

Critical values for beginning of motion vary approximately in the range $2 < F_c^* < 6$ for $0.2 < \frac{d}{D} < 1$ in Figure 2. This means that small depth variations from $0.2D$ to D cause large critical variations of F_c^* . For $\frac{d}{D} > 1$ there is a small increment of F_c^* for large depth increments.

2.2.2 Bed load sediment sorting

Equilibrium sorting of coarse mobile bed load sediment in meander bends is considered. A theory of two-dimensional bed load transport of graded material, including the effects of gravity on lateral slopes and secondary currents, is developed. This theory is coupled with a simple treatment of flow in bends, an analytically determined bend shape, and the condition of the continuity of each grade size range in the transport to describe sorting. The theory indicates that the locus of coarse sediment shifts from the inside bank to the outside bank near the bend apex.

Meandering streams with heterogeneous sediment loads move different grain sizes in different proportions and directions, this results in a fairly consistent pattern of sorting. Downstream of a bend apex, the point bar on the inside tends to be finer than the pool on the outside. In addition, the upper parts of the point bars tend to be coarser at the upstream end and finer at the downstream end. The above two tendencies are embodied in a shift in the locus of the coarsest sediment from the inside to the outside of a bend with progression around it (Parker & Andrews, 1986).

2.3. Governing equations in Delft3D

2.3.1 Introduction

In this section, we will present in detail the governing equations that are used in Delft3D for 2D hydrodynamic and morphological modelling.

2.3.2 Hydrodynamic equations

Delft3D-FLOW solves the Navier Stokes equations for an incompressible fluid, under the shallow water and the Boussinesq assumptions. In the vertical momentum equation the vertical accelerations are neglected, which leads to the hydrostatic pressure equation. In 2D models the vertical velocities are computed from the continuity equation. The set of partial differential equations in combination with an appropriate set of initial and boundary conditions is solved on a finite difference grid.

In the horizontal direction Delft3D-FLOW offers the opportunity to use:

- Cartesian rectangular co-ordinates (x, y).
- Orthogonal curvilinear co-ordinates (ξ, η).
- Spherical co-ordinates (λ, φ).

The boundaries of a river, an estuary or a coastal sea are in general curved and are not smoothly represented on a rectangular grid. The boundary becomes irregular and may introduce significant discretization errors. To reduce these errors boundary fitted orthogonal curvilinear co-ordinates are used. Curvilinear co-ordinates also allow local grid refinement in areas with large horizontal gradients.

Spherical co-ordinates are a special case of orthogonal curvilinear co-ordinates with:

$$\begin{aligned}
 \xi &= \lambda \\
 \eta &= \phi \\
 \sqrt{G_{\xi\xi}} &= R \cos \phi \\
 \sqrt{G_{\eta\eta}} &= R
 \end{aligned} \tag{2.32}$$

In which λ is the longitude, ϕ is the latitude and R is the radius of the Earth (6370 km).

- **Continuity equation**

The depth-averaged continuity equation is given by:

$$\frac{\partial \zeta}{\partial t} + \frac{1}{\sqrt{G_{\xi\xi}} \sqrt{G_{\eta\eta}}} \frac{\partial \left[(d + \zeta) U \sqrt{G_{\xi\xi}} \right]}{\partial \xi} + \frac{1}{\sqrt{G_{\xi\xi}} \sqrt{G_{\eta\eta}}} \frac{\partial \left[(d + \zeta) V \sqrt{G_{\xi\xi}} \right]}{\partial \eta} = Q \tag{2.33}$$

In which ζ = slope, d = water depth, with Q representing the contributions per unit area due to the discharge or withdrawal of water, precipitation and evaporation:

$$Q = H \int_{-\gamma}^{\gamma} (q_{in} - q_{out}) d\sigma + P - E \tag{2.34}$$

where q_{in} and q_{out} are the local sources and sinks of water per unit of volume (1/s), respectively, P the non-local source term of precipitation and E non-local sink term due to evaporation.

We remark that the intake of, for example, a power plant is a withdrawal of water and should be modelled as a sink. At the free surface there may be a source due to precipitation or a sink due to evaporation.

2.2.3 Depth-averaged flow

For 2D depth-averaged flow the shear-stress at the bed induced by a turbulent flow is assumed to be given by a quadratic friction law:

$$\bar{\tau}_b = \frac{\rho \cdot g \bar{U} |\bar{U}|}{C_{2D}} \tag{2.35}$$

Where $|\bar{U}|$ is the magnitude of the depth-averaged horizontal velocity.

The 2D-Chézy coefficient 2D C can be determined according to one of the following three formulations:

• **Chézy formulation:**

$$C_{2D} = \text{Chézy coefficient (m}^{1/2}/\text{s)}.$$

• **Manning's formulation:**

$$C_{2D} = \frac{\sqrt[3]{H}}{n} \quad (2.36a)$$

Where: H is the total water depth (m).
And n is the Manning coefficient (m^{-1/3} s).

• **White Colebrook's formulation:**

$$C_{2D} = 14.8 \log \left(\frac{\sqrt[3]{H}}{k_s} \right) \quad (2.36b)$$

Where: H is the total water depth.
And k_s is the Nikuradse roughness length.

2.3.4 Secondary flow (feature available in σ-grid only)

The flow in a river bend is basically three-dimensional. The velocity has a component in the plane perpendicular to the river axis. This component is directed to the inner bend near the riverbed and directed to the outer bend near the water surface, see Figure 2-4.

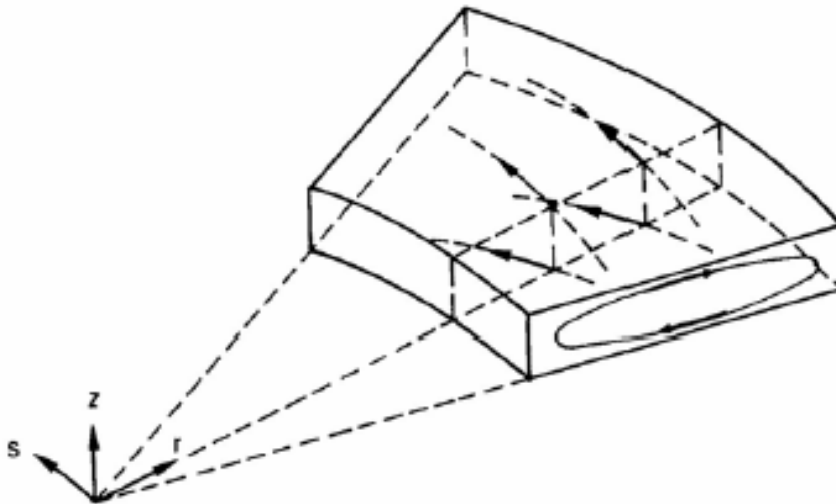


Figure 2.4: Secondary flow definition in Delft 2D model

This so-called 'secondary flow' (spiral motion) is of importance for the calculation of changes of the riverbed in morphological models and the dispersion of matter. In a 2D model the secondary flow is resolved on the vertical grid, but in 2D depth-averaged simulations the secondary flow has to be determined indirectly using a secondary flow model. It strongly varies over the vertical but its magnitude is small compared to the characteristic horizontal flow velocity.

The secondary flow will be defined here as the velocity component $v(\sigma)$ normal to the depth-averaged main flow. The spiral motion intensity of the secondary flow I is a measure for the magnitude of this velocity component along the vertical:

$$I = \int_{-1}^1 |v(\sigma)| d\sigma \quad (3.37)$$

The vertical distribution of the secondary flow is assumed to be a universal function of the vertical co-ordinate $f(\sigma)$. The actual local velocity distribution originates from a multiplication of this universal function with the spiral motion intensity; see (Kalkwijk and Booij, 1986):

$$v(\sigma) = f(\sigma)I \quad (3.38)$$

A vertical distribution for a river bend is given in Figure 3.10. The spiral motion intensity I can also be used to determine the deviation of the direction of the bed shear stress from the direction of the depth-averaged flow.

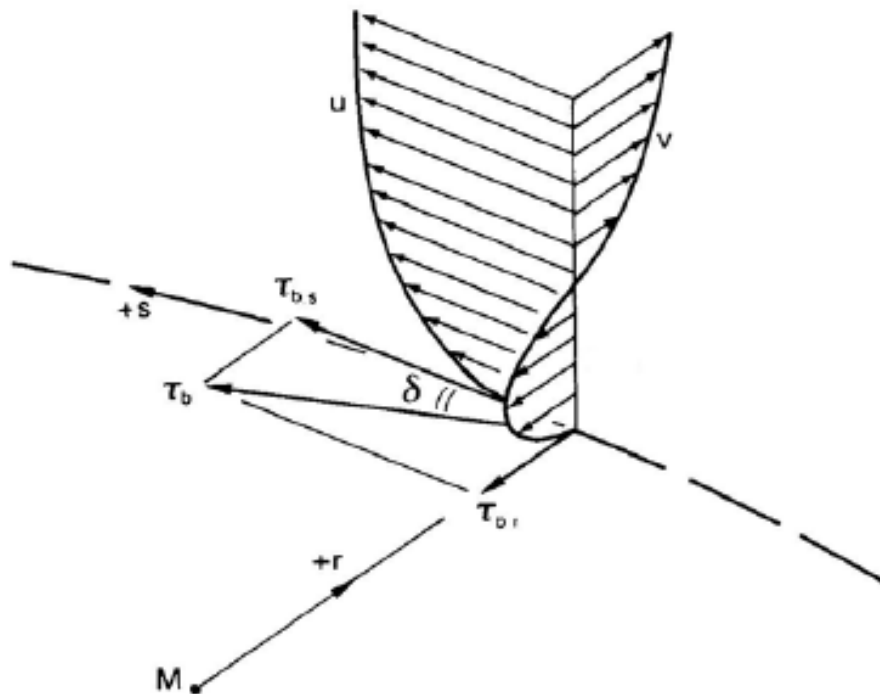


Figure 3.10: vertical distribution for a river bend

The component of the bed shear stress normal to the depth-averaged flow direction

τ_{br} reads:

$$\tau_{br} = -\rho \alpha \left(1 - \frac{\alpha}{\nu} \right) |U| I \quad (2.39)$$

Where α is defined in eq. (2.38) and U is the magnitude of the depth-averaged velocity. To take into account the effect of the secondary flow on the depth-averaged flow, the depth-averaged shallow water equations have to be extended with:

- An additional advection-diffusion equation to account for the generation and adaptation of the spiral motion intensity.
- Additional terms in the momentum equations to account for the horizontal effective shear-stresses originating from the secondary flow.

2.3.5 Effect of secondary flow on depth-averaged momentum equations

To account for the effect of the secondary flow on the depth-averaged flow, the momentum equations have to be extended with additional shear stresses. To close the equations these stresses are coupled to parameters of the depth-averaged flow field. The main flow is assumed to have a logarithmic velocity profile and the secondary flow originates from a multiplication of a universal function with the spiral motion intensity, see (Kalkwijk and Booij, 1986). Depth averaging of the 3D equations leads to correction terms in the depth-averaged momentum equations for the effect of spiral motion:

$$F_{s\xi} = \frac{1}{d + \xi} \left\{ \frac{1}{\sqrt{G_{\xi\xi}}} \frac{\partial [(d + \xi)T_{\xi\xi}]}{\partial \xi} + \frac{1}{\sqrt{G_{\eta\eta}}} \frac{\partial [(d + \xi)T_{\xi\eta}]}{\partial \eta} \right\} + \left\{ \frac{\nu T_{\xi\eta}}{\sqrt{G_{\xi\xi}} \sqrt{G_{\eta\eta}}} \frac{\partial \sqrt{G_{\xi\xi}}}{\partial \eta} + \frac{\nu T_{\xi\xi}}{\sqrt{G_{\xi\xi}} \sqrt{G_{\eta\eta}}} \frac{\partial \sqrt{G_{\eta\eta}}}{\partial \xi} \right\} \quad (2.40a)$$

and

$$F_{s\eta} = \frac{1}{d + \xi} \left\{ \frac{1}{\sqrt{G_{\xi\xi}}} \frac{\partial [(d + \xi)T_{\eta\xi}]}{\partial \xi} + \frac{1}{\sqrt{G_{\eta\eta}}} \frac{\partial [(d + \xi)T_{\eta\eta}]}{\partial \eta} \right\} + \left\{ \frac{\nu T_{\eta\eta}}{\sqrt{G_{\xi\xi}} \sqrt{G_{\eta\eta}}} \frac{\partial \sqrt{G_{\xi\xi}}}{\partial \eta} + \frac{\nu T_{\eta\xi}}{\sqrt{G_{\xi\xi}} \sqrt{G_{\eta\eta}}} \frac{\partial \sqrt{G_{\eta\eta}}}{\partial \xi} \right\} \quad (2.40b)$$

With the shear-stresses, resulting from the secondary flow, modelled as:

$$T_{\xi\xi} = -\gamma \beta UV \quad (2.41a)$$

$$T_{\eta\xi} = T_{\xi\eta} = \beta (U^\gamma - V^\gamma) \quad (2.41b)$$

$$T_{\eta\eta} = \gamma \beta UV \quad (2.41c)$$

and

$$\beta = \beta^* \frac{(d + \zeta)}{R_s^*} \quad (2.41d)$$

$$\beta^* = \beta_c (\alpha - 1)^{0.7} \alpha^\gamma + 3\gamma \alpha^\gamma \quad (2.41e)$$

$\beta_c \in [0, 1]$, correction coefficient specified by user

$$\alpha = \frac{\sqrt{g}}{\kappa C_{vD}} < 1 \quad (2.42)$$

With R_s^* the effective radius of curvature of a 2D streamline to be derived from the intensity of the spiral motion and κ the Von Karman constant.

2.4. Transport equations

2.4.1 Introduction

In this particular report we are more interested in bed load transport and all computations were made basis on bed load transportation without taking suspended load into considerations

2.4.2 Bed-load sediment transport of non-cohesive sediment

Bed-load transport is calculated for all “sand” sediment fractions by broadly following the approach described Van Rijn (1993, 2000). This accounts for the near-bed sediment transport occurring below the reference height a described above.

The approach first computes the magnitude and direction of the bed-load “sand” transport using by Van Rijn. The computed sediment transport vectors are then relocated from water level points to velocity points using an “upwind” computational

scheme to ensure numerical stability. Finally the transport components are adjusted for bed-slope effects.

But for the Meuse River some sort of calibration test was made and it was found that the equation of Meyer-Peter-Muller (1948) is the best for graded sediment with the overall calibration factor of 1.0, because they noted that the computer computation with this equation gives two times the measurement quantities.

4.4.3 Sediment transport components per fraction

The bed-load components $s_{b\xi i}$ and $s_{b\eta i}$ (on a curvilinear ξ, η grid) follow from the volumetric bed-load transport rate s_{bi} per fraction by:

$$\begin{aligned} s_{b\eta i} &= s_{bi} \sin(\beta_i) \\ s_{b\xi i} &= s_{bi} \cos(\beta_i) \end{aligned} \quad (4.43)$$

Where β_i is the direction of sediment transport for fraction i .

The local bed-load transport rate per fraction is described using a standard transport formula. For the two-dimensional approach the Meyer-Peter and Muller formula, and the Ashida and Michiue formula, prepared for graded sediment simulations in two dimensions, are provided. The following is focussed on the application of the Ashida and Michiue formula. It should be remarked that extension of Ashida and Michiue formula to two-dimensions is not unambiguous, and permits alternative formulations. Generally the formula is expressed as:

$$s_{bi} = \gamma \sqrt{\Delta g D_i} \tau_{*ei}^{\gamma} \left(1 - K_c \frac{\tau_{*ci}}{\tau_{*fi}} \right) \left(1 - \sqrt{K_c \frac{\tau_{*ci}}{\tau_{*fi}}} \right) \quad (4.44)$$

in which D_i is the characteristic diameter of fraction i , g is the acceleration due to gravity, Δ is the relative density of the sediment ($\Delta = (\rho_s/\rho) - 1$ where ρ_s and ρ are mass density of sediment and water), τ_{*fi} is the non-dimensional shear stress, τ_{*ei} is the effective non-dimensional shear stress, and τ_{*ci} is the non-dimensional critical shear stress. Furthermore, K_c is a correction factor on the magnitude of the transport rate for the influence of bed slope. The non-dimensional shear stresses for each fraction can be based on the representative grain size D_i and the shear velocity u_* as follows:

$$\tau_{*ei} = \frac{u_*^{\gamma}}{\Delta g D_i} \left[1 + \frac{1}{\kappa} \ln \left(\frac{h}{D_m \{1 + \tau_{*m}\}} \right) \right]^{\gamma}; \quad \tau_{*m} = \frac{u_*^{\gamma}}{\Delta g D_m}; \quad \tau_{*fi} = \frac{u_*^{\gamma}}{\Delta g D_i}; \quad \tau_{*ci} = \zeta_i \tau_{*cm} \quad (4.45)$$

Where h is the local water depth, D_m is the mean grain size of the bed material, τ_{*cm} is the critical non-dimensional shear stress (Shields value) for grain size D_m ($\tau_{*cm} \approx 0.045$), ζ_i is the coefficient for hiding and exposure. In the presented formulation for τ_{*ei} a type of ripple factor is included, although other formulations are provided in the model as well. For the hiding and exposure coefficient it is common to use the Egiazaroff's formulation adjusted by Ashida and Michiue:

$$\zeta_i = \left[\frac{\log_{10}(\lambda^q)}{\log_{10}(\lambda^q D_i / D_m)} \right]^\gamma \quad \text{if } \frac{D_i}{D_m} \geq \lambda \cdot \xi ; \quad \zeta_i = \lambda \cdot \lambda^0 \frac{D_m}{D_i} \quad \text{if } \frac{D_i}{D_m} < \lambda \cdot \xi \quad (3.46)$$

Due to the downhill gravitational transport component, the transport direction and transport magnitude in a 3D model does not necessarily coincide with the direction of the bed shear stress of the flow, and the transport capacity on a horizontal bed. In the Ashida and Michiue formula these bed-inclination effects influence the transport rate through the correction factor K_c , and the direction of sediment transport through an expression for β_i (see equation 3.44). The direction of sediment transport β_i is found to be of major importance for the development of typical 3D morphological features.

The slope effect on sediment-transport magnitude K_c can be expressed as:

$$K_c = 1 + \frac{1}{\mu_s} \left[\left(1 + \frac{1}{\Delta} \right) \cos(\alpha) \frac{1}{g_\xi} \frac{\partial z_b}{\partial \xi} + \sin(\alpha) \frac{1}{g_\eta} \frac{\partial z_b}{\partial \eta} \right] \quad (3.47)$$

Here g_ξ and g_η are co-ordinate transformation coefficients, α is the flow direction near the bed, and μ_s is the static friction coefficient for sediment.

The slope effect on the direction of sediment transport can be expressed by extending the direction formula for uniform sediment to a more general graded sediment formulation, in which effects of hiding and exposure, and bed forms are also accounted for. Further simplification of this general formula (for the moment, on basis of numerical experiments) led to the following formula:

$$\tan(\beta_i) = \frac{\sin(\alpha) - \frac{1}{f_{si}} \frac{1}{g_\eta} \frac{\partial z_b}{\partial \eta}}{\cos(\alpha) - \frac{1}{f_{si}} \frac{1}{g_\xi} \frac{\partial z_b}{\partial \xi}} \quad \text{with} \quad f_{si} = \frac{A_{sh}}{\Pi} \left(\frac{\tau_{*fi}}{\tau_{*ci}} \right) \left(\frac{D_m}{D_i} \right)^{D_{sh}} \quad (3.48)$$

Where A_{sh} is a calibration coefficient generally taken equal to unity, D_{sh} a coefficient determining the dependence of the Shields number on D_i or D_m (e.g. $D_{sh} = 0$ or -1), and $\Pi = K_{ld} + 1/\mu_s$ with K_{ld} is the ratio of the lift force to drag force on the grains ($K_{ld} \approx \lambda \cdot \lambda^0$).

3.5. Active Layer-approach for erosion and deposition of fractions

The basic bed-layer concept used here is that of Ribberink, in which the bed is subdivided in transport layer with thickness δ_a , an exchange layer (optional) with thickness δ_{ex} and a substratum with top level z_s , as shown in Figure 3.6. In this Figure p_i is the probability of a size fraction (with $\sum p_{i,a} = 1$, $\sum p_{i,ex} = 1$, $\sum p_{i,s} = 1$) z_b is the

average bed level ($z_b = z. + \delta_{ex} + \delta_a$), and ϕ_i is the vertical sediment flux through the interface. The active layer represents the upper layer containing the material, which is taking part in the actual sediment-transport process, and its thickness is generally related to the average height of bed forms (dunes, ripples). The exchange layer, between active layer and substratum is sometimes used for stabilization of the approach. This second-layer is introduced by Ribberink to incorporate the effect of variability of through depths and related vertical sorting, and to partially avoid elliptic mathematical behaviour of the equations of the one-layer concept. For the present paper the exchange layer is not further included in the following theoretical descriptions and analyses. The non-moving substratum is either schematized with a homogeneous composition, or it is schematized by a number of sub-layers for which a bookkeeping system the substrate composition, taking into account the history of its deposits. These changes in substrate during a simulation occur for instance when due to sedimentation processes material transported from upstream is deposited and added to the substratum.

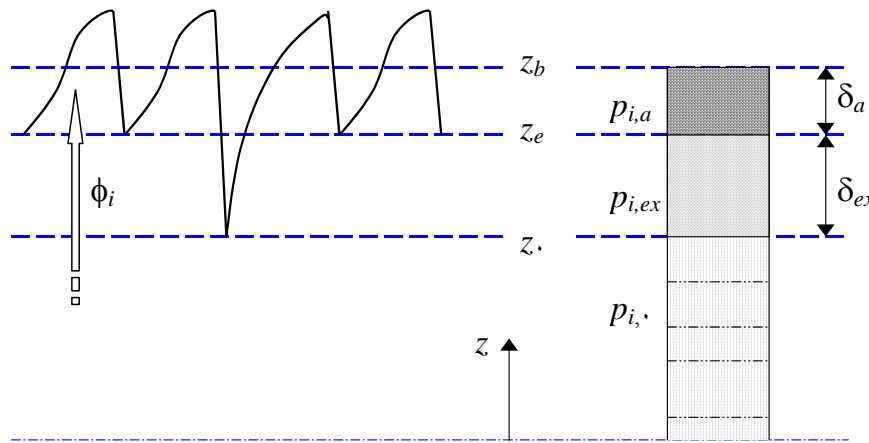


Figure 2.1: The bed-layer schematization after Ribberink (1988), where sub-script i is associated to sediment size fraction i

The layer-concept of Ribberink, is extended to two dimensions, and is governed by the following sediment continuity equation per size fraction (for bed-load transport):

$$(1 - \epsilon_p) \left[\frac{\partial p_{i,a} \delta_a}{\partial t} + p_i(z.) \frac{\partial z.}{\partial t} \right] + \frac{\partial s_{bxi}}{\partial x} + \frac{\partial s_{byi}}{\partial y} = \cdot \quad p_i(z.) = \begin{cases} p_{i,a} & \text{sedimentation} \\ p_{i,cdot} & \text{erosion} \end{cases}$$

In which t is time, x and y are Cartesian co-ordinates, $p_i(z.)$ is the probability of occurrence of a sediment size fraction i at level $z.$ (taken equal to $p_{i,a}$ during sedimentation, and taken equal to $p_{i,cdot}$ during erosion), and $s_{bxi}(x, y, t)$ and $s_{byi}(x, y, t)$ are the bed-load transport components per unit of width for fraction i . In the Delft 2D-Rivers modelling approach the equations are projected on an orthogonal curvilinear grid with ξ, η . co-ordinates. In this paper the ξ . coordinate is the main-flow direction (usually the direction of the river axis). Projections of s_{bxi} and s_{byi} on the curvilinear grid are called $s_{b\xi i}$ and $s_{b\eta i}$.

3. The Meuse River

3.1. Introduction

The Meuse River originates in France on the plateau of Langres, then flows through Belgium and enters The Netherlands at Eijsden (near Maastricht). The total length of the river from its origin at Pouilly-en - Bassigny to the Hollands Diep estuary is about 490 km. The river constitutes a natural international border between the Netherlands and Belgium from Eijsden to Maastricht and from Borgharen to Stevenweert. This part of approximately 60 kilometers is the only major gravel-bed river in The Netherlands, and because it is no longer used for navigation, there is ample opportunity for nature restoration. The reach is called Grensmaas (Border Meuse) in The Netherlands and Gemeenschappelijke Maas (Common Meuse) in Flanders (Klaassen et al, 1998) and (Berkhout, 2003).

The common Meuse flows through a relatively narrow valley and has a gradient of almost 0.40 m/km. At Grevenbicht it crosses the Feldebiss fault, which divides the valley into two distinct geomorphological settings. Upstream of this fault, uplift and erosion have produced pronounced Pleistocene river terraces. Downstream the river has deposited thick layers of gravel in the subsiding Roer valley graben. The mining of this gravel has produced a landscape with numerous deep lakes.

3.2. The Meuse and the Meuse Valley together

After the floods in 1993 and 1995, it became clear that the people, who live, work and enjoy their leisure time in the Meuse Valley are not well enough protected against flooding, this also the view taken by the Delta Plan for Major Rivers. Immediately after the floods in 1995, low embankments were quickly built around population centres, but they still do not provide the necessary protection.

In addition to safety, there are other issues at stake. The government is keen to transport as many goods as possible by water instead of by road. This will reduce traffic congestion and is good for the environment. At present, however, some stretches of waterway are not able to handle modern vessels. Plans to increase the scale of inland shipping will only make these problems worse. This is another reason for the government to look into improving the Meuse Route.

Further issue is related to the ecology of the river's winter-bed, the object of growing concern. The work carried out to make the Meuse a safer river also opens up opportunities to encourage and reinforce nature in the winter-bed. The government is therefore eager to examine and exploit these opportunities. These are the three aims of the overall Zandmaas/Maasroute project: to raise the level of protection, to improve the waterway and, where possible, to use these changes to benefit nature. It is obvious that these three aims should be tackled in a single project. The associated measures will, after all, be implemented in the same stretch of the Meuse and will therefore have a direct impact on one another. Furthermore, by dealing with these in one and the same project, it will only be necessary to go through one set of decision-making procedures. An integrated approach of this type also makes it easier to explain which measures are

required, and what the relationships are between them. (Zandmaas / Maasroute – Route paper /EIS)

For all these reasons, it has been decided to merge the Zandmaas project (flood protection) and the Maasroute project (improvements to the waterway) into a single project, the Zandmaas/Maasroute project.

3.3. Hydrological conditions

The size of the Meuse catchment area is about 33,000 km², of which 10,000 km² is in France, 13,000 km² in Belgium, 8,000 km² in Germany, and 6,000 km² in The Netherlands. The French Meuse flows through wide valleys with permeable soil. This allows water to infiltrate providing an important source for the low base-flow in the dry season. Large parts of the catchment area, especially in Belgium, have an impermeable soil, causing the river to react quickly to any precipitation. In case of heavy rainfall in France or Belgium flood discharges will reach the common Meuse within three days as a maximum. The discharge of the steep and impermeable Wallon branches will arrive within half a day (Berkhout, 2003).

The Meuse is a rain-fed river. This causes large variations in discharges. The river has an average flow of about 200 m³/s and flood discharges about 3000 m³/s. The year-average flow of the Meuse at Borgharen in the period of 1911 to 2002 is 240 m³/s. Most high discharges occur during the wet season, which begins in October and ends in April. The maximum flood discharges of 1993 and 1990 were calculated to be 3039 and 2746 m³/s respectively, the MHW-discharge (the design flood) is set on 3800 m³/s (Berkhout, 2003).

3.4. Gravel-sand content of the sediments

The gravel-sand content of the sediments is another way to represent the spatial variation of the sediments. Figure 3.1 gives the percentage of gravel ($D_j \geq 2$ mm) content along the Meuse River. In this Figure it is possible to notice that the average sand content exceeds the 50% around km 100 approximately, which is also the reach where the gravel-sand transition occurs. Inspection of the spatial variation in D_{10} , D_{50} and D_{90} confirmed such location (Murillo-Muñoz, 1998). In Figure 3, two peaks in the sand content are observed, notably around km 70 and 90. These peaks may be produced by the barrages of Linne and Roermond respectively, which induce sedimentation of sand during low flow conditions

3.5. Sediment transport rates and measurements

Regarding the sediment transport rates there is great variability of data reported in the literature. Waterloopkundig Laboratorium (1994) reports that the average sediment transport rate of the Common Meuse River at Borgharen is approximately 30×10^3 m³/y; but at Linne it is reported to be about 26×10^3 m³/y, while 19×10^3 m³/y at Kessel and 9×10^3 m³/y at Ravenstein are mentioned for the more downstream reach (Gerretsen, 1978). The reduction between Borgharen and Kessel may be to tectonic effects (Murillo and Klaassen, 2006).

Furthermore, it has been observed in the Meuse River that the transported sediment load depends on whether or not the armour layer has been mobilized during a previous flood.

Klaassen (1986) indicated that if the armour layer remains stable when the smaller floods are passing little sediment is transported. Once the armour layer is mobilized the substratum material is available and the sediment load increases rapidly. This phenomenon has been estimated to occur at discharges higher than $120 \text{ m}^3/\text{s}$ (Klaassen, 1981), which coincide with the present estimated bank-full discharge. During the receding part of the flood the armour layer is built up once again but at a lower level, and on top of the eroded layer sediments are deposited. These deposited (and often finer) sediments are available for transport and therefore after a flood period this material can be transported at smaller discharges until the armour layer is exposed again. Hence, the composition of the armour layer and the sediment transport is a function of the magnitude of previous floods (Duizendstra, 1999). A high flood will give a finer armour layer and more eroded sediment on top of the restored armour layer after the flood (Klaassen, 1986).

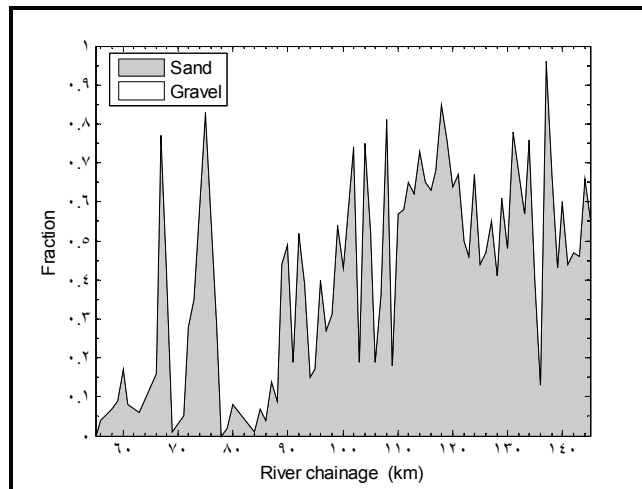


Figure 3.1: Gravel and sand content along the Meuse River.

Sediment transport in a river can be subdivided into bed load transport, suspended load transport and wash load transport. Measurements of sediment transport have only taken place on a very limited scale in the Grensmaas. Relevant publications concerning sediment transport measurements are given in the table 3.1 below.

Only a few publications are available which concern sediment transport measurements in the Grensmaas. Duizendstra (1999) was the only one who carried out sediment transport measurements during discharge values exceeding the (assumed) critical value for the break up of armour layers. The accuracy of the Helley Smith sampler during high discharge values with transportation of very coarse gravel particles is not known. However, it can be concluded that there are not enough data available to obtain complete insight into the formation of break up of armor layers and the effect on the sediment transport in the Grensmaas (Lambeek, 1996).

Author	Discharge m ³ /s	Location	Location (km)	Type of transport	Instrument
Bed load and suspended load transport					
Rijkswaterstaat 1978	< 700	Roosteren	04	Bed load + suspended load	Btma, Delft bottle
Schoonman, 1991 Burgdorffer, 1993	203 - 1000	Eijsden, Maaseik	4, 02	Bed load + suspended load	Helley Smith AZTM, PFS
Duizendstra et al 1994	723 - 780	Stein, Maaseik	29, 02	Bed load	Helley Smith
Duizendstra, 1990	1300 - 2600	Stein, Maaseik	29, 02	Bed load	Helley Smith
Wash load transport					
RIWA, RID, 1979	-	Eijsden	4	Wash load	
Van der Veen, 1990	-	Eijsden	4	Wash load	
Fioole, 1992	-	Eijsden	4	Wash load	

Table 3.1: Relevant publications concerning sediment transport data Grensmaas Source: Mer Project Grensmaas

3.1. Bed level and bed slope

Bed levels along the Meuse have changed significantly in the upper part of the river. These changes are due to the impressive degradation process that the river has suffered during the last century as a result of training works and subsurface mining. In the area near Maasband this has resulted in degradation of some 0 m while in others reaches the degradation is less severe but still considerable. On the contrary, minimum degradation has been observed in the lower parts of the river, with a number of reaches experiencing some aggradations

Measured bed levels along the Meuse are shown in Figure 3.4. From these levels the slope of the river bed is estimated and the resulting lines represent the trend of the bed elevation. The trend of the data in the upper part of the river indicates a slope of 0.0 m/km whilst for the lower reach a value of 0.10 m/km is found. It is possible to observe also that the change in the slope occurs between km 70-80. However, a close inspection of the bed levels indicates that in period 1909-1916 the change in slope was more gradual with a sharper transition near the km 90, where probably the gravel-sand transition was formed (Murillo-Muñoz, 1998). This suggests that the current location

of the transition in the bed slope is probably the results of the intensive degradation process induced by the human interference in the system.

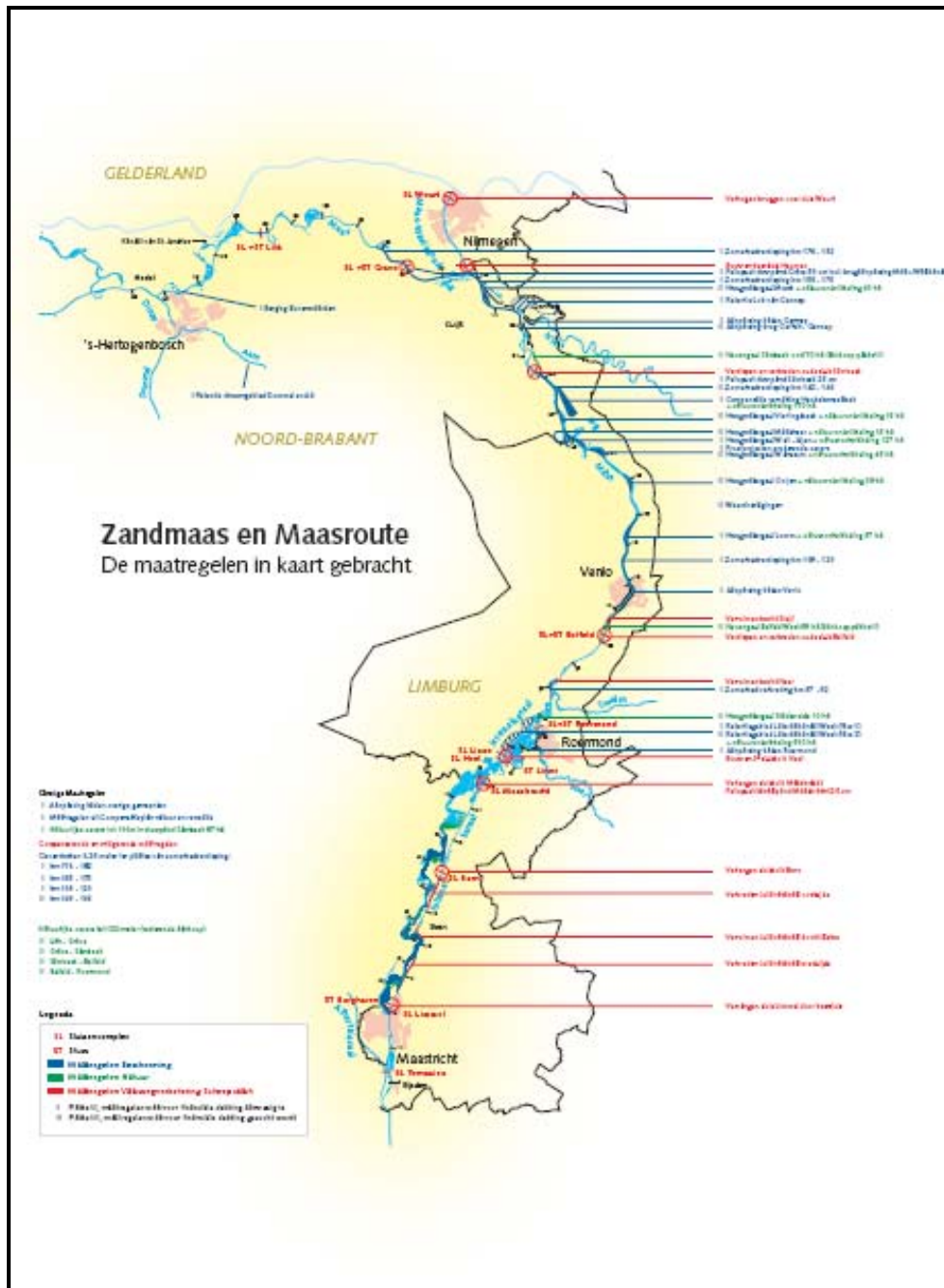


Figure 3.1: Meuse River

3.7. Characteristics of the river bed

The Common Meuse is the gravel-bed river with a bed slope of about 1.0×10^{-3} . This is about five times steeper than other Dutch rivers and brings along high flow velocities. The bank full flow velocity is $1 - 1.5$ m/s at the surface (Berkhout, 2003). The river consists of an incised channel and shows large meander bends. The width is reasonably constant around 80 m due to river training in the 19th century. Between km chainage 60 and 90 the slope reduces from 1.0×10^{-3} to 1.5×10^{-3} (see Figure 3.6). Over a length of about 20 km between km chainage 90 and 110 the median diameter of the riverbed also become smaller (D_{50} reduced from 10 mm to 5 mm) (Murillo – Munoz, 1998).

The riverbed in the Common Meuse shows an armour layer (Klaassen, 1981). The top layer consists of much coarser grains than the sub-layers. This top layer protects the underlying fine material from being entrained during normal discharges. Because of the limited availability of mobile grains the transport capacity in the river is often much larger than the actual transport (factor 100) (Berkhout, 2003).

The median size of the bed material is about 10 mm, or possibly somewhat higher because there are indications that there has been a bias in the choice of the sample locations. The gravel bed has a pronounced armour layer during most of the flows. Only during floods, a few days per year, this armour layer become unstable, this leads to transport of the fine bed material in large quantities. The sediment transport is about 0.5×10^6 m³/year (Klaassen, 1988; Klaassen, 1981). The armour layer consists of gravel with diameters between 10 and 100 mm (Klaassen et al, 1998).

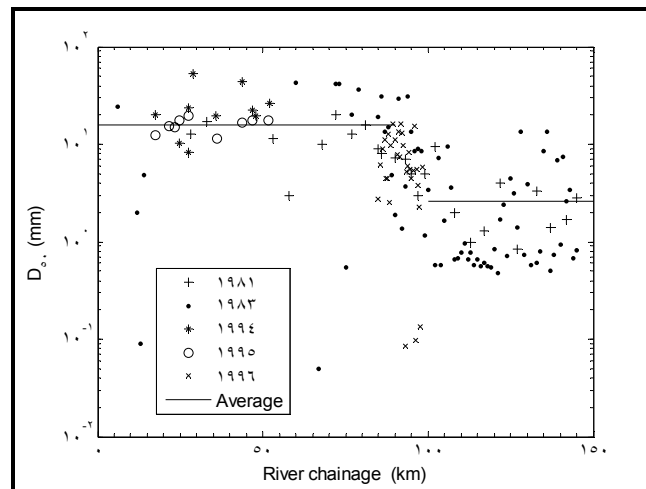


Figure 3.7: Variation of the D_{50} in the bed material along the Meuse River.

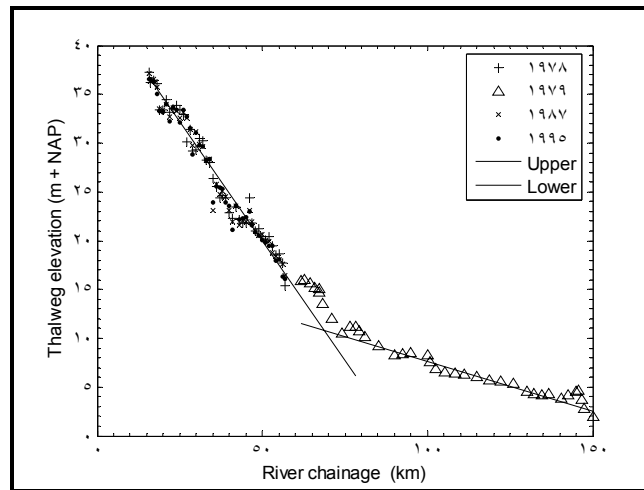


Figure 3.4: Trend of the thalweg elevation along the Meuse River.

3.8. About Maaswerken

The Maaswerken project organisation was set up by the Ministry of Transport, Public Works and Water Management, the Province of Limburg, and the Ministry of Agriculture, Nature Management and Fisheries under the Delta Plan for Major Rivers. After the floods of 1993 and 1995, this plan provided for the construction of embankments along the Meuse to offer better protection to vulnerable areas. The likelihood of flooding is now no greater than 1:50 per annum. This Figure should be reduced to 1:200 per annum. Flood protection is thus an important goal of the Maaswerken.

When the Maaswerken was launched in April 1997, the existing Grensmaas and Zandmaas / Maasroute projects were brought together. The Maaswerken is responsible for developing plans and implementing these two projects.

The measures required to increase the level of flood protection, improve the waterway and tin courage nature development wilt have an impact on the river system and the waterway. The Meuse and the Juliana Canal are of such importance as waterways that a decision is required under the Route Act before work can proceed. An environmental impact assessment (EIA) is also necessary, as it is linked to the procedure set out under the Route Act. Olie of the components of the EIA is the Environmental Impact Statement (EIS).

Because this project also involves taking other decisions that wilt influence the environment, the need for an EIS is evident. For example, olie of the consequences of the Zandmaal/Maalroute measures is that soil and sediment will be excavated. If the excavation covers more than 100 hectares, an environmental impact assessment is required. Sand and gravel are extracted, but allow soil which is unmarketable and sometimes diffusely polluted. Such soil may need to be stored in depots. Depots that exceed a capacity of 500,000 cubic metres require an environmental impact assessment to be carried out as well.

The same requirement may apply if the soil is treated. Further EIA measures may become necessary, depending on the choices made, and the Zandmaal/Mansroute EIS must describe these reassures.

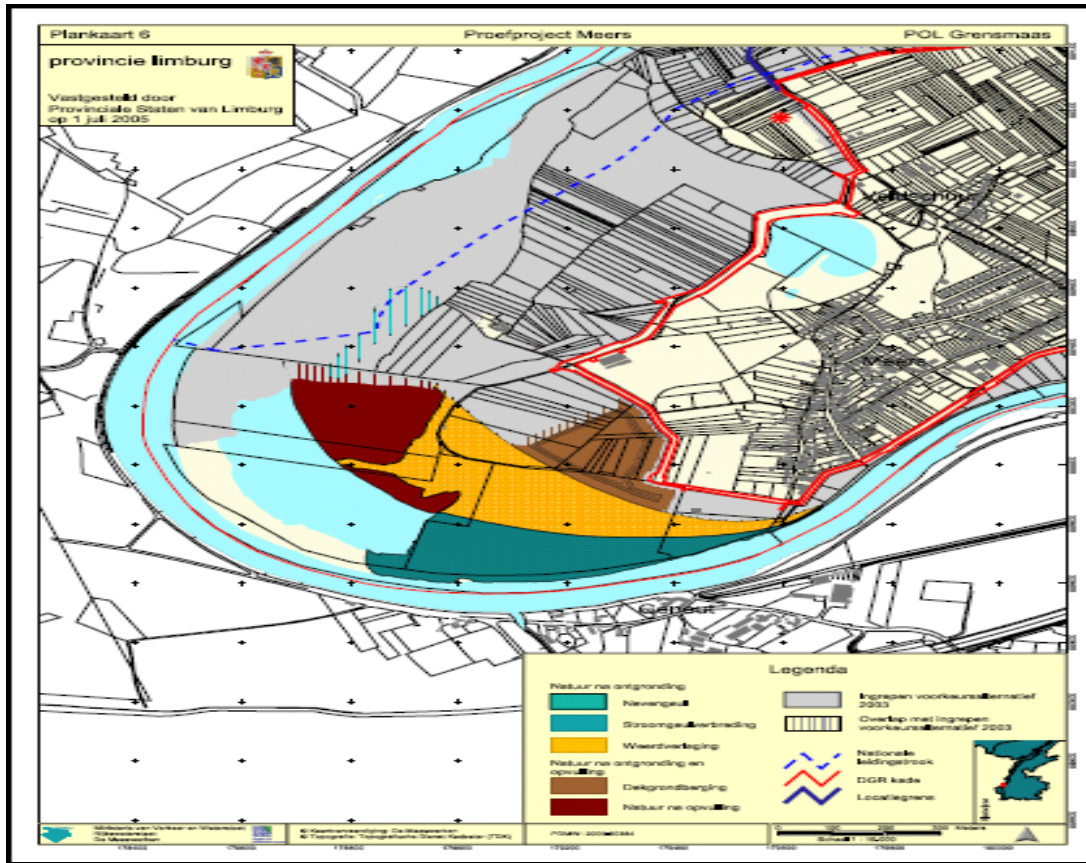


Figure 3.5: Meuse River at Meers (planned excavations)



Figure 3.6: Meuse River at Meers

3.9. Socio – economic functions of the Meuse

Naturally, the primary function of the Meuse is discharging water and sediment. But it is also used for a lot of other purposes. Traditionally floodplains are used for housing and agriculture, and nowadays for nature development, and recreation. The water in the river is used as cooling water and to provide water supply. The Meuse is part of an important transport network in the trans-European inland waterways along with the Waal, the Rhine-Scheldt Canal and the Albert Canal (Belgium). Weirs are used to make sure that the river is navigable during the whole year. Part of the waterway is the Juliana Canal parallel to the Common Meuse. An indication of the importance of the Meuse River for navigation can be given using Sambeek lock. In 1996 a total of 50700 vessels passed through with a combined capacity of 41 million tons. More than 70% of the freight is accounted for by sand and gravel. To put these numbers in perspective, it should be noted that 16000 vessels pass at Lobith each year a combined freight of 10 million ton (Middelkoop, 1998). Hence the transport on the Meuse River is about 1/3 of the Rhine River.

3.10. Natural and human interventions in the river bed morphology

The natural Meuse River of the last centuries was a typical island river with at least 100 islands. Most of these islands have disappeared due to river training in the 19th century, but the ones that still exist have changed very little over the last two centuries. The biggest changes in the course of the river Meuse were the result of normalization and canalization works between 1800 and 1940. During this period the all-shallow and wide river was reduced to one uniform channel. Between 1900 and 1930 weirs and locks were built in The Netherlands and Belgium in order to improve shipping conditions. This was also the main motivation to built canals along the river Meuse. The conditions that were created by this normalization lead to further incision of the riverbed and which was accelerated by large-scale of gravel mining.

In 1992 the Ministry of Transport, Public works and Water management, the Ministry of agriculture, nature management and fisheries and Province of Limburg agreed to develop a joint plan to use the revenue of gravel mining for nature development (Grensmaas project). This should result in a widened channel of the Common Meuse in which a great diversity of the natural habitats could develop. At the same time the widened river reduces the risks of flood discharges, after the floods of 1993 and 1990 the aim of the project were adjusted in order to reduce the effects of such high discharges even more.

Subsequently this project was merged in April 1997 with a project for the improvement of navigation conditions in the Dutch Meuse together with limited nature development (Zandmaas / Maasroute). This project and the resulting project organization are called

“De Maaswerken”. Its goals are to present a set of interventions for the Dutch Meuse combining the needs for flood protection, intensified navigation and nature development. Some temporal measures to increase protection against future floods are carried out. Structural flood protection measures and interventions to improve nature and shipping conditions and to gain incomes with gravel mining are still in development. Nevertheless, this will certainly involve adjustments of the river profile accompanied by morphological response in future.

The extent to which interventions contribute to the morphological behaviour in the future is difficult to determine. This is due to the very large time scale over which interventions in the Common Meuse influence the river morphology. As a lot of human activities around the river have taken place in the last centuries, the effects will occur simultaneously.

3.11. Data availability

For the purpose of studying the existing problem in the Meuse River and trying to reproduce the morphological phenomena happen during 2002-2003 floods using Delft2D software, different kind of data were requested to be provided, in order to defining as much as possible the character of the river and its boundary and initial conditions to the model. The required data were consists of:

- Hydrological data for the Meuse River (hourly basis)
- Bed topography of the river at and near to the problem area for different time references (before the project, after the project and before the flood and after the project and the flood)
- Roughness of the main channel and the floodplain
- Cross-sections of the river
- Sediment transport quantities (most interested in bed load transport which used in the model)
- Grain size distribution of the sediment transport, bed composition and bank composition
- Bank erosion rate
- Input and output of WAQUA model (which contain some of the required items)
- Some other data sets (Aerial photo, GIS photos before and after the flood, etc.)

The process of identification and collection of data took quite some time (about three months) till provided for us to be used in the model, but most of the required items were covered, in below some important ones will be mention:

The discharge data was provided from 1999 to 2004 in daily basis, and also for the flood period is provided in hourly basis. Also the water level is provided in hourly basis for some period of the flood, and a rating curve is provided for km 38 as shown in Figures below:

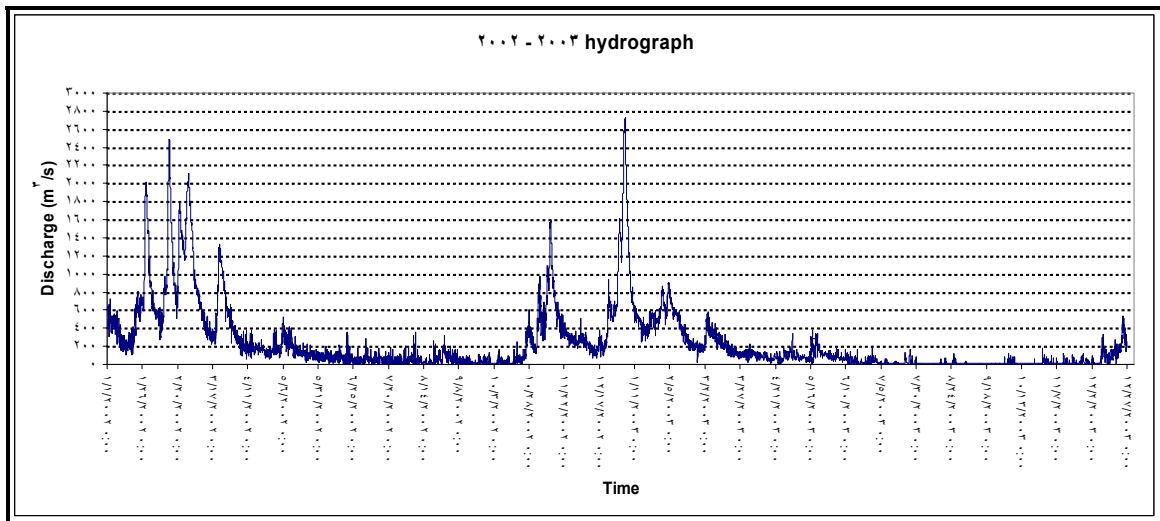


Figure 3.7: 2002-2003 hydrograph

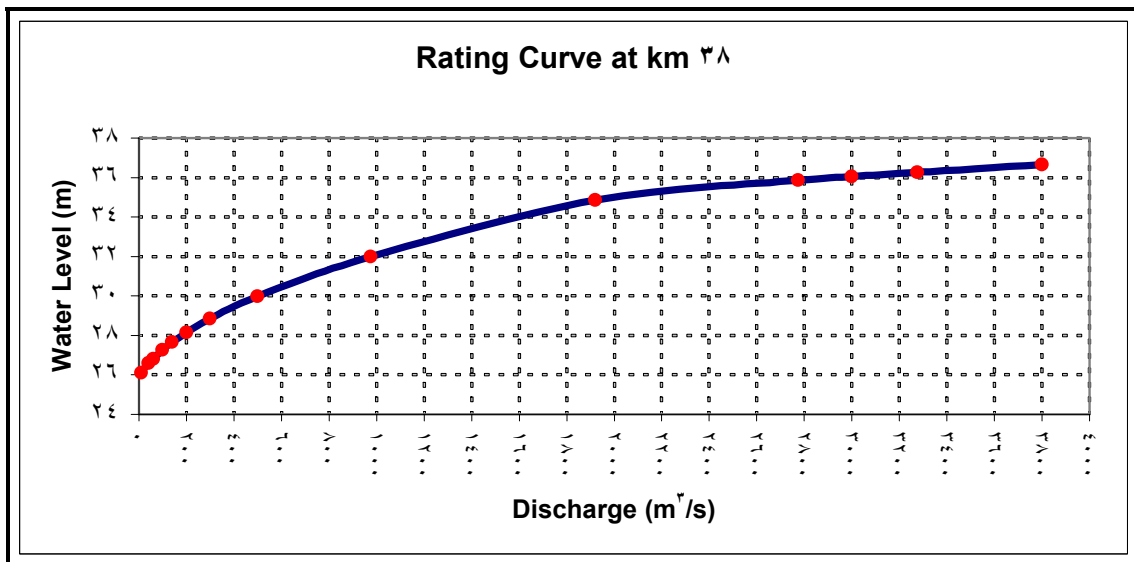


Figure 3.8: Rating curve for the Meuse River at km 38

The bed topography, roughness, cross-sections, land boundaries and other geometric feature inside the floodplain were provided in term of WAQUA schematizations for different time intervals, (1998 before the project) and (2003 after the project)

The grain size distribution was provided for bed material composition, indicating each of top-layer and sub-layers 1 & 2 as shown below:

Sediment Particles (mm)	Relative Cumulative Fractions		
	Top layer	Sub - Layer 1	Sub - Layer 2
362	1	1	1
206	1	1	1
181	1	1	1
128	1	1	1
91	0.98	0.99	0.99
64	0.86	0.9	0.9
40	0.63	0.76	0.82
22	0.38	0.58	0.66
22.4	0.23	0.49	0.51
16	0.07	0.4	0.38
11.2	0.02	0.30	0.29
8	0	0.31	0.22
0.6	0	0.28	0.17
4	0	0.20	0.14
2.8	0	0.21	0.11
2	0	0.18	0.09
1.4	0	0.14	0.08
1	0	0.11	0.07
0.80	0	0.1	0.06
0.6	0	0.07	0.04
0.42	0	0.00	0.03
0.3	0	0.03	0.02
0.21	0	0.01	0.01
0.10	0	0	0
0.100	0	0	0
0.070	0	0	0
0.053	0	0	0

Table 3.2: Grain size distribution of the bed composition for each of top layer and two sub-layers.

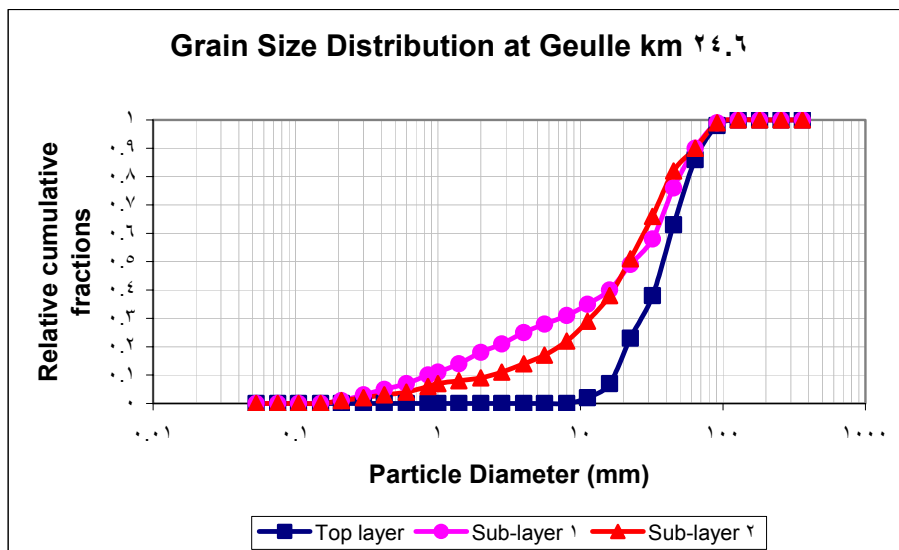


Figure 3.3: Grain size distribution of the bed composition for each of top layer and two sub-layers.

4. Model Description

4.1. Introduction

The numerical hydrodynamic modelling system Delft3D-FLOW solves the unsteady shallow water equations in two (depth-averaged) or in three dimensions. The system of equations consists of the horizontal equations of motion, the continuity equation, and the transport equations for conservative constituents. The equations are formulated in orthogonal curvilinear co-ordinates or in spherical co-ordinates on the globe. In Delft3D-FLOW models with a rectangular grid (Cartesian frame of reference) are considered as a simplified form of a curvilinear grid. In curvilinear co-ordinates, the free surface level and bathymetry are related to a flat horizontal plane of reference, whereas in spherical coordinates the reference plane follows the Earth's curvature.

Every numerical model needs different kinds of data for preparing an input file. The quality and accuracy of the data directly affects the accuracy of the result of the model. Data should be selected carefully if many data are available.

The required data for the present study on the Common Meuse is provided by different organizations and companies, such as RIZA, pilot project Meers and De Maaswerken.

For the purpose of preparing a good input file to our model we requested different sort of data for representing the area of interest and introducing the important elements and features into the model that have a significant effect on the result.

The requested data consisted of several items, such as discharges, water level records, bed roughness, bed topography for different situations (pre project, post project and before the flood, post project and after the flood), grain size distribution of bed material, quantity of sediment transport (bed load transport) and WAQUA model schematisation.

The data provided covered most of the required items. Still some other data should be provided, but the process of collecting them took a long period of time, which limited the remaining study time.

4.2. Model Setup

Model setup is a vital step in the numerical modelling. All input files should be prepared individually and then connected together inside the model in an appropriate way. Below a short description is given of model setup and required input data for Delft3D.

4.2.1 Selecting boundaries of the model

The boundaries of the model should be selected at a distance far from the area of interest such that the effect errors at the boundaries will not reach the study area. In this particular study both upstream and downstream boundary were selected about 5 km far from the area of interest.

The upstream boundary was selected at Geulle at km 14.6 and the downstream boundary located 2 km below Leut (i.e. at km 18). The length of the river reach within the model is about 13.0 km.

The land boundary (width of floodplain) is selected with the help of the WAQUA schematization as indicated by a light blue colour in Figure 4.2.

4.2.2 Grid generation

Mostly in numerical modelling the first input file that should be prepared is the computational grid generation. It is considered as the heart of the model input data, because the whole processing depends on the grids. The quality of the grid file has a large influence on all processes of the model (morphological and hydro-dynamic). Coarsening the grid gives less accurate results and refining it will increase the computational time of the model. There are some parameters should be taken into consideration while the grid system is developed like orthogonality and smoothness of the grids.

The data provided included a prepared grid file for the Meers location on the Meuse River, but unfortunately this grid file was not suitable for morphological computations, because in some areas the grid lines did not follow the direction of the main channel as shown in Figure 4.1. This might cause some computational instability especially at low flow condition. Nevertheless grid generation for the Meers location was not an easy task, because there are two difficult bends of the river with a wide floodplain.

There are several techniques to generate grid system for a specific area; firstly for regular shapes the easier way is to generate the grids by some programming technique, secondly if the area of interest will be a river with a narrow floodplain the grid can be generated first for the main channel, then it can be extended to the floodplain considering the restriction of the parameters mentioned above (orthogonality and smoothness), finally when the river has a wide flood plain the grid generation become more difficult and the first step in this case is to draw the summer bank of the river and then drawing some perpendicular lines at equal distances (preferable) to these banks.

Later on these perpendicular lines should be extended to cover the floodplain area in the way to reduce somewhat the effect of the bends in the river through the wide floodplain which considered as the most difficult part of the grid generations for such areas. After that the grid will be generated for the whole area and the processes of orthogonality and smoothness will be continued for the grid cells part by part till they will be under acceptable ranges, but it will be very time consuming processes, which was the case in this particular study.

It can be concluded from the above descriptions the preparing the grid file will affect the overall result of the model and the study itself, so that it should be made very carefully and considering most of the circumstances

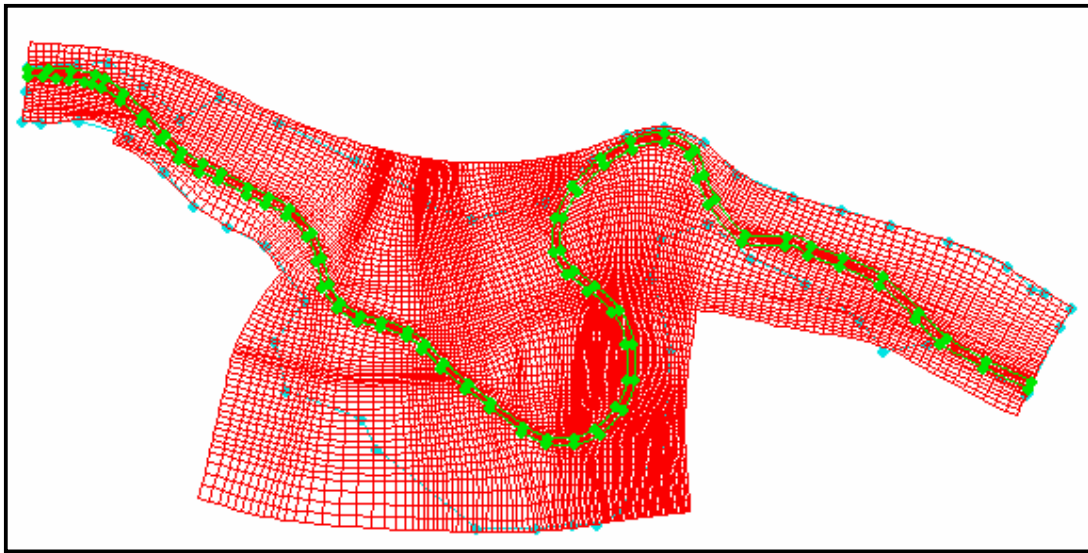


Figure 4.1: Grid schematisation in WAQUA model

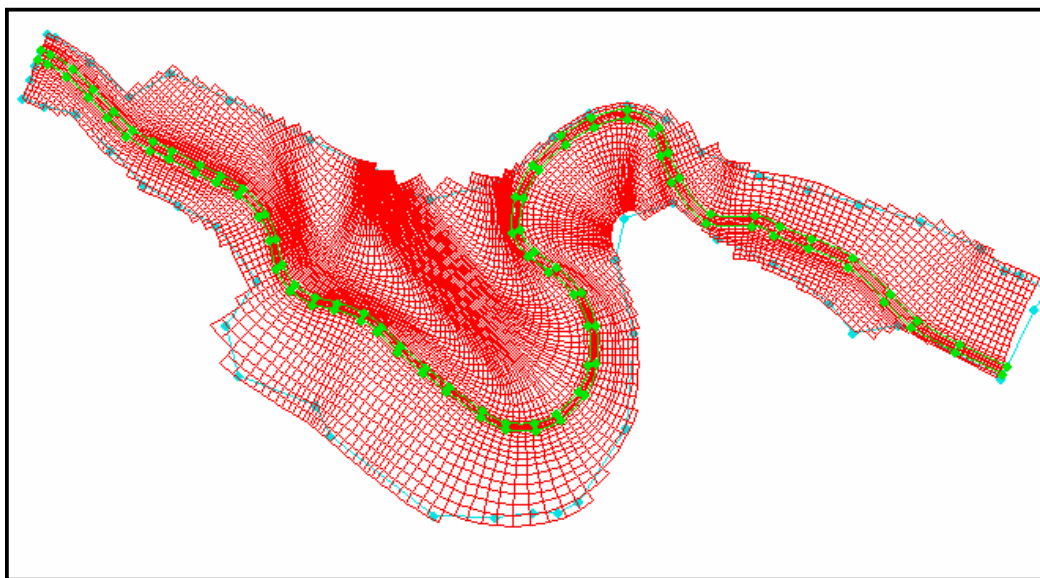


Figure 4.2: Grid schematisation in Delft 2D model

4.2.3 Selection of time step (Δt)

The time step should be selected in such a way that the computation remains stable. Generally, you can choose the time step based on accuracy arguments only, in most cases stability is not an issue. The accuracy is, among several other parameters, such as the reproduction of the important spatial length scales by the numerical grid, dependent on the Courant number (Cr), defined by:

$$Cr = \frac{\Delta t \cdot \sqrt{gh}}{\{\Delta x, \Delta y\}}$$

Where Δt is the time step (in seconds), g is the acceleration due to gravity, h is the (total) water depth, and $\{\Delta x, \Delta y\}$ is a characteristic value (in many cases the minimal value) of the grid spacing in either direction.

Generally, the Courant number should not exceed a value of **ten**, but for problems with rather small variations in both space and time the Courant number can be taken substantially larger.

We can obtain the minimum value of $\{\Delta x$ and $\Delta y\}$ from the grid generation and they are about,

$$\Delta x = 2.12 \text{ m}$$

$$\Delta y = 4.29 \text{ m}$$

If we assume the water depth will be about (0 m) and the acceleration of gravity about 10 N/s^2 , the estimated time step can be calculated from the above equation as below:

$$10 = \frac{\Delta t \cdot \sqrt{10 \cdot 0}}{2.12} \Rightarrow \Delta t \cong 3 \text{ seconds} = 0.05 \text{ minutes}$$

The time step obtained is very small which mostly increases the overall computational time of the model, and the minimum values of the grid cells $\{\Delta x$ and $\Delta y\}$ are not located inside the main channel, but far at the end of the floodplain. For that reason another time step was tested ($\Delta t = 0.1 \text{ min.}$), and the water level, velocity and the secondary currents were checked, as shown in Figures 4.3 – 4.5:

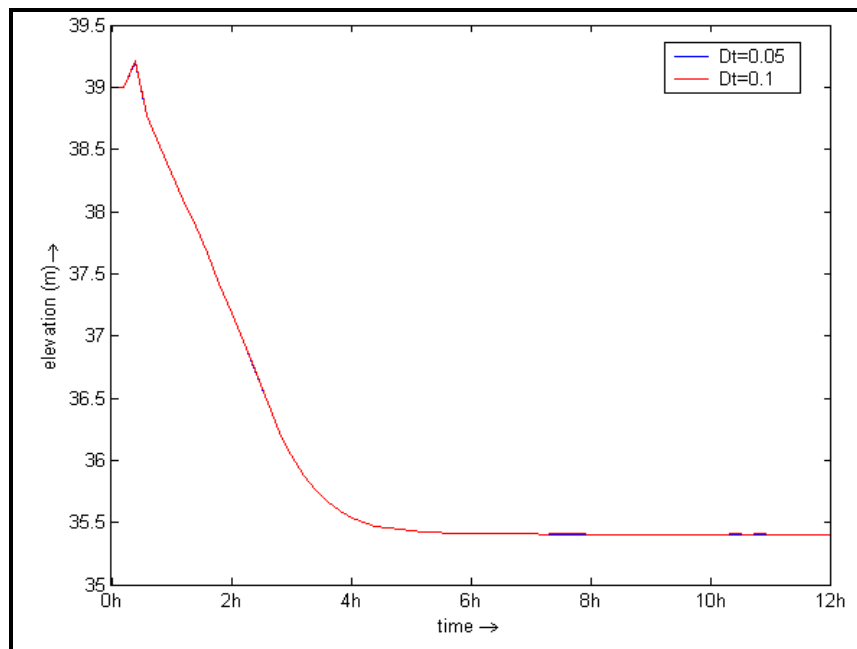


Figure 4.1: Water level for different time steps

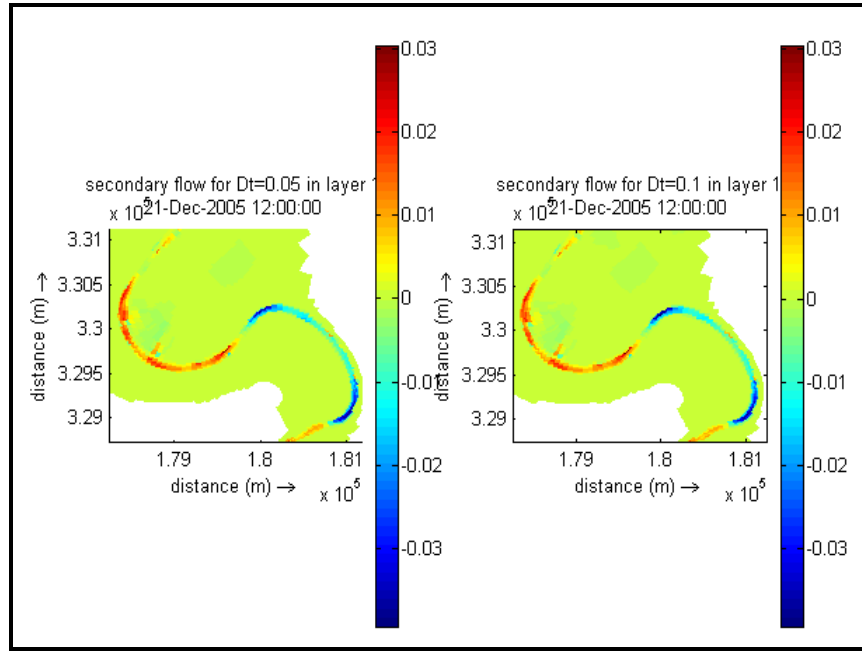


Figure 4.1: Secondary flow intensity for different time steps

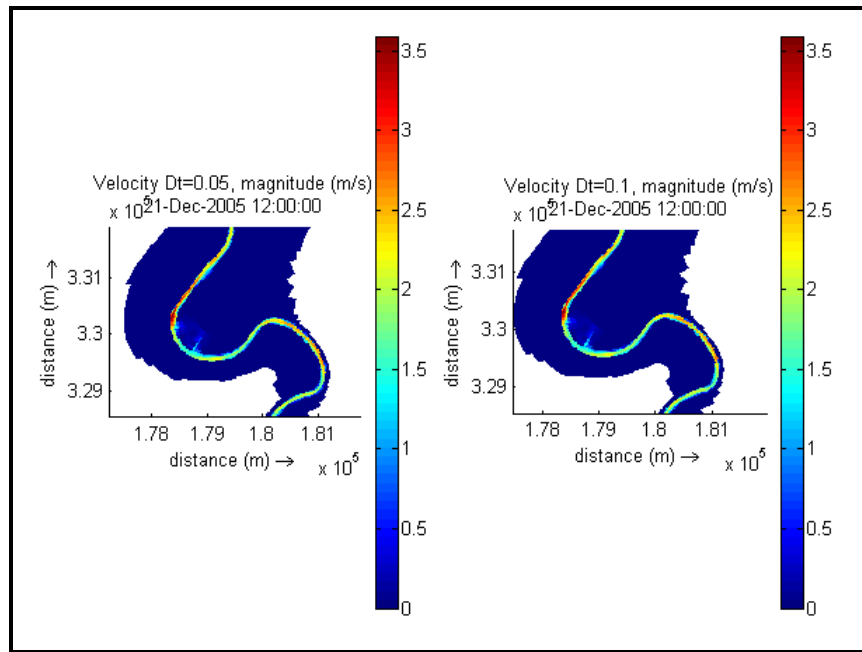


Figure 4.2: Depth averaged velocity for different time steps

From the above results we can conclude that by increasing the time step from 0.05 min to 0.1 min any considerable changes were not noted in the output parameters shown in Figures 4.3 – 4.6. Then it is decided to increase the time step and for other simulations 0.1 min will be used.

Nevertheless, the time step for the morphological computations should be checked also according to the Curren number, and it can be determined with the equation:

$$Cr = \frac{n \cdot s}{h}$$

Where Cr is the Currant number, n is the power of transport formula (ρ), s is the sediment transport rate (m³/s) in two directions (2D modelling is used), and h is the water depth (m).

The value of Currant number can be determined using Delft2D quick plot and the result is as shown in the Figure 4.7 below:

From the Figure 4.7 we can note that the value of currant number is very small and larger time step can be used, but increasing the time step might affect hydrodynamic condition of the model.

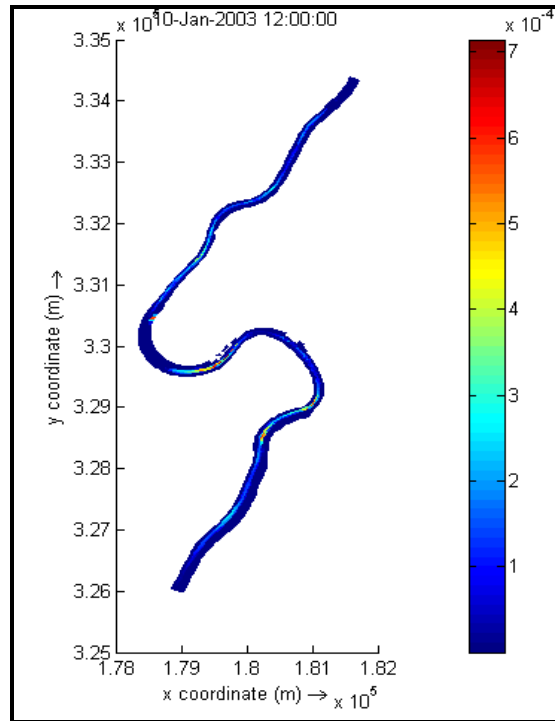


Figure 4.4: Value of Currant number for morphological model

4.2.4 Initial conditions

The initial conditions for the model consist of bed topography (erroneously called bathymetry in Delft2D), water levels, geometric features in the river and floodplain and other inflowing and out-flowing discharges or sediments inside the selected reach.

- **Bed topography**

The bathymetry file should be prepared according to the grid system of the model (Figure 4.2). For this study the bed topography was provided as input data of WAQUA model, based on the grid system of WAQUA. These files had to convert to Delft2D bathymetry input files.

The data provided for different time references of WAQUA were a 1998 schematization and a 2003 schematization. The 1998 schematization was converted to a Delft2D bathymetry file (after some adjustments) and used for the without project situation. The other one (2003) was combined with some measurements for the excavation site and the main channel of 1998, and used for the With project situation. In Figure 4.6 a sample of the bathymetry file is shown which was used for the without project case.

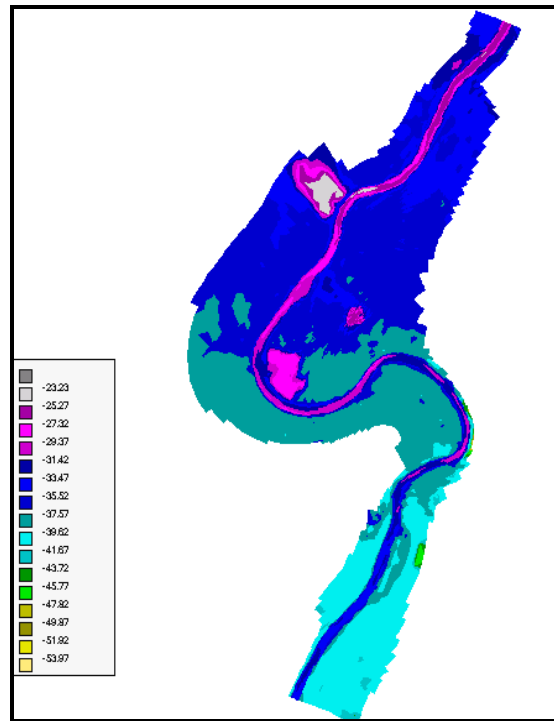


Figure 4.6: Bathymetry of 1998 used in Delft2D model

- **Local weirs, roads and other geometric features inside the floodplain.**

Before doing a hydro-dynamic simulation with Delft2D, it was important to introduce some other geometric features that occur in the floodplain area such as roads, summer dikes, weirs and some sort of protection structures which protect particular areas of the project. The detailed file was prepared for the WAQUA model and could not be used in Delft2D for two reasons: different grid system and different file format. However, with the help of the WAQUA file those which have significant effect on the flow pattern have been determined and a new file of 2D weirs was prepared to be another element of the Delft2D input file.

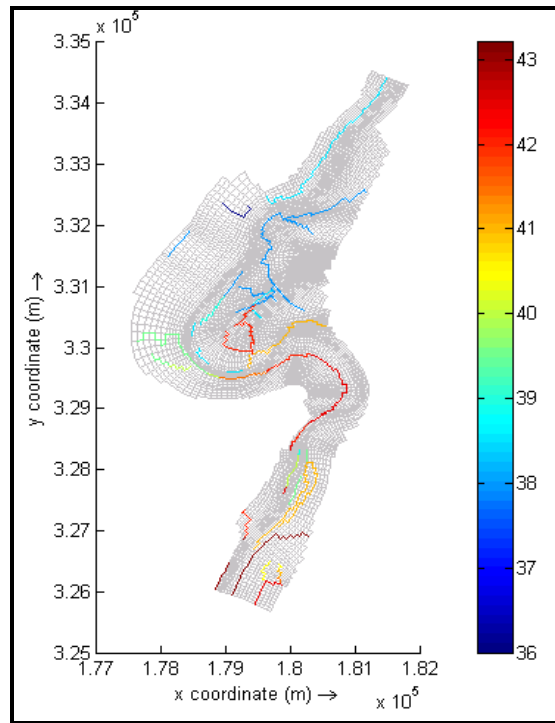


Figure 4.1: 2D weirs schematisation in the floodplain used in Delft 2D model

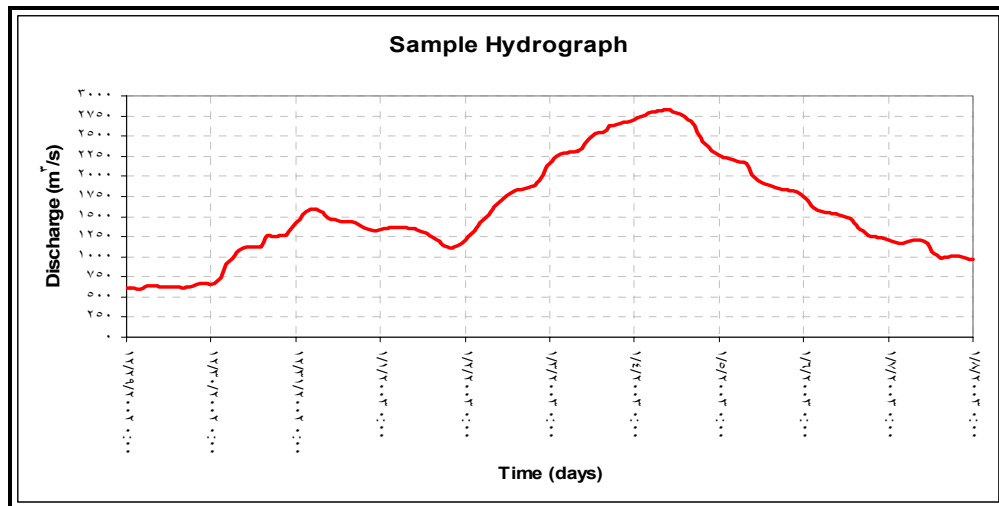


Figure 4.2: Sample hydrograph for upstream boundary condition used in Delft 2D model

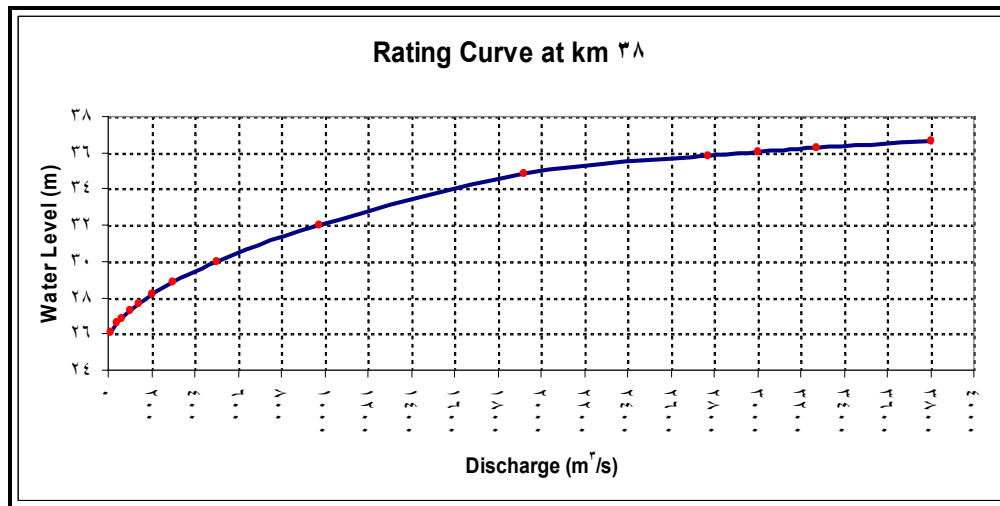


Figure 4.10: Q-H relation (rating curve) at km 38 for downstream boundary condition used in Delft2D model

Fixing the bed level (constant bed level) of the upstream boundary, was the choice of indicating the inflow sediment to the model, with this condition the model able to introduce any sediment that will be eroded at the first cell after the boundary, and the same amount of sediment will entered to the model.

From the data given in chapter 3 for the grain size distribution, provided three layers (top layer and sub layers 1 & 2). All layers were defined in the model, and the grain sizes were divided over 5 different fractions starting from 0.2 mm diameter to 110 mm diameter as shown in tables 4.11:

Sediment Fractions	% of Top layer	% of Sub-layer 1	% of Sub-layer 2
0.2-3.0 mm	0	21	10
3.0-8.0 mm	0	10	11
8.0-22.0 mm	22	19	29
22.0-42.0 mm	40	26	31
42.0-110.0 mm	38	24	19
Total	100	100	100

Table 4.11: Sediment fractions and their relative occurrence for the different layers used in Delft2D

4.2.5 Roughness files (Chézy coefficient)

With the WAQUA schematization a detailed roughness file was provided for the whole area, but because the grid system distribution was changed, it was not possible to use it in Delft2D. Nevertheless, creating such detailed file for the main channel and the floodplain is not impossible but it is very difficult in a short period of time. Because of that with the help of the WAQUA input file a constant Chézy coefficient was selected for the main channel ($40 \text{ m}^{1/3}/\text{s}$) and another one for the floodplain ($36 \text{ m}^{1/3}/\text{s}$), as shown in the Figure 4.10:

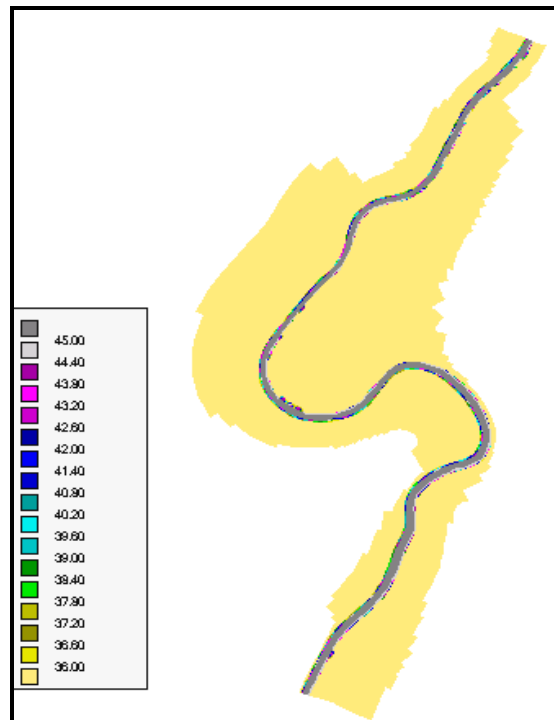


Figure 4.11: Roughness schematisation (based on Chézy coefficient) used in Delft 2D model

4.2.6 Observation points and cross-sections

The observation points and cross-sections are required in the model setup for the purpose of monitoring and storing historical results in particular locations and interest points. The prepared and used points and cross-sections are shown in Figure 4.12:

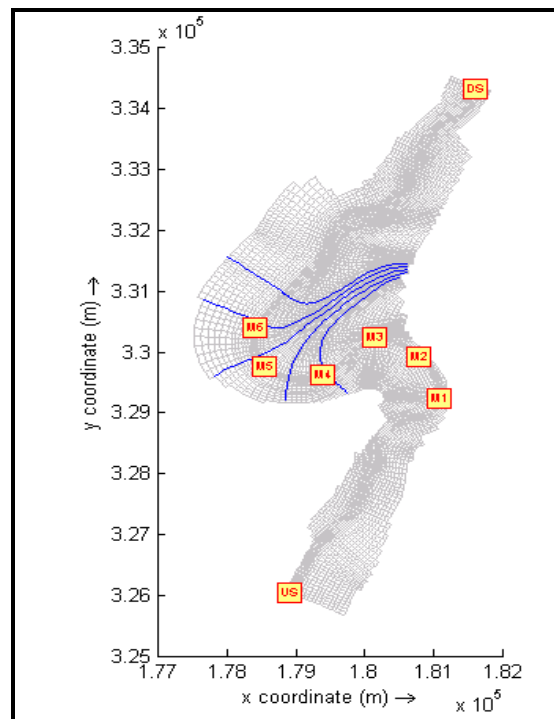


Figure 4.12: Observation points and cross-sections used in Delft 2D model

Finally by collecting all these files and conditions and defining them in Delft2D along with some other aspects which can be used in the user interface, the first setup of the model was finished. It can be checked, calibrated or verified in the next step. But before that it is important to know what type of equations (in general) has been implemented in Delft2D (see chapter 2).

• Model Calibration and Verification

•.1. Introduction

The aim of the calibration is to obtain a model that is representative for the Meuse River and properly reflects the hydraulic and morphological phenomena in the river.

Several parameters are available to influence the morphological processes calculated by a model. The amount of coefficients and the nature of them depend on the sediment formulas used.

An ideal morphological model should be calibrated for different conditions such as flow (hydrodynamic of the model), transport formula and morphological parameters that have effect directly on the changes.

Flow or hydrodynamic calibration is should be done with different values of roughness coefficient, either in the main channel and the flood plain, because in reality the roughness of the surface is differ from point to another, and the best solution is to prepare the roughness coefficient for the grid generation of the model i.e. for each grid cells introduce roughness coefficient.

Calibration for the transport formula is can be done by calibrating different parameters of the formula, for example if Meyer–Peter–Muller (MPM) formula is used, normally the calibration will be done for:

Overall calibration factor (TRF): with this factor the transport rate quantities can be controlled between the measured and computed one. This factor will affect the direct change of the sediment transport magnitude. This has effect on the time-scale of morphological development.

Critical Shields parameter θ_{cr} : determines the hydraulic conditions at which sediment is entrained. A lower critical Shields value will increase the total sediment transport.

Ripple factor μ : represents the percentage of the total shear stress that is the result of particle roughness. The additional roughness is caused by bed forms (dunes). The relative contribution of the particles to the total roughness decreases as the dunes get larger. A smaller ripple factor will lead to less sediment transport and smaller morphological changes.

Morphological parameters include all of the parameters that contribute in the morphological changes in both time and space scales, the most important parameters that should be calibrated are:

Effective layer thickness δ_{eff} : this factor influences the arte at which the river bed adjusted to the condition on the river. Therefore, it also influences the rate at which morphological changes move further down stream. A thin layer will be able to coarsen much faster than a thick layer. This difference in time influences the magnitude of the morphological effects.

Morphological factor (MORFAC): this factor either by speeding up the morphological changes, or by affecting the hydrodynamic condition of the model (distorting the hydrodynamics) will influence the morphological changes.

In this particular study the calibration was not carried out for the transport formula (Meyer – Peter – Muller), because this formula is already calibrated with graded sediment for the Meuse River, and it seems that this formula gives a quantity of sediment transport which is twice the measured one. This means the overall calibration factor is $\cdot 2$.

Unfortunately the thickness of the transport layer (active layer) also was not calibrated because of the time limitation and it was estimated to be more-less equal to the top-layer of bed composition which is about 0.20 m. The thickness of this layer influences the rate at which the river bed adjusts to the condition in the rivers. Therefore, it also influences the rate at which morphological changes move further downstream. A thin layer will be able to coarsen much faster than a thick layer. This difference in time influences the magnitude of the morphological effects (Berkhout, 2003).

Mr Di Silvio and Mr Peviani described a formula for determining the thickness of transport layer in mountain rivers in Italy which mostly likely to be gravel bed rivers as shown in below:

$$\delta = \gamma * d_a$$

where δ = is the thickness of transport layer . This equation related the transport layer thickness to the d_a of the armour layer.

3.1. Effect of main channel roughness on the water level (Chézy coefficient)

For the purpose of determining the effect of the Chézy coefficient on the water level and flow pattern another simulation was made by changing the value of the Chézy coefficient of the main channel from 40 m^{1/2}/s to 47 m^{1/2}/s, and by fixing the value of Chézy coefficient of the floodplain to be 36 m^{1/2}/s, the result is shown in Figure 3.1:

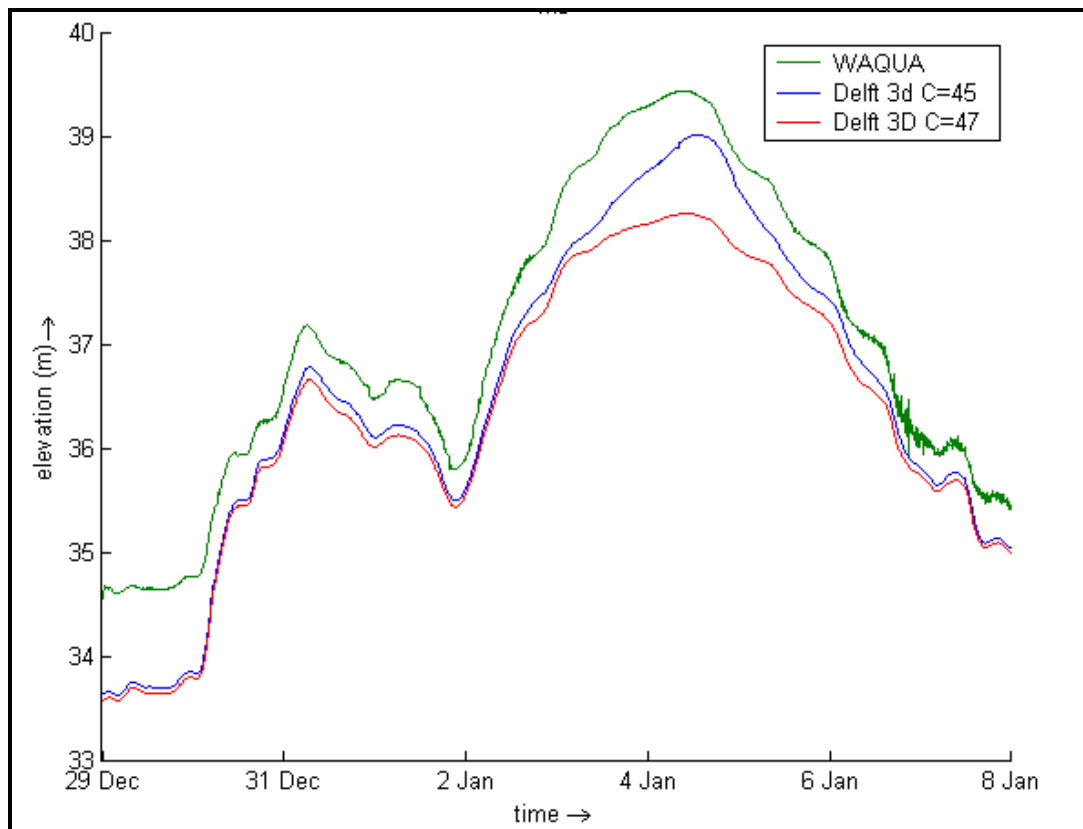


Figure 3.1: Effect of Chézy value on water level

From this Figure we can conclude that the Chézy coefficient has a significant effect on the water level at peak flow. It lowered water level more than 0.5m at peak flood, whereas only slight changes appeared for the rest.

2.3. Model verification (hydrodynamic)

After the model setup, it is important to make some sort of calibration and verification; if the field measurements or lab measurements are available the calibration test of the model should be made for determining different factors and parameters to be put into the model for later use.

In this particular study only some verification tests were made for the model because the output file of another package (WAQUA) was available (calibrated for water levels in the river and the floodplain). We had to compare the Delft2D flow condition with it, and to play with some parameters for improving the flow condition to be the same or close to that of the WAQUA model. Nevertheless, some sort of sensitivity analysis was made by altering some parameters and significant changes of the output were noticed.

The first verification was made for the water level in the river by comparing the result of the Delft2D and WAQUA models. Delft2D has several options to define input files, for example as shown in the Figure 2.2, in numerical parameter menu it is possible to calculate the bed levels at water level points by interpolating the values at the corner of each grid cells or direct calculating at the middle of the grid cells (the option **from depth point**).

Usually in Delft2D the depth file is defined in the model by taking the values at the grid cell corners and the water level is usually computed at the centre of the cells. It can be noted from the Figure that there are several options for interpolating the depth at each grid cell such as max., mean, min., and from depth point. The first three options use interpolation between the values and the last option takes the computation at the point of depth.

Max means that the interpolation will take the maximum value between the points, which gives an over estimation of the conveyance capacity of the main channel and will lead to an underestimation of the water level in the river, whereas, min means vice versa i.e. it takes the minimum value and it will give an underestimation of the conveyance capacity of the main channel and high water level. The mean is the average of them and will be somewhere in between max and min.

From the explanatory Figures 2.3-2.6, if the dashed lines be the simple cross section defined in the model, and the solid lines be the cross-sections interpolated between the points, the definition of max, min, and mean will be as below:-

Figure 2.4 is representing interpolation between points by taking the maximum value (selecting max) and it can be noted that the cross section is larger than the original one (dash line), whereas the interpolation by taking the minimum value (selecting min) will reduce the cross-section of the river as shown in Figure 2.5. However averaging them will produce a better choice where the cross-section is more close to the defined one (selecting mean) as shown in Figure 2.6.

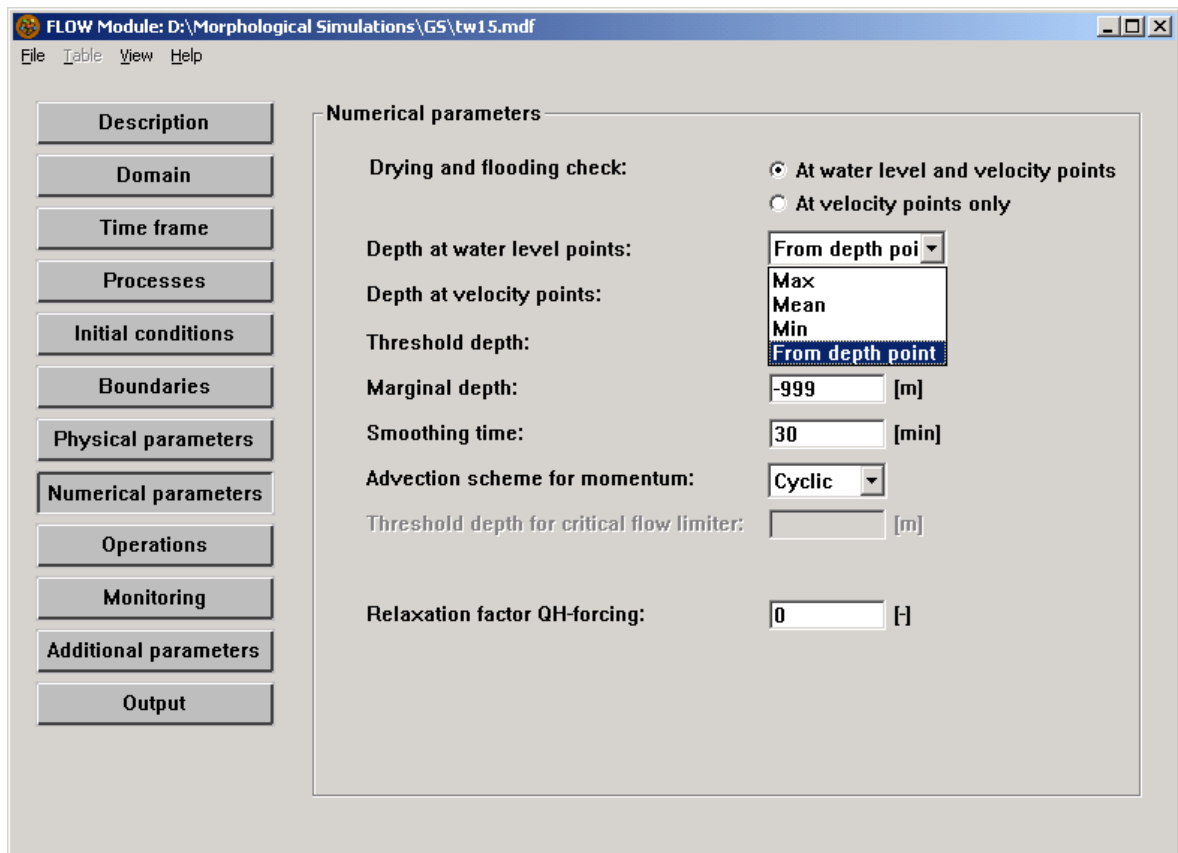


Figure 3.1: defining input files in to Delft 2D

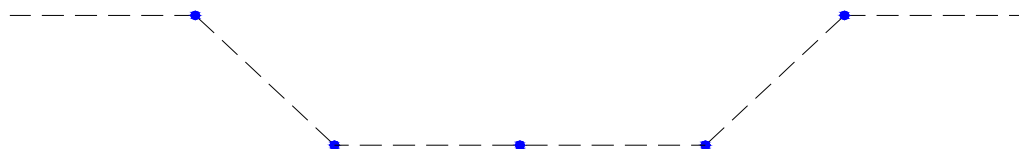


Figure 3.2: Simple schematisation of river section



Figure 3.4: cross-section in case of selecting max

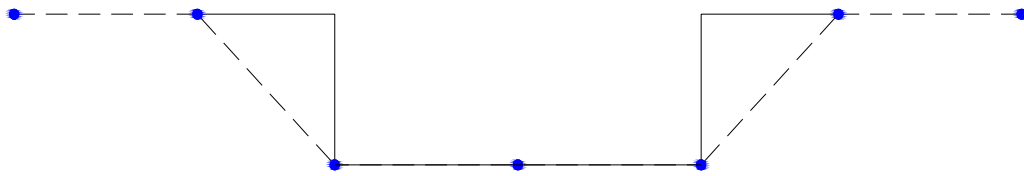


Figure 2.2: cross-section in case of selecting min

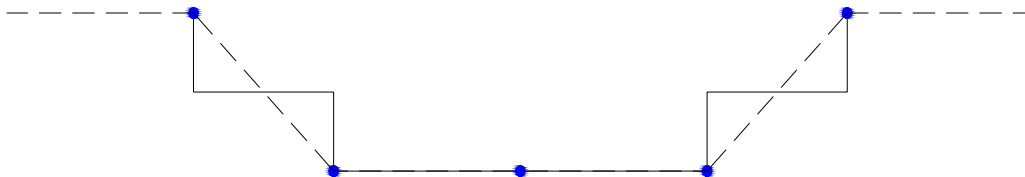


Figure 2.3: cross-section in case of selecting mean

The sensitivity analysis was made for verifying the water levels in Delft 2D by comparing them to those in WAQUA. The result is shown 2.4:-

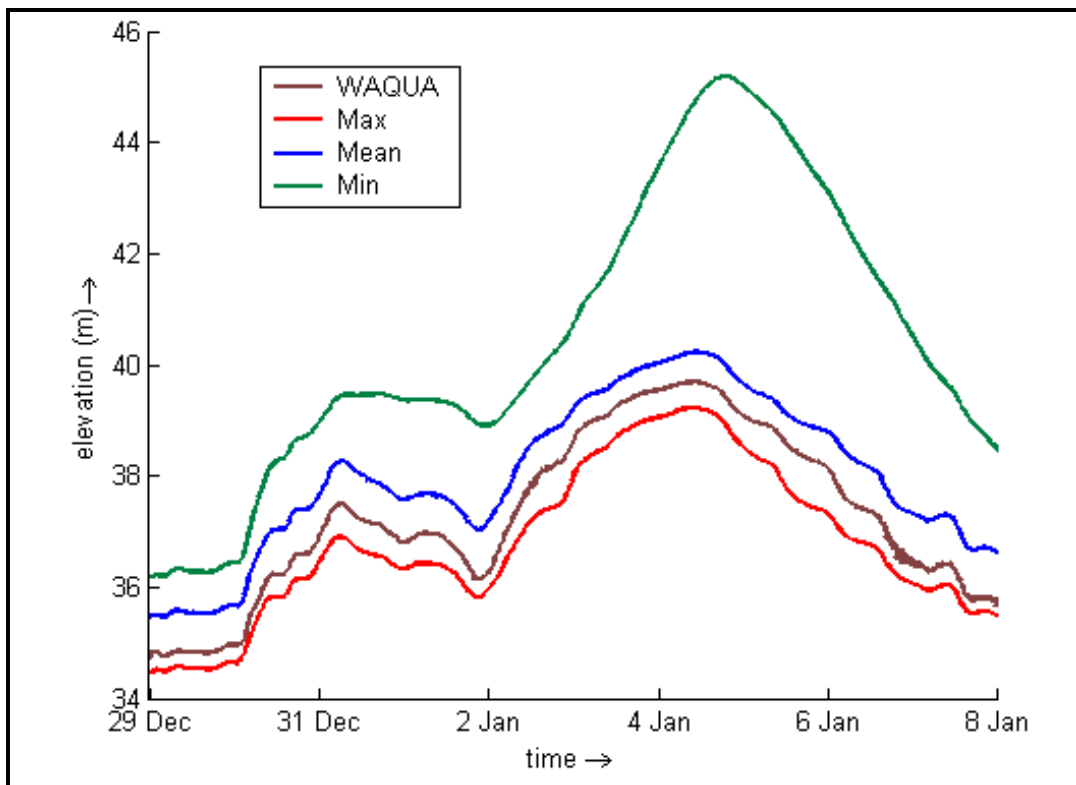


Figure 2.4: Sensitivity analysis for water level in Delft 2D

It can be noted from Figure 2.4 that in the case of selecting **Min**, as explained before, the conveyance capacity of the main channel is underestimated and we can note a rapid increase in water level especially under peak flow conditions.

The water level in the **WAQUA** model seems to be between the cases of **Max** and **Mean**.

For making the water level condition in Delft3D to be more close to the condition in WAQUA, we took the **average** of **Max** and **Mean** by converting the output file of each of them to the input file and creating a new depth file for the model. The result is shown in Figure 9.1:

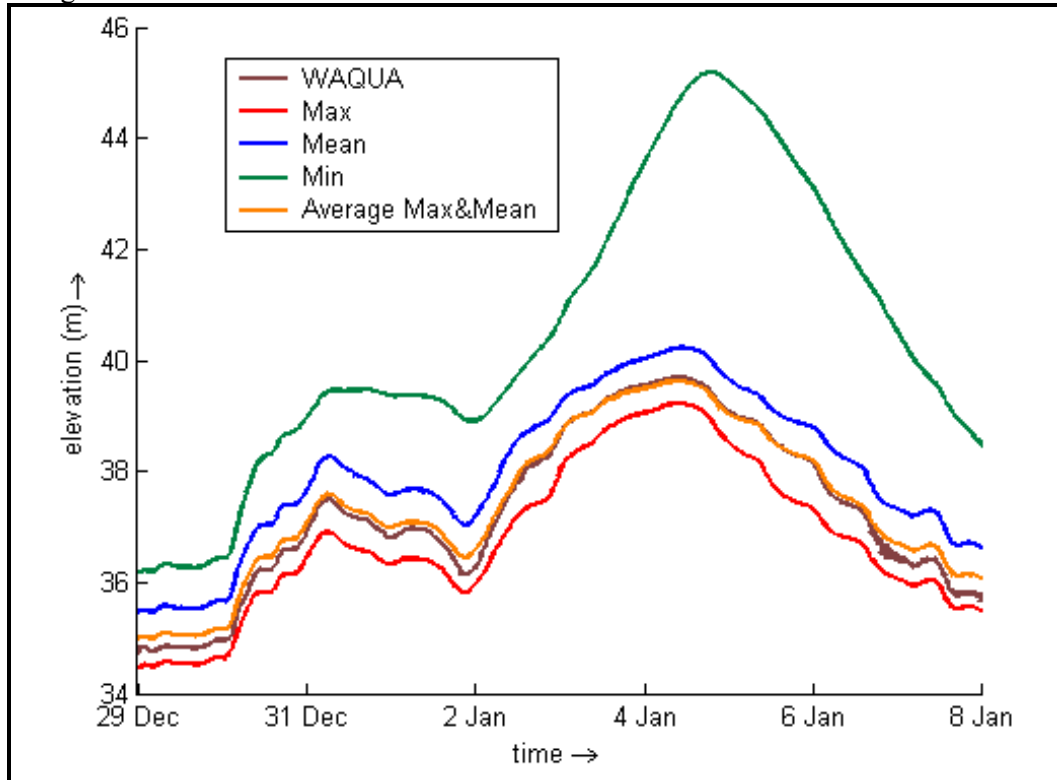


Figure 9.1: Verification of water level in Delft 3D

We can see easily from the Figure 9.1 that the new line which represents the average value of **Mean** and **Max** is more close to the condition in the WAQUA model. And here the verification for the hydrodynamic flow condition can be stopped to start with the next and important part of the modelling for this study, which is the morphological computation with graded sediment.

9.4. Selection of morphological factor (MORFAC)

9.4.1 Introduction

One of the complications inherent in carrying out morphological projections on the basis of hydrodynamic flows is that morphological developments take place on a time scale several times longer than typical flow changes (for example, tidal flows change significantly in a period of hours, whereas the morphology of a coastline will usually take weeks, months, or years to change significantly). One technique for approaching

this problem is to use a “morphological time scale factor” whereby the speed of the changes in the morphology is scaled up to a rate that it begins to have a significant impact on the hydrodynamic flows.

This can be achieved by specifying a non-unity value for the variable MORFAC in the morphology input file.

The implementation of the morphological time scale factor is achieved by simply multiplying the erosion and deposition fluxes from the bed to the flow and vice-versa by the MORFAC-factor, at each computational time-step. This allows accelerated bed-level changes to be incorporated dynamically into the hydrodynamic flow calculations.

While the maximum morphological time scale factor that can be included in a morphodynamic model without affecting the accuracy of the model will depend on the particular situation being modelled, and will remain a matter of judgement, tests have shown that the computations remain stable in moderately morphologically active situations even with MORFAC-factors in excess of 1000. We also note that setting MORFAC = 1 is often a convenient method of preventing both the flow depth and the quantity of sediment available at the bottom from updating, if an investigation of a steady state solution is required (Delft 2D flow manual, 2009).

Some test case simulations were made for both without project and with project by selecting a 10 days hydrograph from the 2002 – 2003 hydrograph. Different morphological factors were used with original and squeezed hydrographs as explained below:

5.4.2 Hydrodynamic and morphological time of 10 days (10 days hydrograph and morphological factor 1)

In this case the hydrodynamic and morphological updating is as under normal real conditions without speeding up the morphological changes in the bed topography of the river.

As explained in chapters 1 & 3, the Meuse River is the only gravel bed river in the Netherlands, and the armouring phenomena are present in the gravel bed reach, where the particle sizes were relatively coarse at the top layer and paved the river bed. During most period of the year this pavement remains stable till the peak will come and induce large shear force on the bed material. Sometimes this armoured layer will break down and the bed material will be entrained by the flow.

In order to study these phenomena, as a first trial the peak flood hydrograph of 2002-2003 was used in most of the simulation, because we want to have insight into the changes will happen due to this flood.

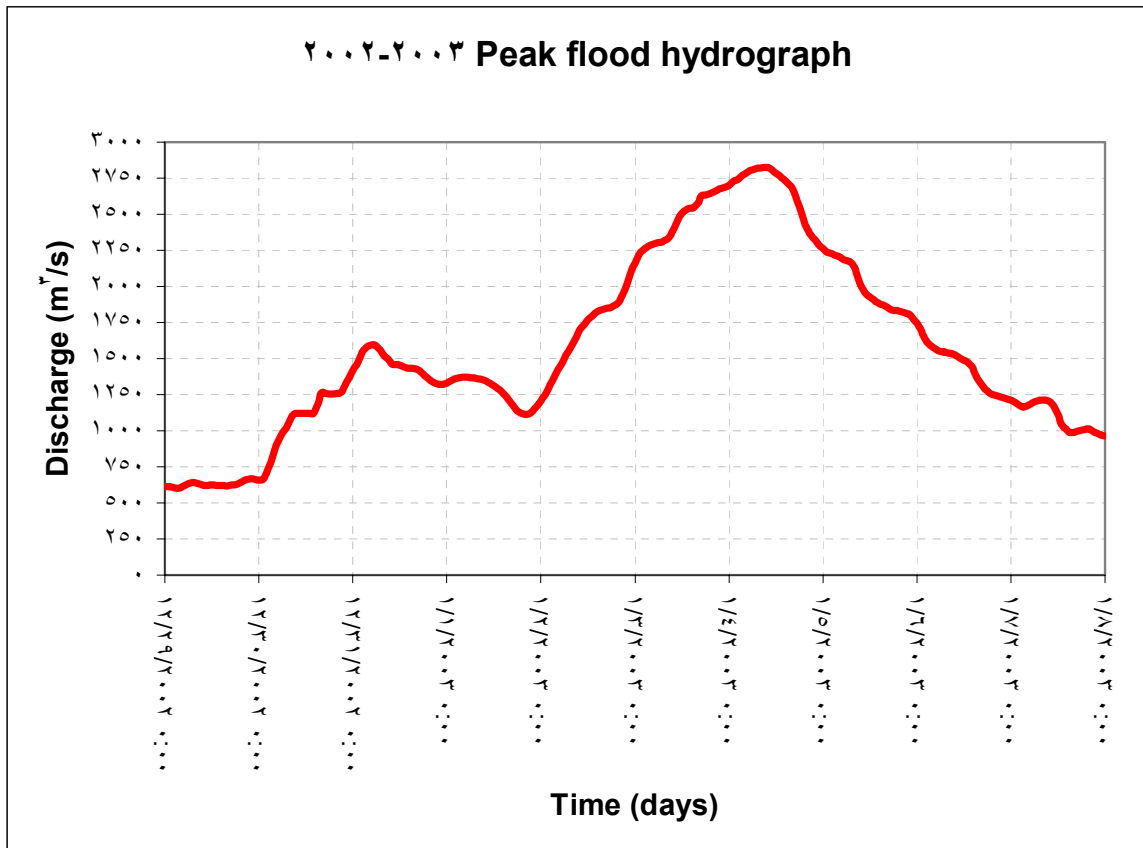


Figure 0.9: Normal peak hydrograph of 2002-2003 floods.

After entering all required information and defining data to the model, the morphological computations were started and some results were obtained as shown in Figures 0.10 – 0.11:

In Figures 0.10 – 0.11 the dark red is maximum sedimentation and dark blue is maximum erosion.

In Figure 0.10 the cumulative erosion and deposition is shown for indicating and determining what was the possible effect of the 2002-2003 peak flood if the project was not implemented in this location (Meers), it can be seen that there are no changes in the floodplain far from the main channel, but also it is not clear for the part of the floodplain near to the main channel.

If the main channel and a part of the floodplain are zoomed as shown in Figure 0.11 the difference will be more clear.

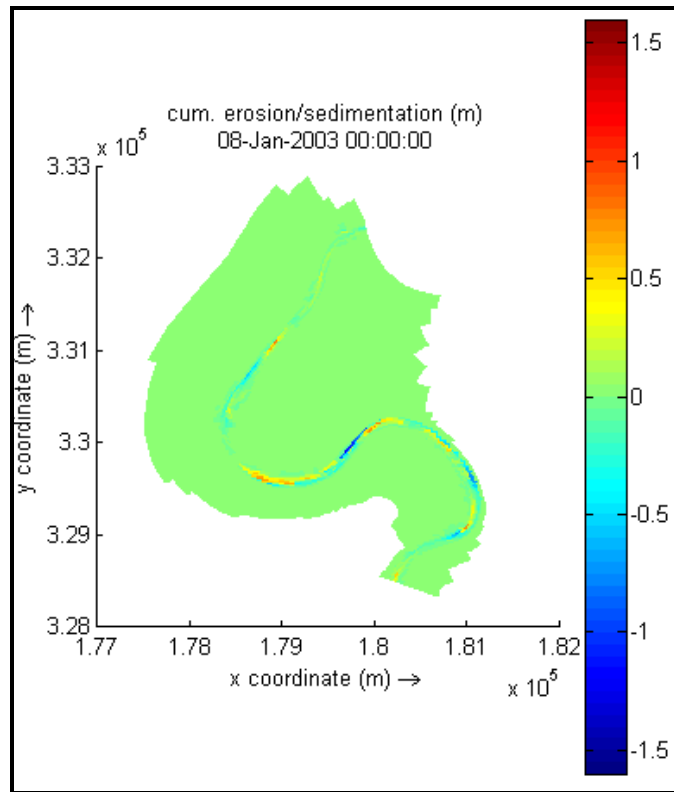


Figure 9.10: Cumulative erosion and deposition for 10 days hydrograph and morph. factor 1.

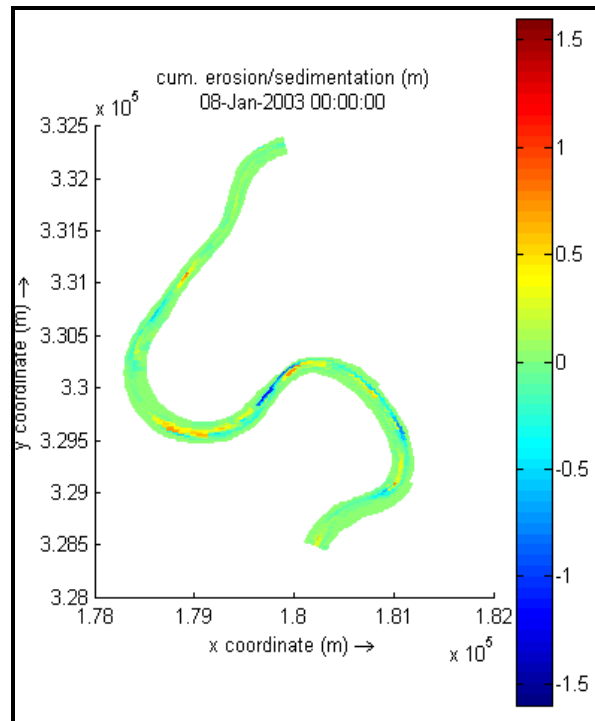


Figure 9.11: Cumulative erosion and deposition in the main channel for 10 days hydrograph and morph. factor 1.

It can be concluded from the Figures 0.10 – 0.11 that also if the project is not implemented some sedimentation and erosion was possible due to the effect of this flood peak hydrograph.

0.4.3 Hydrodynamic time of 2.0 days and morphological time of 1.0 days (2.0 days hydrograph and morphological factor ξ)

The inflow hydrograph used in section (0.4.2) is squeezed by a factor of ξ . This is done by dividing each discharge duration in the normal hydrograph by a factor ξ , this was for reducing the computational time of the model. And the morphological changes were multiplied by a factor ξ also, thus for speeding up the morphological changes with shorter duration hydrograph to 1.0 days morphology.

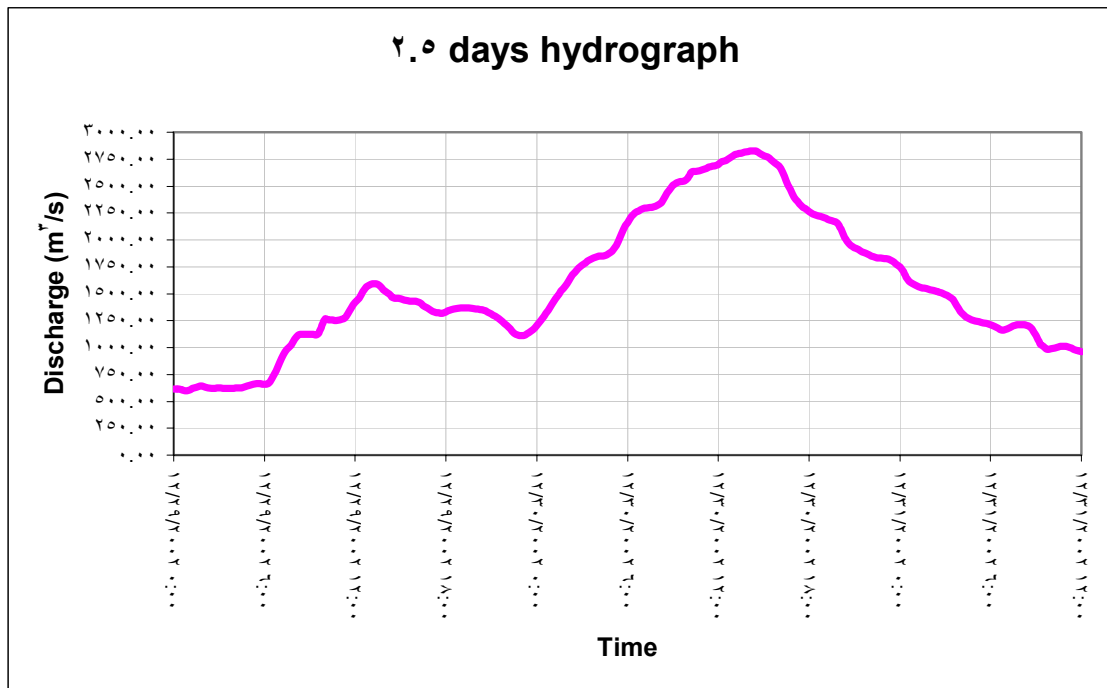


Figure 0.12: Squeezed hydrograph of 2.0-2.0 floods by factor ξ .

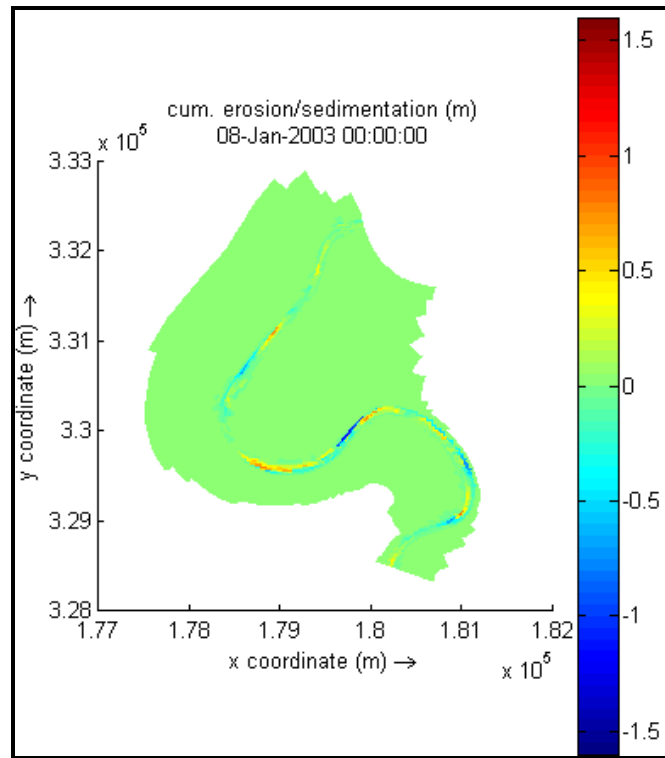


Figure 9.13: Cumulative erosion and deposition for 2.0 days hydrograph and morph. factor 4.

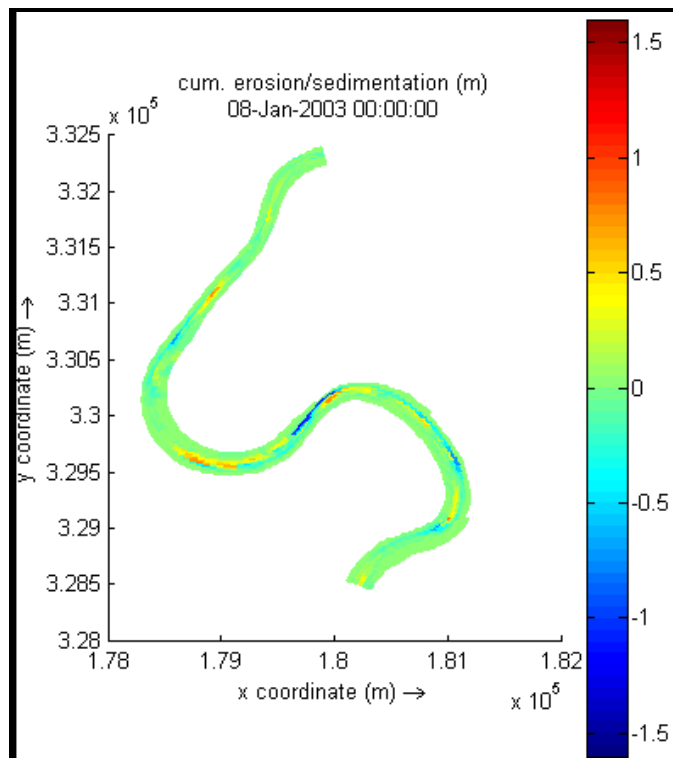


Figure 9.14: Cumulative erosion and deposition in the main channel for 2.0 days hydrograph and morph. factor 4.

If we note to the Figures 0.13 – 0.14, the erosion and sedimentation pattern is mostly the same as of the previous case. It might be there is some difference in magnitude but it cannot be identified here, and it will be more clear when the comparison will be carried out for the different cases.

0.4.4 Hydrodynamic time of 1.20 days and morphological time of 10 days (1.20 days hydrograph and morphological factor λ)

The inflow hydrograph used in section (0.4.2) is squeezed by a factor of λ . This is done by dividing each discharge duration in the normal hydrograph by a factor λ , this was for reducing the computational time of the model. And the morphological changes were multiplied by a factor λ also, for speeding up the morphological changes with a shorter duration hydrograph to 10 days morphology.

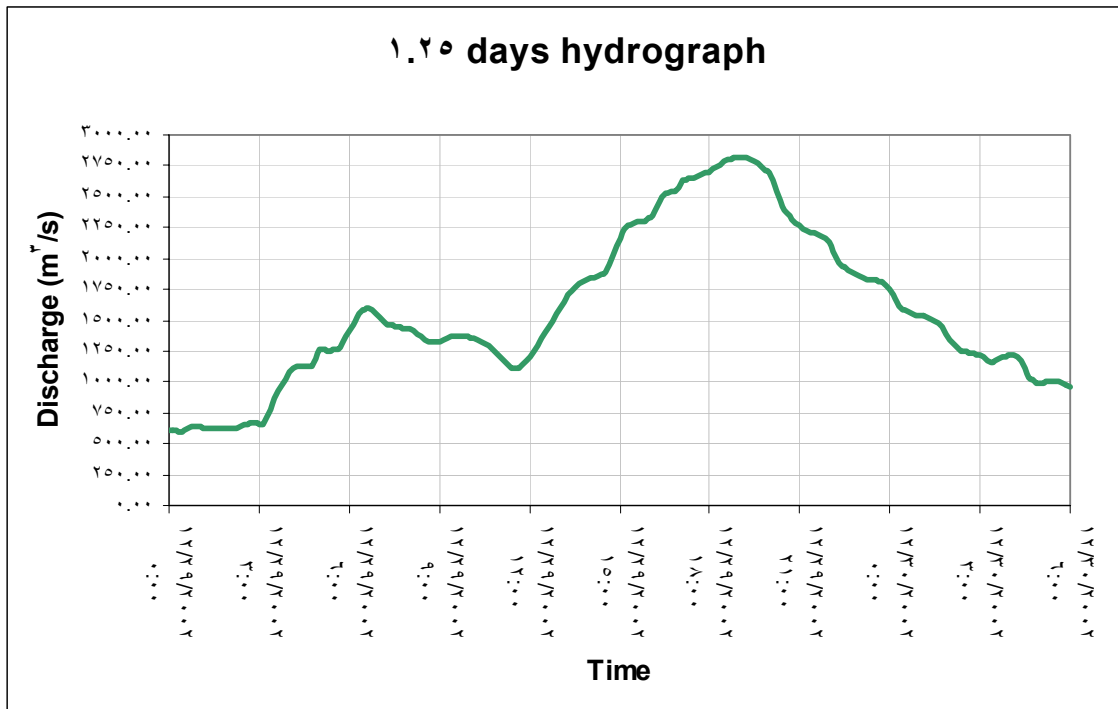


Figure 0.10: Squeezed hydrograph of 2002-2003 floods by factor λ .

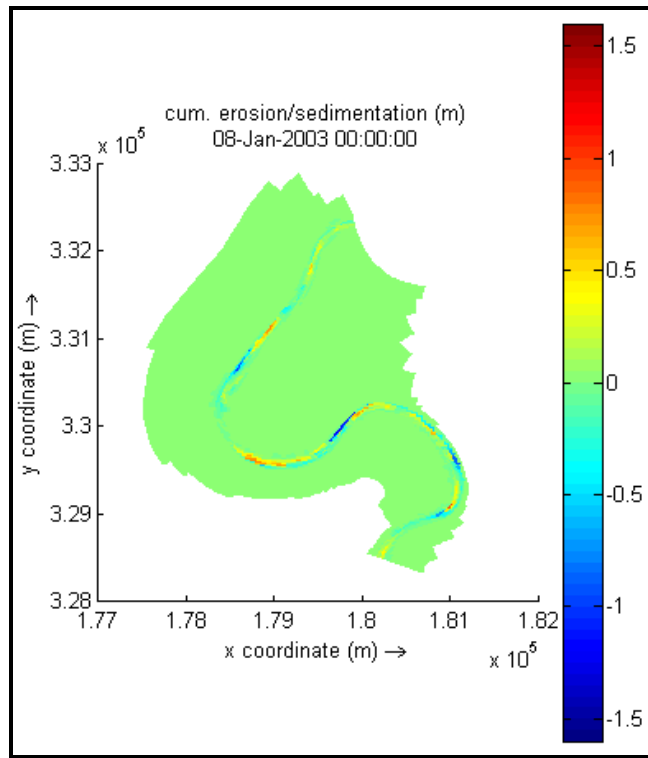


Figure 9.16: Cumulative erosion & deposition for 1.20 days hydrograph and morph. factor 1.

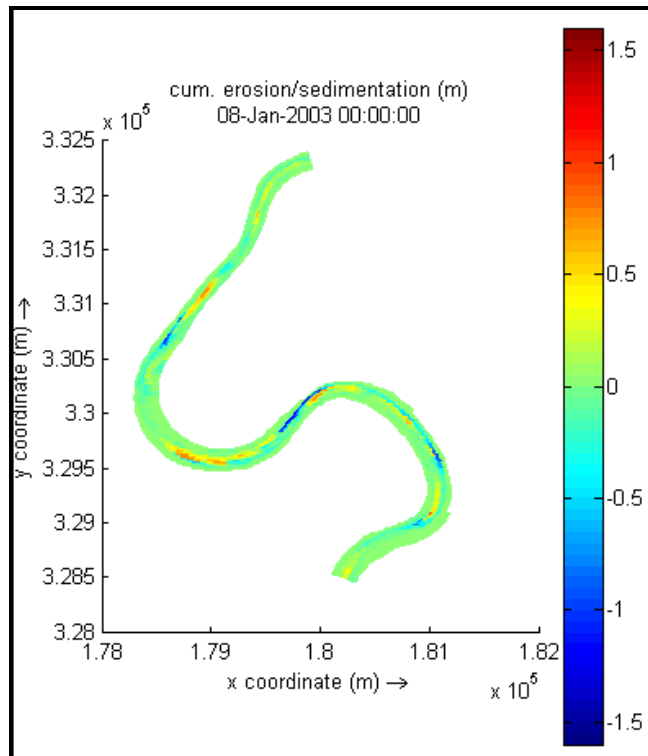


Figure 9.17: Cumulative erosion and deposition in the main channel for 1.20 days hydrograph and morph. factor 1.

Also in this case the same pattern is repeated in terms of cumulative erosion and deposition but still the effect of hydrograph squeezing and using different morphological factors is not clear for this short morphological change time which is equal for all cases (10 days morphological time for all three cases).

If the above three hydrographs are drawn together the difference between them can be easily noted. In order to study the effect of the hydrograph squeezing and the morphological factor, some comparisons were made and the result is as shown in Figures 0.19 – 0.27.

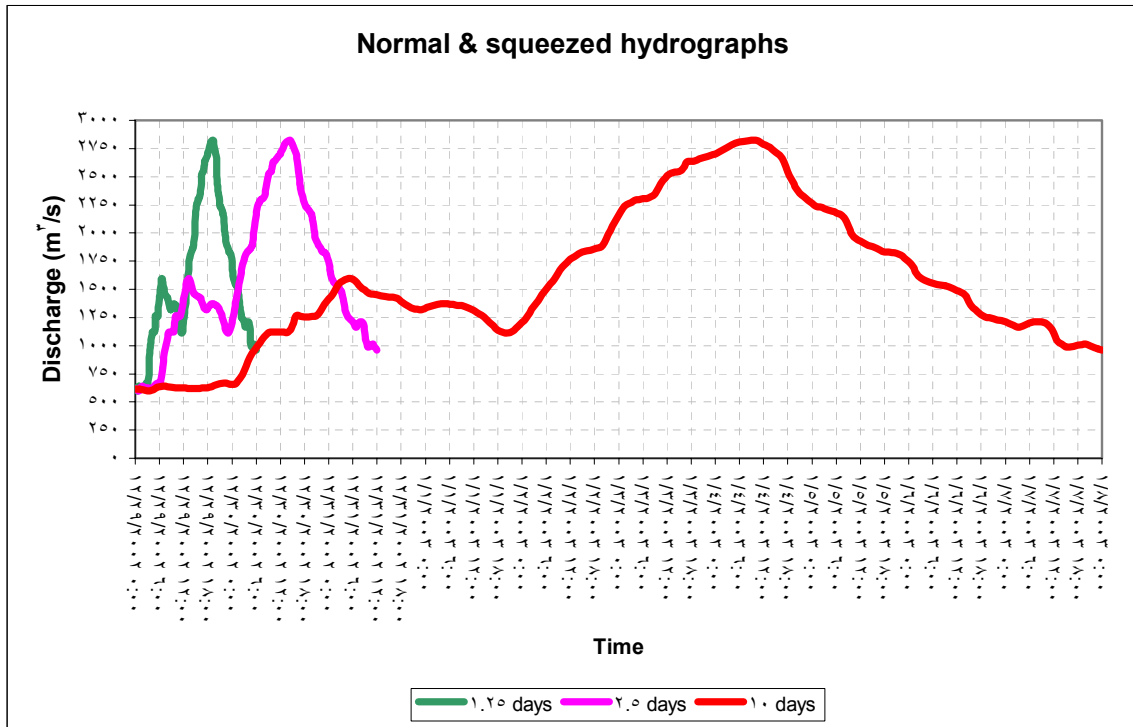


Figure 0.18: Normal and squeezed hydrograph of 2002-2003 floods.

From Figure 0.18 the difference between the hydrographs easily and clearly can be noted, but the consequences of this squeezing (reduction in computational time) is shown in Figures 0.19 – 0.27:

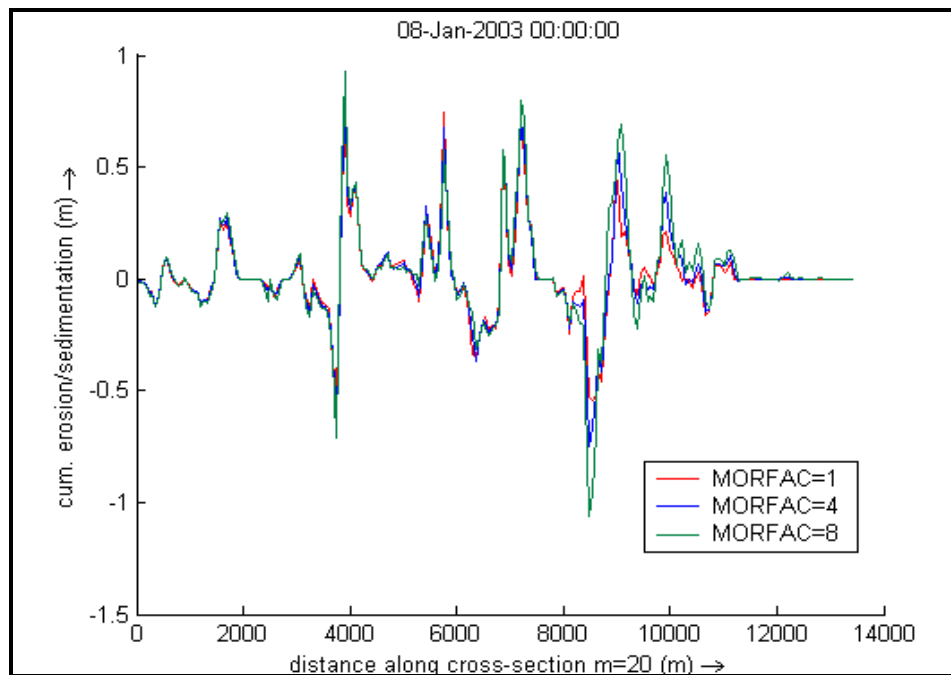


Figure 0.19: Cumulative erosion and sedimentation along longitudinal profile first line from the left bank (zero value is located at km 24.0 of the river).

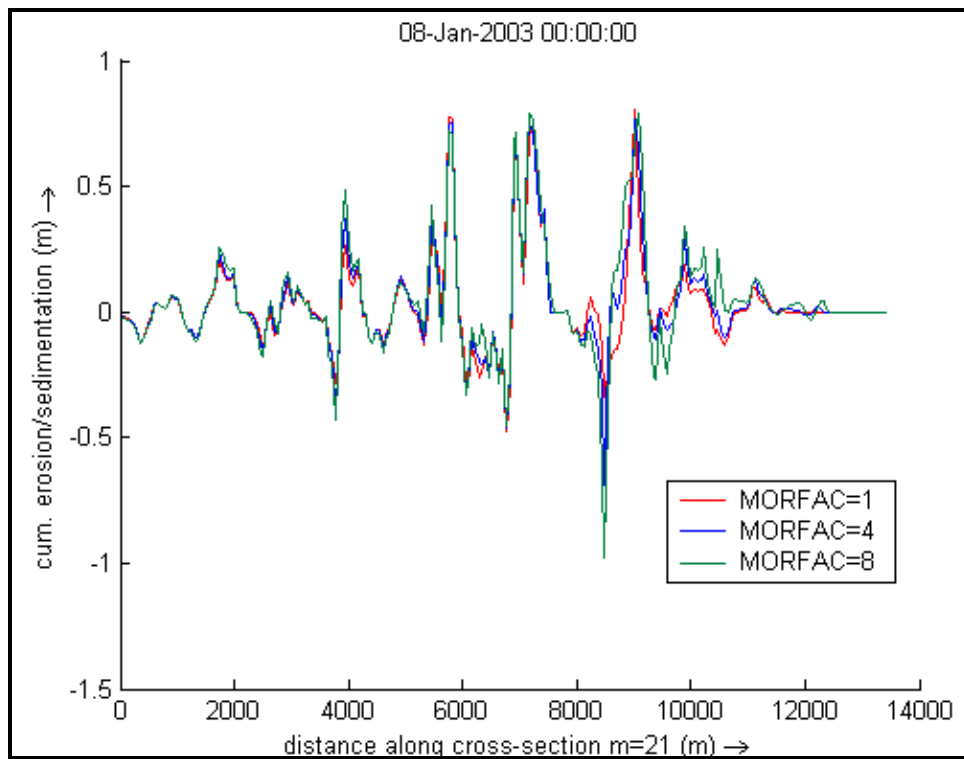


Figure 0.20: Cumulative erosion and sedimentation along longitudinal profile second line from the left bank (zero value is located at km 24.0 of the river).

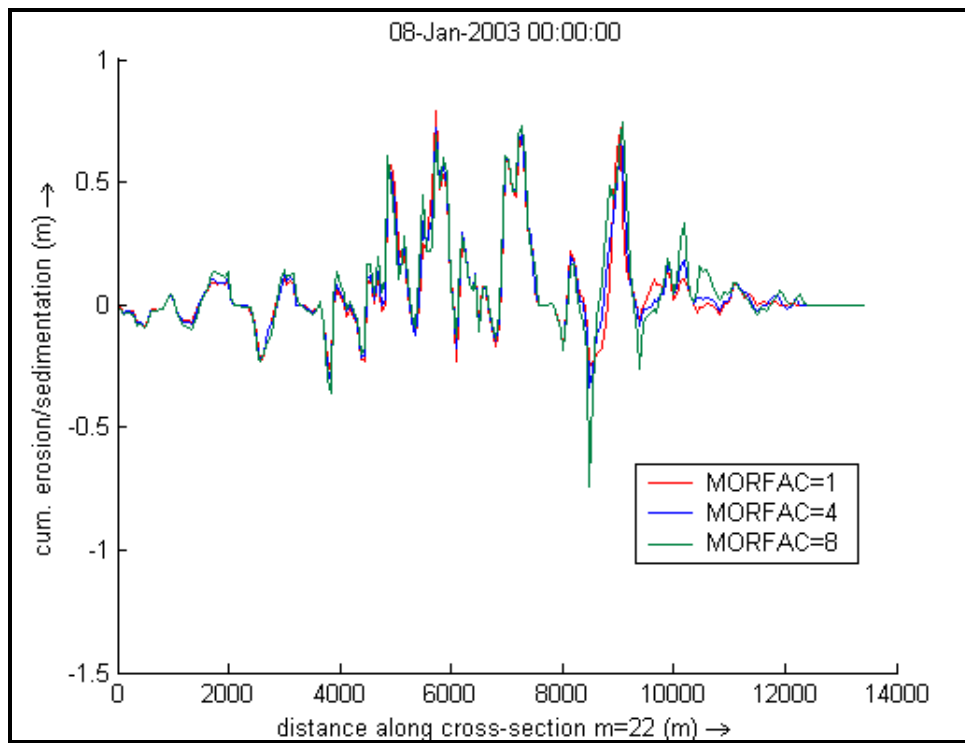


Figure 9.21: Cumulative erosion and sedimentation along longitudinal profile third line from the left bank (zero value is located at km 24.0 of the river).

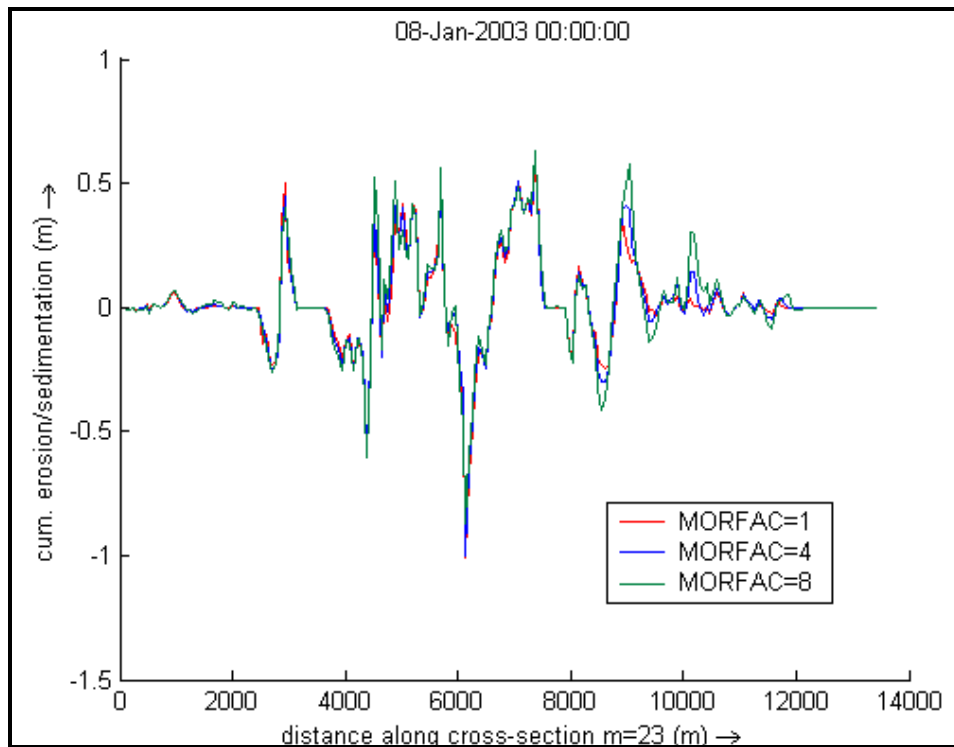


Figure 9.22: Cumulative erosion and sedimentation along longitudinal profile fourth line from the left bank (zero value is located at km 24.0 of the river)..

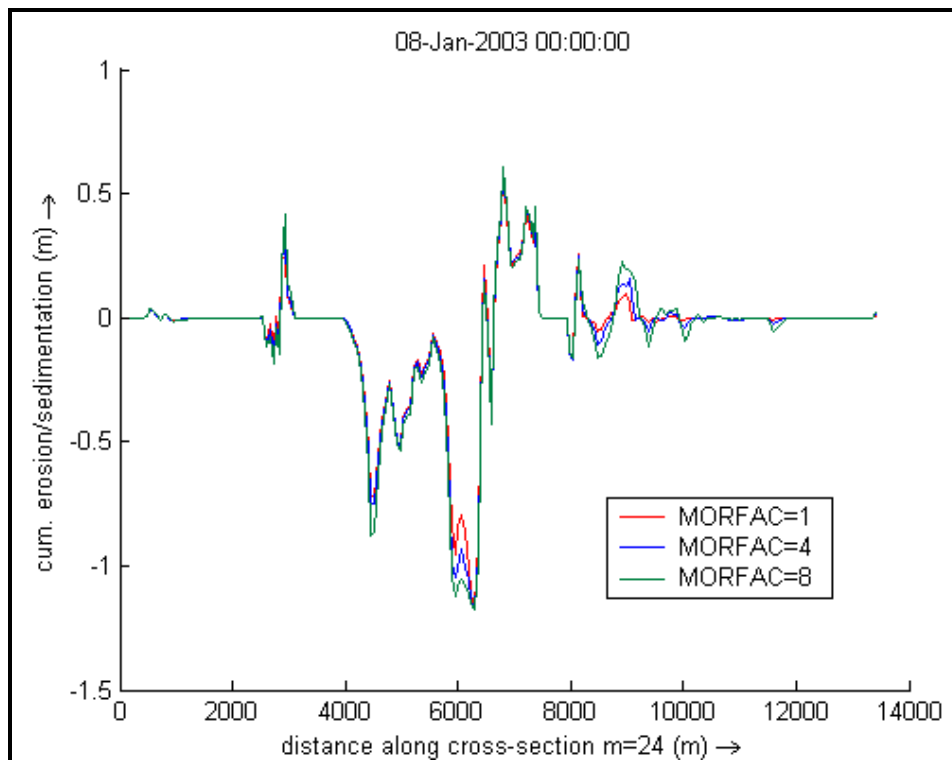


Figure 9.22: Cumulative erosion and sedimentation along longitudinal profile final line at right bank (zero value is located at km 24.0 of the river).

These Figures represent the cumulative erosion and sedimentation along longitudinal cross-sections of the river at each of the five grids lines (20, 21, 22, 23, and 24).

If a careful look is taken to the results, it can be noted that there are some differences between them, especially for the case of using morphological factor 8 (green line), whereas the differences are much less between the red and blue lines.

It is difficult to decide whether or not the morphological factor can be used, because if the results are not the same for different morphological factors and equal morphological time (hydrograph squeezing), at the end we can not depend on the result for our decisions.

For that purpose it is better to go further into detail of the results by taking or considering some specific points or locations along the river (points where extreme erosion and sedimentation had taken place), and to compare the above three cases to have an idea what are the relative errors in the results while the morphological changes were speeded up by using a higher morphological factor with a shorter hydrograph duration.

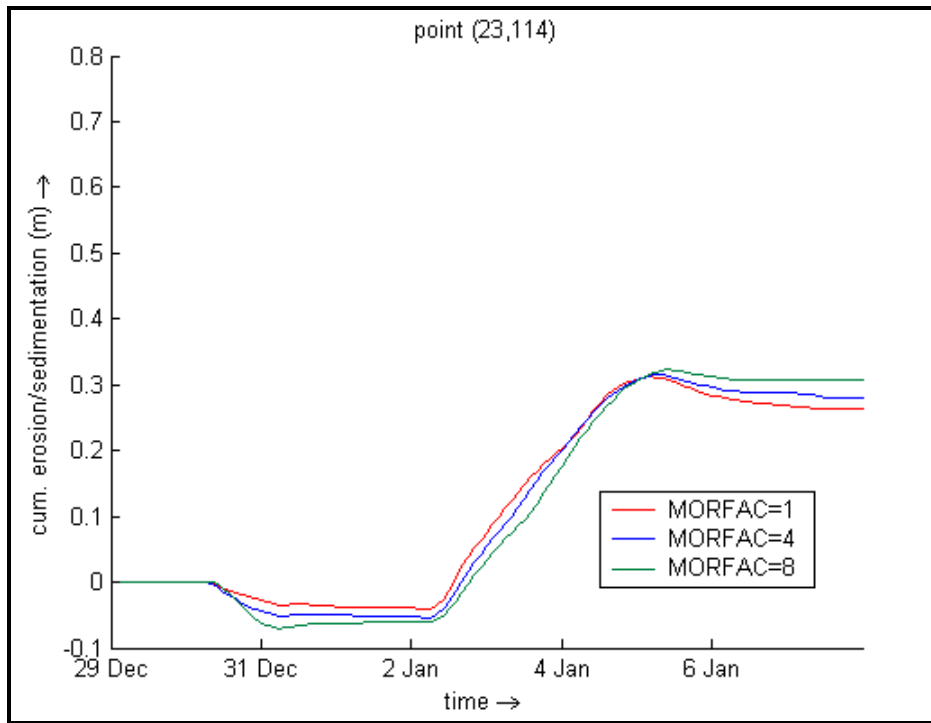


Figure 24: Time dependent cumulative erosion and sedimentation at point where sedimentation had taken place (Without project situation).

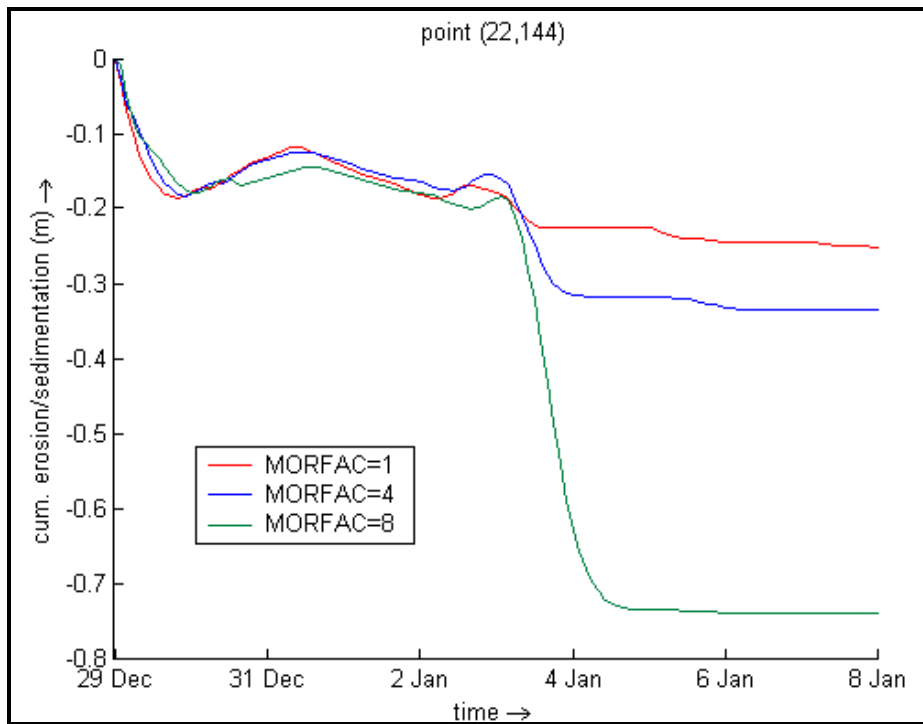


Figure 25: Time dependent cumulative erosion and sedimentation at point where erosion had taken place (Without project situation).

All the above tests were done for the without project case (using the bed topography of 1998). The same tests were also made for the with project case (2001), but it is not relevant to repeat every step. The results for the above two points are shown in Figures 0.26 & 0.27:

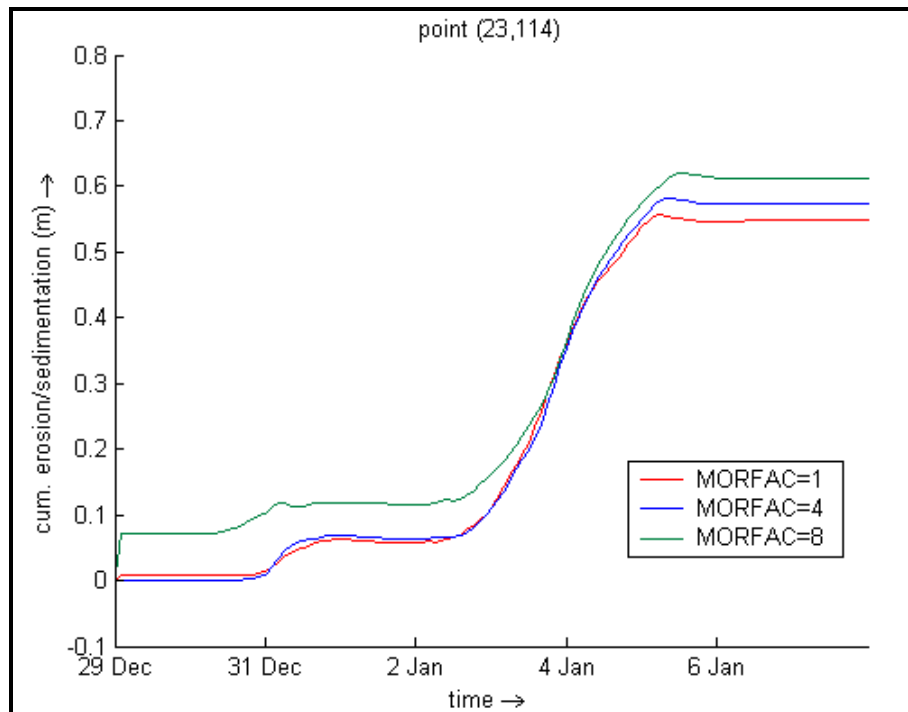


Figure 0.26: Time dependent cumulative erosion and sedimentation at point where sedimentation had taken place (With project situation).

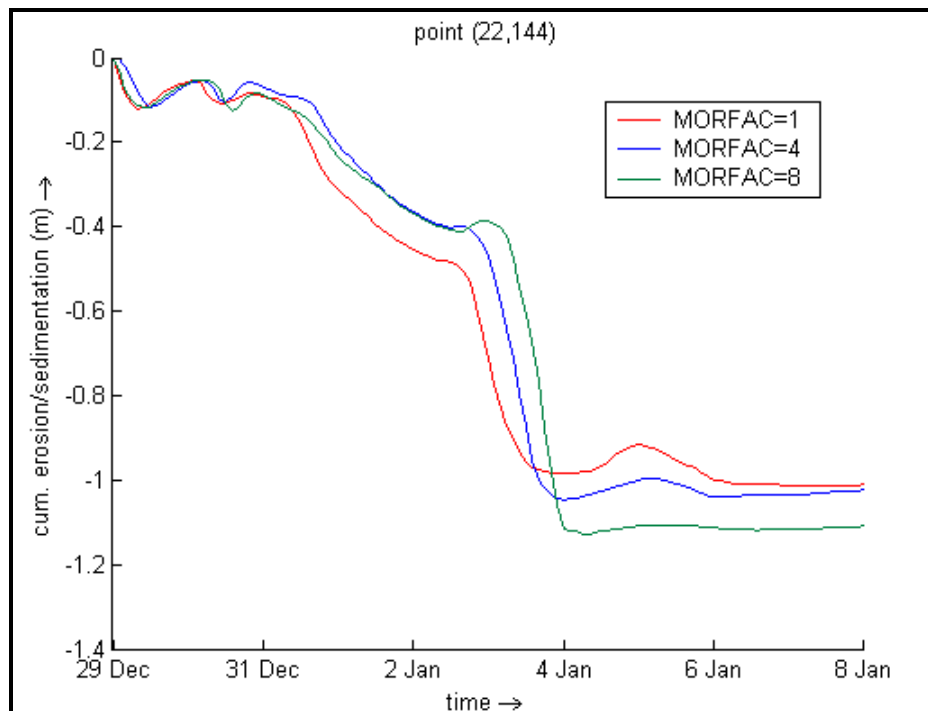


Figure 2.27: Time dependent cumulative erosion and sedimentation at point where erosion had taken place (With project situation).

From Figures 2.24 & 2.25 the difference between results for different morphological factors are clearly figured out. In the case of using MORFAC = 8 (green line) the erosion is at one point almost three times more than when using MORFAC = 1 (red line), while the difference is much less for MORFAC = 4 (blue line). This will attract a conclusion that the result of the green line is not reliable (if the result of the red line is near to the actual situation).

But if we look at Figures 2.26 & 2.27 which represent the same condition but for the With project situation (using 2001 bed topography), it can be noted that the difference of results between the green line (MORFAC=8) and the red line (MORFAC=1) is much less than the difference between the corresponding lines in the Without project situation for the same points. Nevertheless, the difference remains so significant that a modeller could have some fear to use it.

But for MORFAC=4 the difference is not considered significant if no precise results are requested to come out of the model (**mostly qualitative results are needed**), and if only a short period of time is available for having an idea what will be the possible consequences for implementing some sort of measures and projects either in the river itself or at the floodplain close to the main channel.

In this particular study, MORFAC=4 was preferred, due to a limited time availability for carrying out the study and for longer morphological computations.

One important remark should be mentioned that by squeezing the hydrograph the hydrodynamic condition of the model will be affected, and we have to be sure that the hydrodynamic computation remain stable while the hydrograph is squeezed, otherwise unreliable results will come out of the model

6. Model applications and analysis of results

6.1. Introduction

Once the model is properly calibrated, it can be used to simulate different cases. This chapter describes the application of the model to the Pilot Project Meers.

A summary of the results will be presented, and subsequently the results will be analyzed and discussed.

Mostly the results of two different situations will be presented separately and some comparisons will be made on the basis of relative changes in order to view the effect of the implemented project (sediment mining) on this particular location.

For this purpose three different simulations were done for both without project and with project cases using different hydrographs. The comparison will be based on using the same morphological time and inflowing hydrograph for both cases.

The initial condition of the bed material that introduced to the model is contain all fractions, and due to time limitation the model was not run with constant low discharge for obtaining the armouring phenomena, obtaining equilibrium situation in the river.

Index	Situations	Studied in Sections	Hydrograph		Morphology		Initial topography		Comments
			days	Squeezing factor	MORFAC	days	Main channel	Floodplain	
WOP ¹	Without project	Appendix A ¹	1.	ε	ε	1.	1998	1998	For more details look to the referred sections under the third columns
WOP ²		Appendix A ²	3.	ε	ε	3.	1998	1998	
WOP ³		6.2.2	6.	ε	ε	6.	1998	1998	
WP ¹	With Project	Appendix A ³	1.	ε	ε	1.	1998	2002-2003	
WP ²		Appendix A ⁴	3.	ε	ε	3.	1998	2002-2003	
WP ³		6.3.2	6.	ε	ε	6.	1998	2002-2003	

Table 6.1: Overview of cases studied

The studied cases for both situations are described in the table 6.1 above, and it can be seen that the second row represent the cases for without project situations and the same for with project situation is shown in the third row. The numbers written in bold represent the sections where the results of these simulations are shown.

6.2. Without project situation study

6.2.1 Introduction

In this part of the study the major focus will be on morphological changes without the project, to see an insight in what would be the effect of the 2002–2003 floods if the project would not have been implemented. For this purpose the bed topography of 1998 (the only recent available data which was provided before the project) is used to represent the situation before the flood and the project. Also some sort of sensitivity analysis and verification tests were made to the hydrodynamic conditions and compared with WAQUA output before we enter into the morphological computations using Delft3D.

The top layer in the river is much coarser than the sub-layers (see table 4.1). This layer might be stable during most periods of the year, except for the peak flood durations when the shear force induced by the flow will be greater than the critical shear stress of the upper layer.

The downstream boundary conditions remain the same for all cases. They consist of a rating curve at km 38, while the upstream boundary conditions were changed for most of the cases either in duration or magnitude of peak flood.

Below some results will be presented for the different case of WOP¹ and for the other cases that were studied, the results will be shown in the appendixes (WOP¹ – A¹ and WOP² – A²).

6.2.2 Case WOP¹: Using 70 days Constructed hydrograph

In this case we constructed a longer hydrograph of 70 days by combining the floods in 2002 with the flood at the end 2002 – beginning 2003. This is equivalent to the 2002–2003 hydrograph, because only the peaks were selected that have considerable effect on the morphology. The selected and merged peaks are shown in the Figure 6.2.

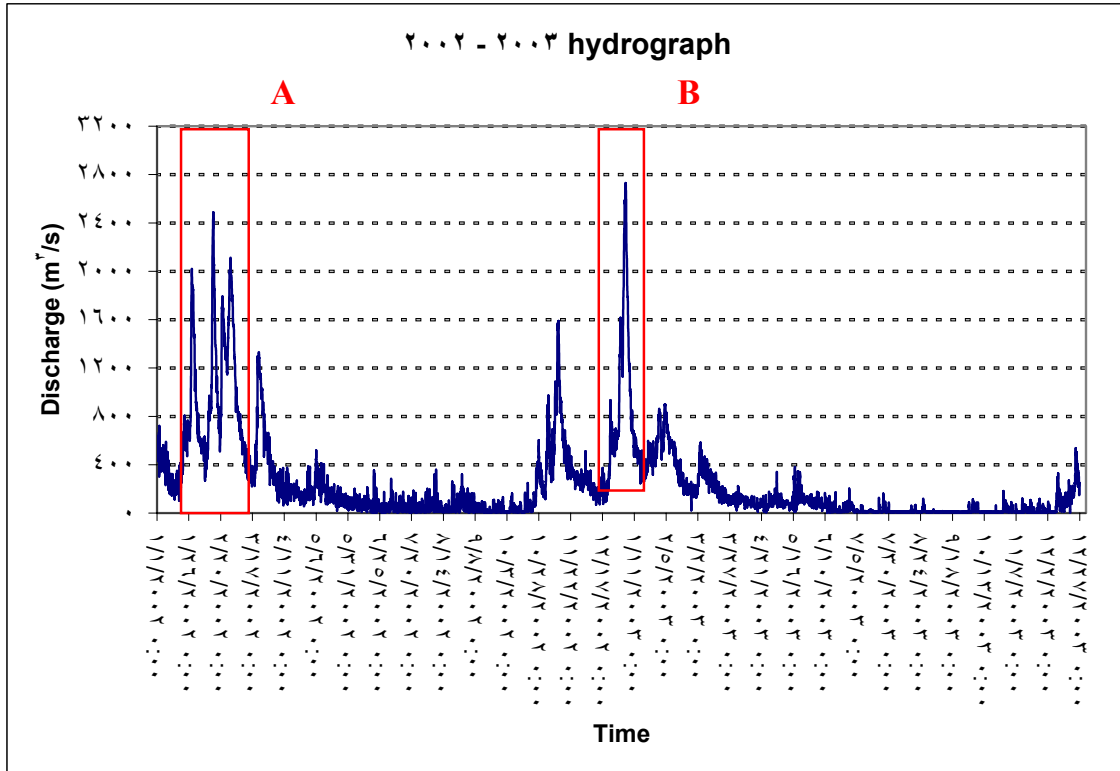


Figure 6.1: 2002-2003 hydrograph.

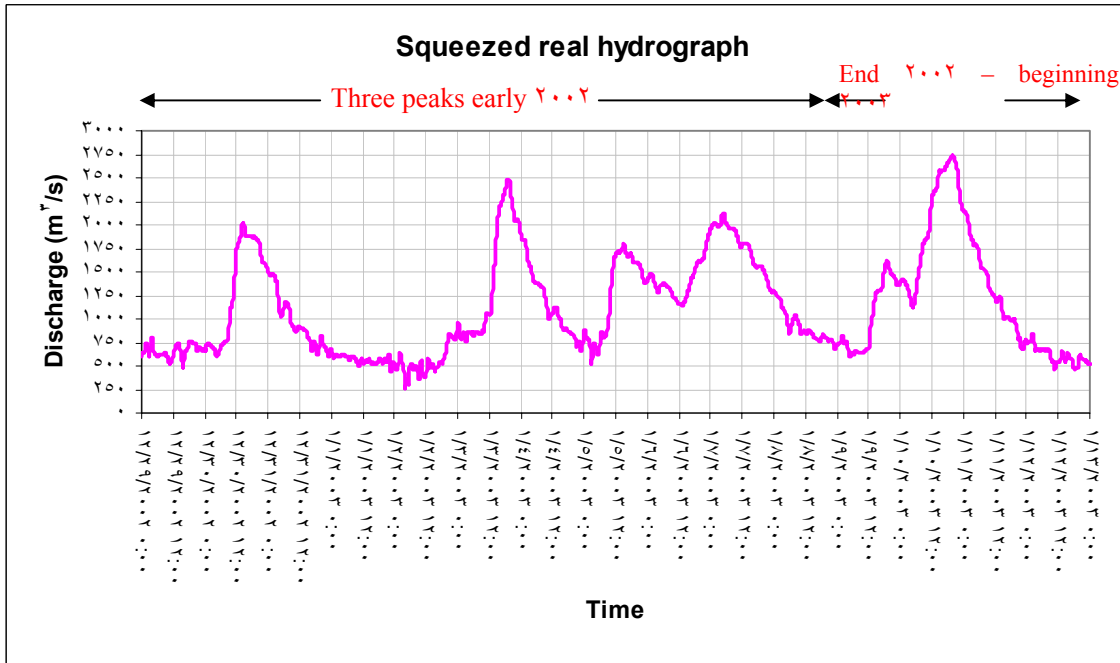


Figure 6.2: Selected peaks from 2002-2003 hydrograph.

The result can be seen in the Figure 6.3 below:

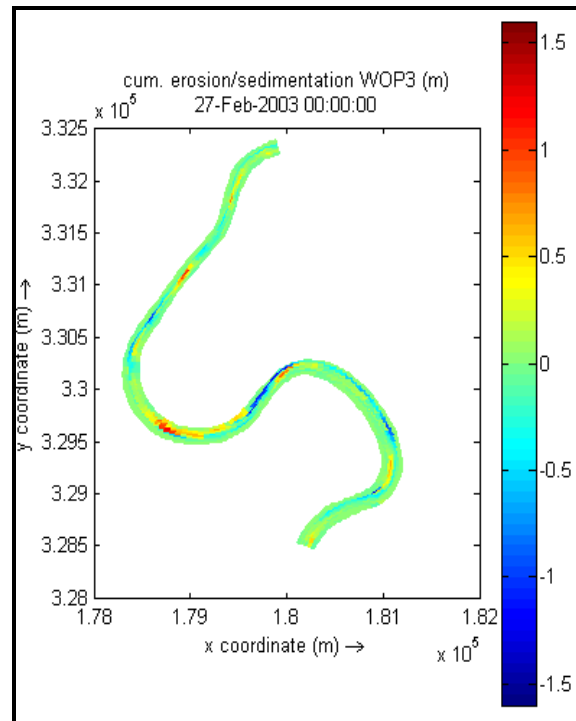


Figure 6.3: Cumulative erosion and sedimentation for 60 days morphological study (squeezed real hydrograph).

Same conclusions can be derived for this case also in term of morphological changes, but here it can be noted that the magnitudes of both erosion and sedimentation is smaller or less than the case WOP2 which shown in the appendix A2. This due to the maximum discharge values used in the simulations, and this result shown in the Figure 6.4, can be considered as better than the others shown in previous cases. Because in this section the morphology of the river was studied with longer durations and the used hydrograph took from the original one of 2002-2003. Later on the comparison between both situations will mostly carrying out depending on the results of this section 6.2.2 WOP2 and section 6.3.2 WP3.

6.3. With project situation study

6.3.1 Introduction

In order to answer the research questions especially whether it is possible to reproduce the phenomena that happened in the Meuse River in the period 2002-2003, this part of study is very important. Because from here we can decide whether if a powerful package like Delft2D with graded sediment can be useful or not in designing the lowering floodplains and the widening of channel in other parts of the river, which mostly have similar characteristics and behaviours.

Most of the input files for the simulations done in this part are the same with the without project situation. The only difference is here the bathymetry of end 2001 should be used.

However this data was not available and some procedures were made for obtaining it (see table 6.1).

For this reason we tried to make best guess for the bed topography of end 2001 by combining the main channel of 1998 with the floodplain 2002-2003 and thus neglecting all morphological changes between 1998 and 2001.

The same cases that were studied for the without project situation are repeated for this situation again, but using the newer bed topography (see also table 6.1).

Before presenting the results of the various cases with project simulations, its better to discuss in advance the effects if a project would be implemented in the Meers location Reference is made to the Figures 6.4 and 6.8:

If we look to the simple cases shown in Figure 6.4a which represent a uniform cross-section and the dash line represent the proposed project for lowering the flood plain at one side of the river. The most possible changes can be determined according to the equations:

$$Q = C \times B \times h \times \sqrt{h \times i}$$

$$u = C \sqrt{h \times i}$$

$$u = \frac{Q}{B \cdot h}$$

where Q is the total discharge, B is the width of the river, h is the water depth, i is the bed slope, C represent the Chézy coefficient, and u is flow velocity.

If we assume that the value of bed slope, Chézy coefficient and the discharge (as a function of distance) are constants, then some rough computations could be carried out

The changes in the morphology will mostly the same as shown in Figure 6.4b, and this due to:

At point A upstream of the river

If we assume that point A will be so far upstream that the project implementation will not affect on it, then the velocity can be determined from equation

$$u_A = C \sqrt{h \times i}$$

At point B

For this point the width of the river is different between upstream and downstream, and then the computation will be as:

Upstream of point B.

At the upstream of this point the bed width is the same of the point A, but the water level is lower (h^*) due to the effect of the project (M^*) curve will be presented at this

area, the velocity will be higher, and as a consequence erosion will start to take place at upstream of point B:

$$u_B = \frac{Q}{B \cdot h_v} > u_A \quad \text{Because } h_v < h$$

Downstream of point B.

At down stream of point B, the bed width will increase, then the velocity will decrease and as a consequence sedimentation will take place

At point C

Upstream of point C mostly will be the same of the downstream of point B where sedimentation taken place. Whereas, at downstream of point C the river returned to situation before.

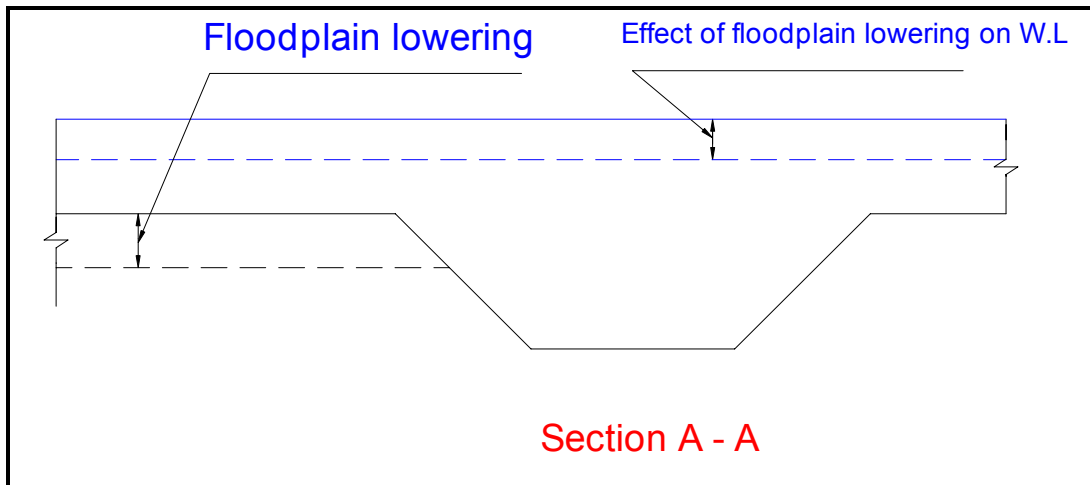


Figure 4.4a: River cross-section

According to the explanations above for the different points the final equilibrium situation caused by project implementation.

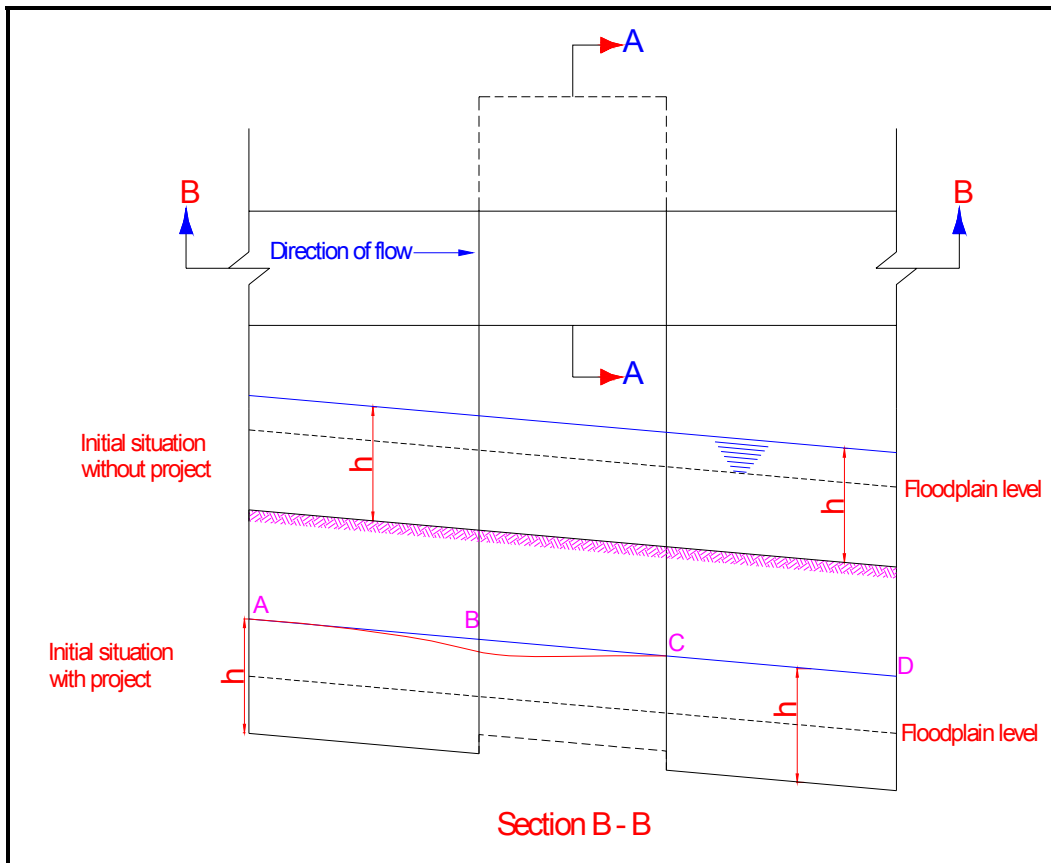


Figure 1.4b: Expected 2D morphological changes after the project implementation

In the case of the Meuse River at Meers the river consists of a bend. Hence the condition is somewhat different from the above explanation for a straight river. Now if we consider a curved river or bend river section shown in the Figure 1.5, and if all simplifications and assumptions made for the case of straight river are used for this case also, then the result will be as shown in the Figure 1.5:-

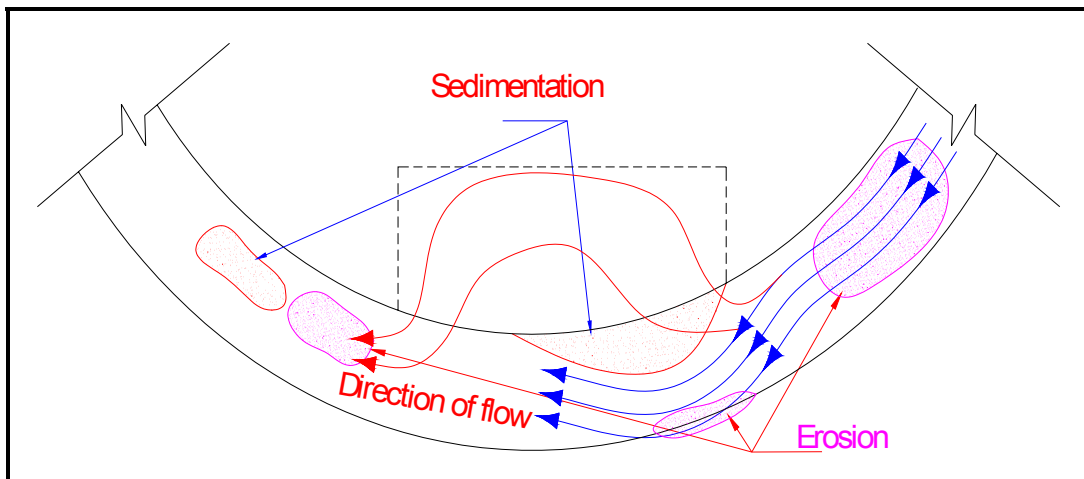


Figure 1.5: Expected 2D morphological changes after the project implementation for river with bends

It is obvious in the curved river is mostly subjected to some sedimentation at the inner bend and erosion at the outer bend also without any project, if the river does not get the equilibrium situations or protections are not implemented at the banks.

When the discharge in the river is below bank full discharge and as shown in the Figure 6.9 the flow will be deviated and directed to the outer bend, due to the sedimentation in the main channel. The velocity might be higher than normal case without decreasing the flow area (without sedimentation in the main channel), and some erosion can be expected along the outer bend.

6.3.2 Case WP3: Using 60 days morphological study

The same hydrograph as used in Section 6.2.2 and shown in Figure 6.5 is used for this case, also for the purpose of determining the effect of the project on morphological changes by considering a real hydrograph for some longer period than other cases. The results are as shown in the Figure 6.6.

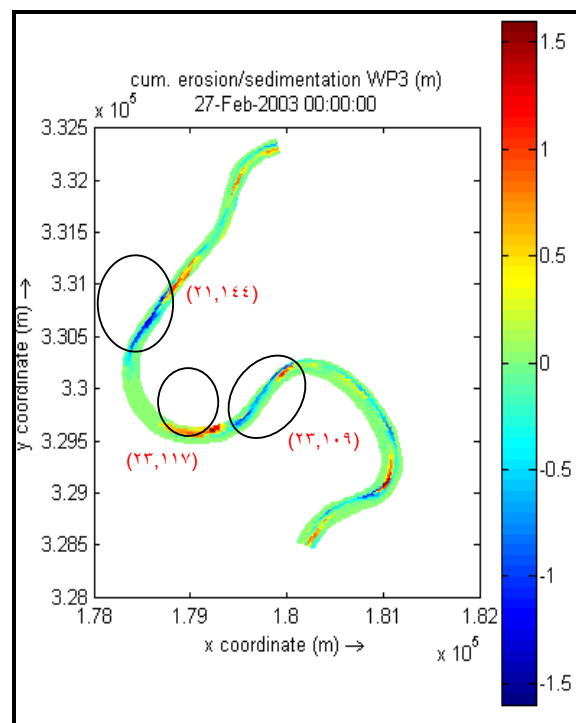


Figure 6.6: Cumulative erosion and sedimentation study in the main channel for 60 days hydrograph.

This case considered as the most relevant for the situation with project, because the simulation is for a longer period, and most of the peaks and discharges in the floods 2002-2003 that have critical effect on the morphological conditions are included.

6.4. Comparison between the without and the with project situations

In this section the results of the two different situations (without project and with project) are compared for determining the effect of the project on the morphological conditions in this affected river reach. There are morphological computations for both

cases for (1, 3, and 6 days) hydrographs (see table 6.1), but here the results of the sections 6.2.2, 6.3.2 will be compared (6 days hydrograph). This is done because the morphological changes were computed for a longer period of time and some part of the real hydrograph of 2002 – 2003 floods is used that have a critical effect.

First of all in this part it is important to show the difference in floodplain topography for both cases (without project and with project) especially at the project location for figuring out what was the major cause of observed phenomena.

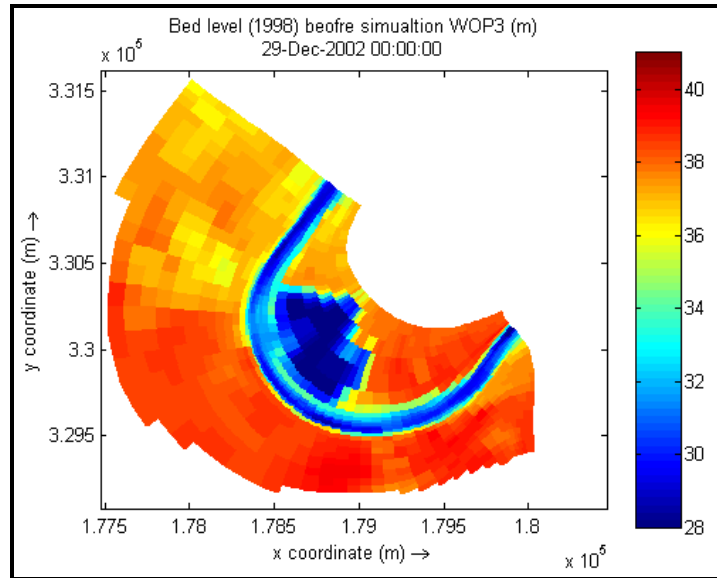


Figure 6.7: Bed topography for the without project case (interest location).

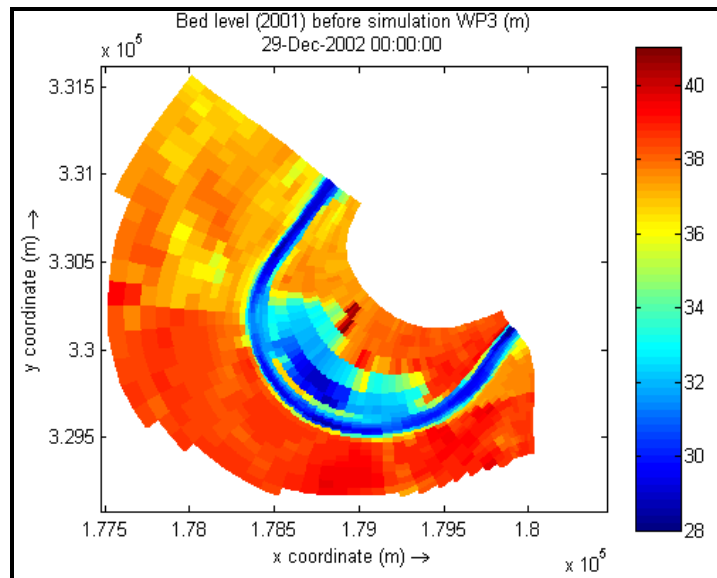


Figure 6.8: Bed topography for the with project case (interest location).

From Figure 6.7 it can be seen that the floodplain at the inner bend of the river (Netherlands side) there is some sort of lake. This due to projects implemented in this area previous to 1998.

Figure 6.8 shows the same location but with the bed topography at end 2001 due to the project implementation the floodplain topography seems to be much lower than the in 1998 in some part of the floodplain and higher in some other parts. This difference could be determined by subtracting bed topography (1998) from (2001), and the result is shown in Figure 6.9.

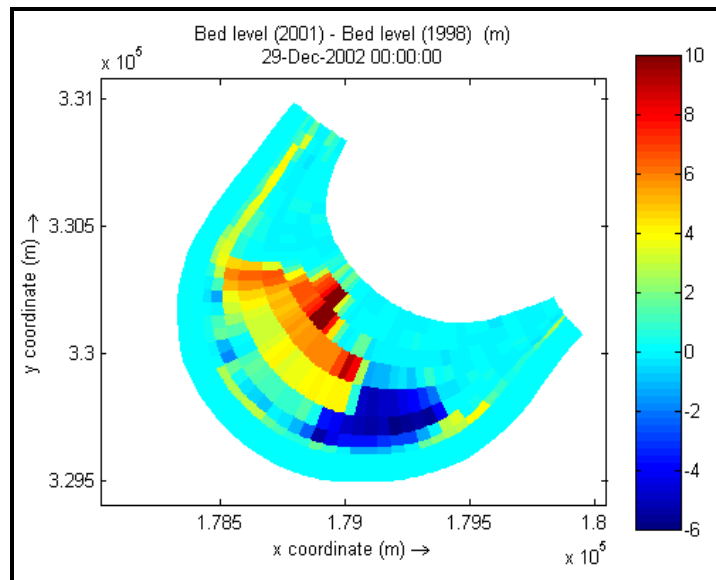


Figure 6.9: Difference of bed topography for with project and without project cases (interest location).

It can be seen easily from the Figure 6.9 that there are major differences between the input data of the model. If we look to the darker blue at the beginning of the bend present that the bed topography of 2001 is almost 6m lower than that of 1998 at this area, and for some other parts is higher.

This lowering of the floodplain close to the main channel will affect the whole flow pattern in the river, because more water will be directed to the floodplain, and the velocity in the main channel will decrease, and as a consequence the sedimentation will take place at this area. But at the downstream of the bend when the water is returning to the main channel (from the floodplain), it will increase the velocity at that area and as a consequence erosion will take place. These phenomena can be noted in the Figure 6.6, for the case of the with project situation.

Also it is important to closely to the area near to the sedimentation and erosion in the main channel, especially at the outer bend, to have an idea about the erosion taken place at that location.

As explained before, when the sedimentation will take place in the main channel, during low flow condition (discharge lower than bank full discharge) the outer bend will be more subjected to erosion because the flow is directed to the bank (see Figure 6.6).

In Figure 7.10 the velocity vectors are shown for the area of the main channel and some bank lines on both sides, and it is not easy to recognize the part of flow that attack the downstream bank (Belgium bank). For that reason the reach of interest is zoomed as shown in Figure 7.11, and there it can be noted that there are some part of the flow directed to the outer bend and crosses the bank lines, which mostly cause some bank erosion at that location. The Figures 7.10 and 7.11 are taken for discharge around 200 m³/s, which is considered as a below bank full discharge level.

In Figure 7.12 it is easy to note that there is some erosion for both situations with and without the project. But for the situation of without the project (dashed line) the erosion is very small and it can neglect. Whereas, for the situation with project the erosion is much more, mostly due to the reasons mentioned before and this prove the flow pattern in the Figures 7.10 and 7.11 shown above.

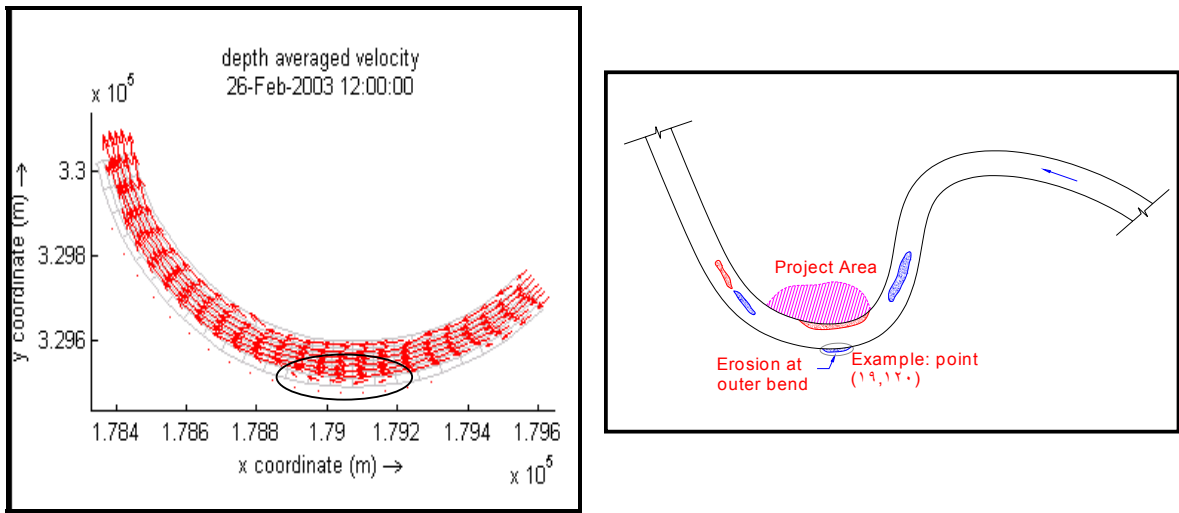


Figure 7.10: Velocity vector for the situation of with project for the case 7.3.3.

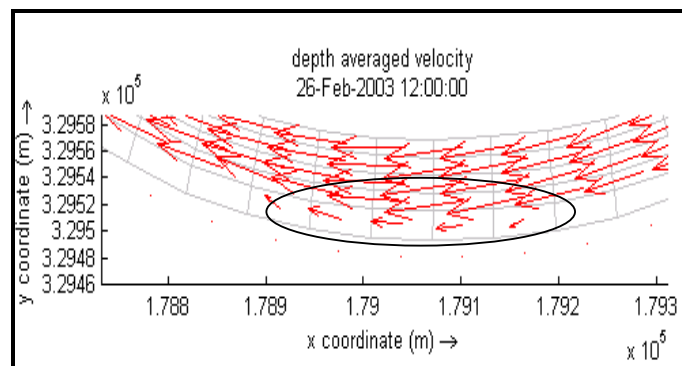


Figure 7.11: Velocity vector for the situation of with project for the case 7.3.3 (zoomed area).

It is important now to take a close look of cumulative erosion and sedimentation of this specific location, for determining either erosion took place or not.

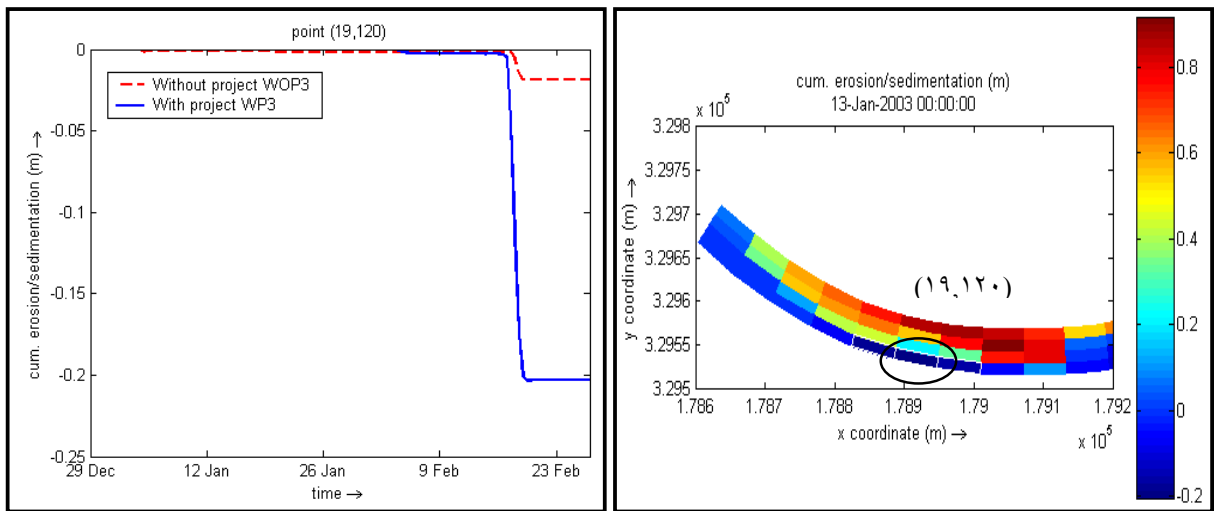


Figure 7.12: Cumulative erosion and sedimentation at outer bend (Belgium bank) for a point (19,120).

Now some more detailed comparisons between the two situations will be made for some locations that are specified in the explanatory Figures that will be attached to each figure to give an idea about the locations of these points in the river.

In Figure 7.1 three points were indicated in reaches of the main channel of the river where phenomena of interest can be observed. The first point is upstream of the project where erosion takes place (23,109), the second point at the location of the project where sedimentation takes place (23,114), and the last point is at downstream of the project where the water flows back to the river main channel and erosion takes place (21,144). The results are shown in the Figures 7.12a – 7.12b.

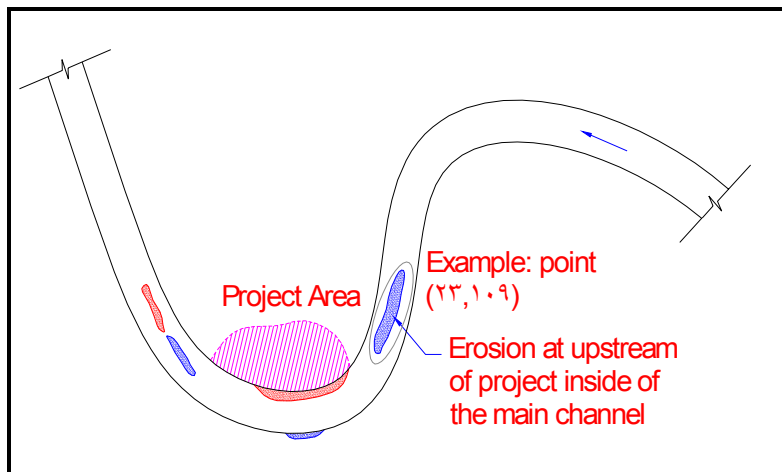


Figure 7.12a: Explanatory figure showing the location of the point (23,109).

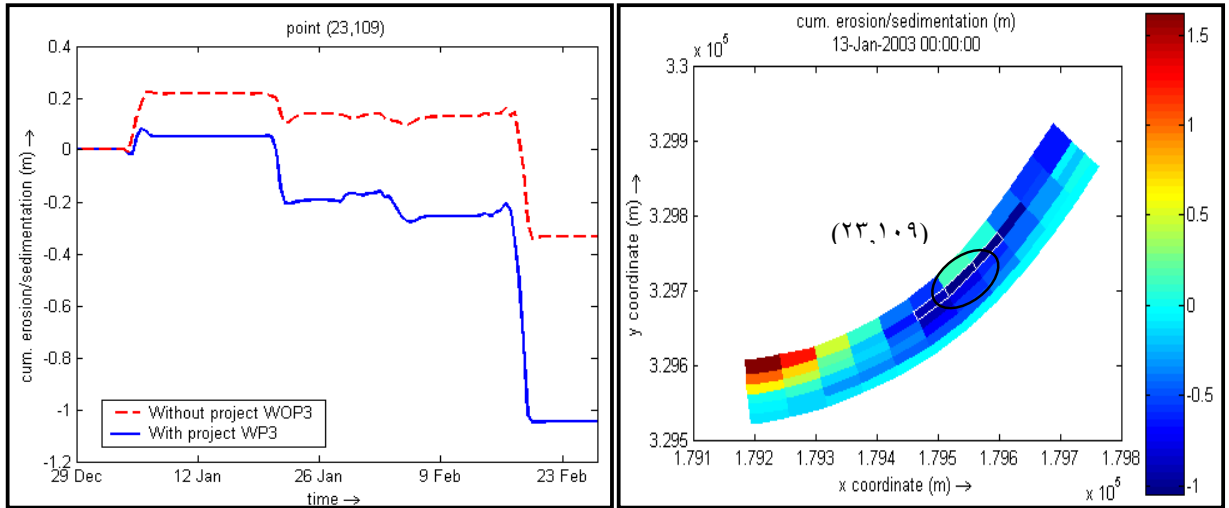


Figure 6.13b: Cumulative erosion and sedimentation at upstream of the project at point (23, 109).

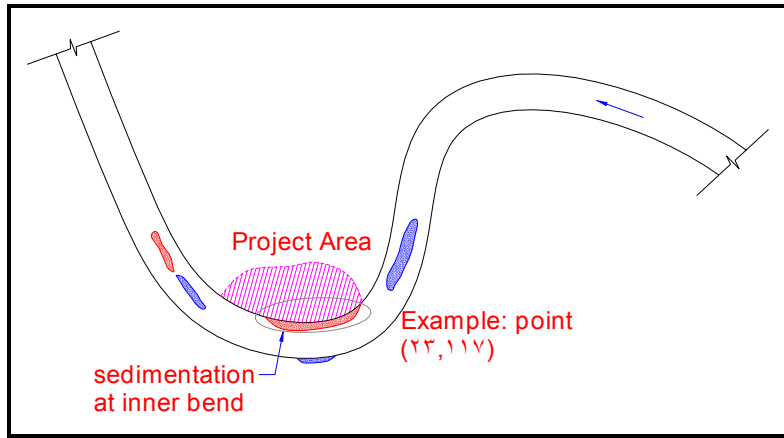


Figure 6.14a: Explanatory figure showing the location of the point (23, 117).

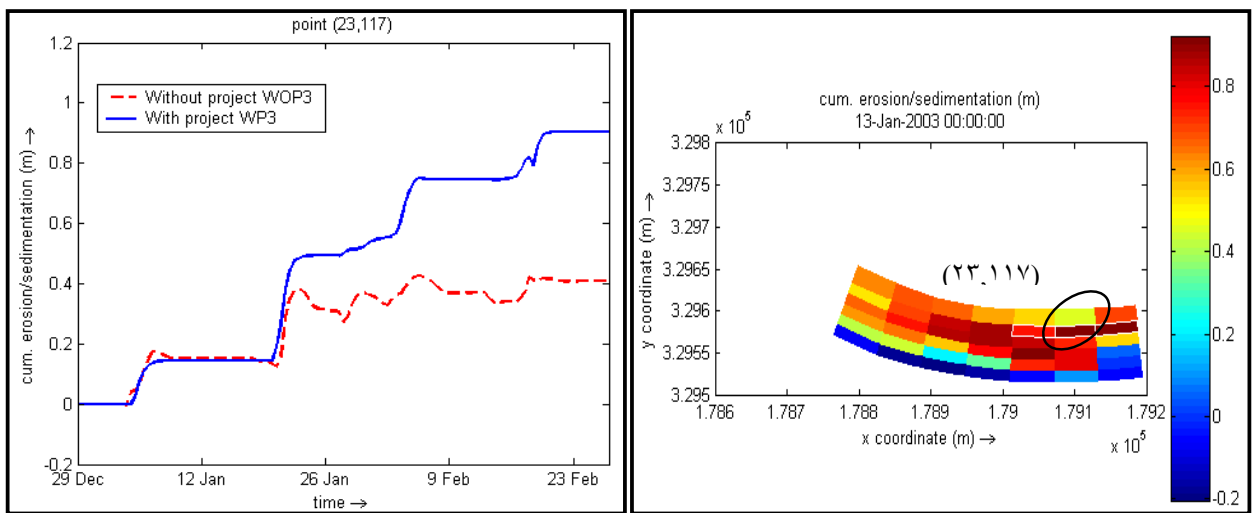


Figure 6.14b: Cumulative erosion and sedimentation location of the project at point (23, 117).

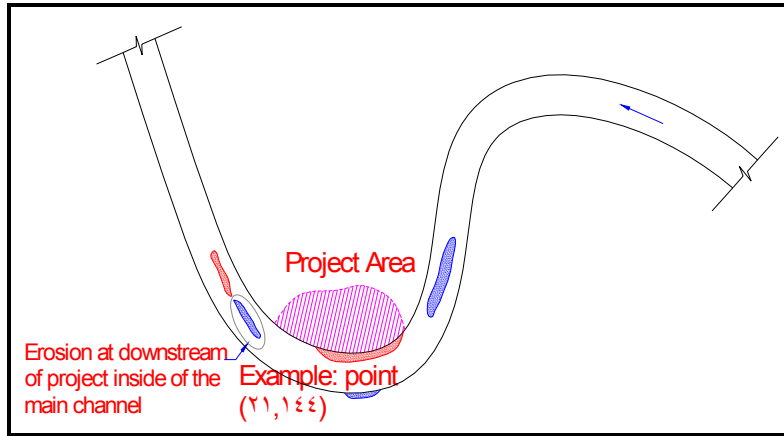


Figure 6.10a: Explanatory figure showing the location of the point (21,144).

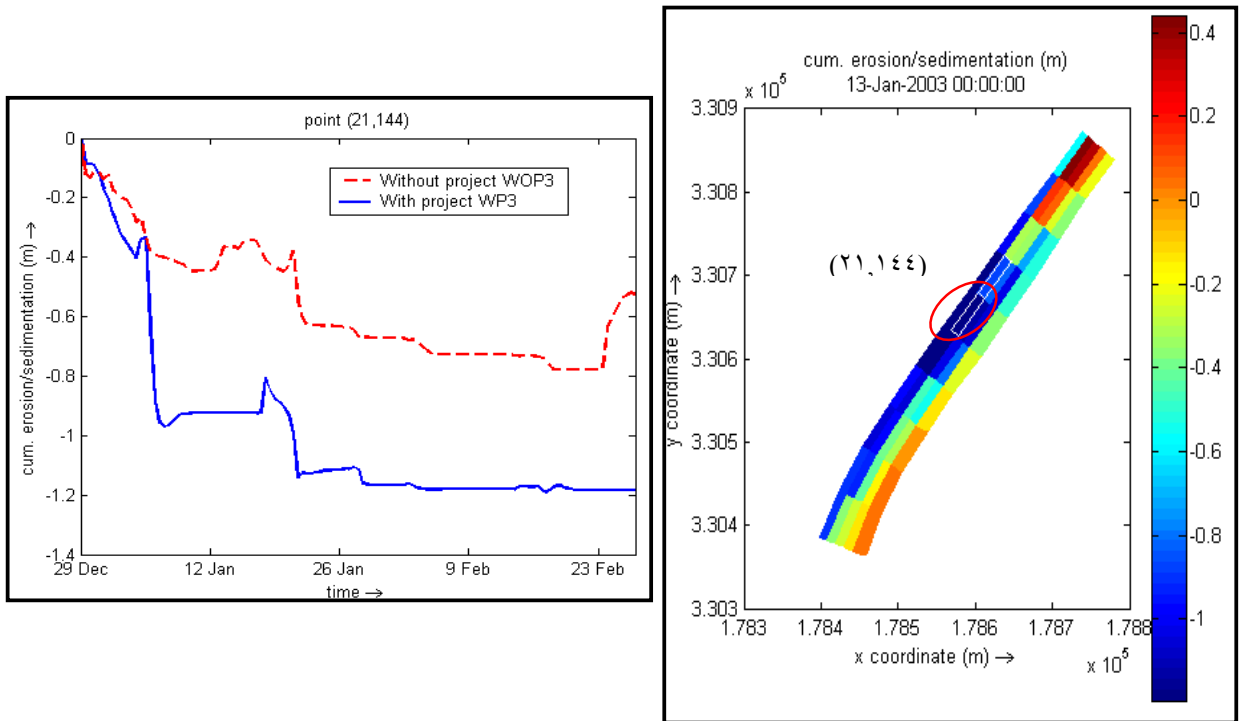


Figure 6.10b: Cumulative erosion and sedimentation downstream of the project at point (21,144).

In the Figures 6.13 through 6.16 the differences between the situations with and without the project can be noted easily in term of cumulative erosion and sedimentation. The dashed red lines represent without project situations and the solid blue lines are used for with project situation. If we look to these Figures we can conclude that the project has large effect on the phenomena happen in that area, but also the sedimentation and erosion for the without project situation is not negligible.

In order to understand these results of sedimentation and erosions presented above, some additional comparison will be made for other parameters like bed levels, water levels, flow velocities, and bed shear stresses for both with and without project situations.

The main channel of the river mostly subjected to all changes, and according to our schematization of the river (that we defined to the model), the model is consist of five grid cells, and its not relevant to present the result for each individual grid lines. For that reason an average value over the cross-section of the river will be given. As shown in the Figures 6.16 through 6.20.

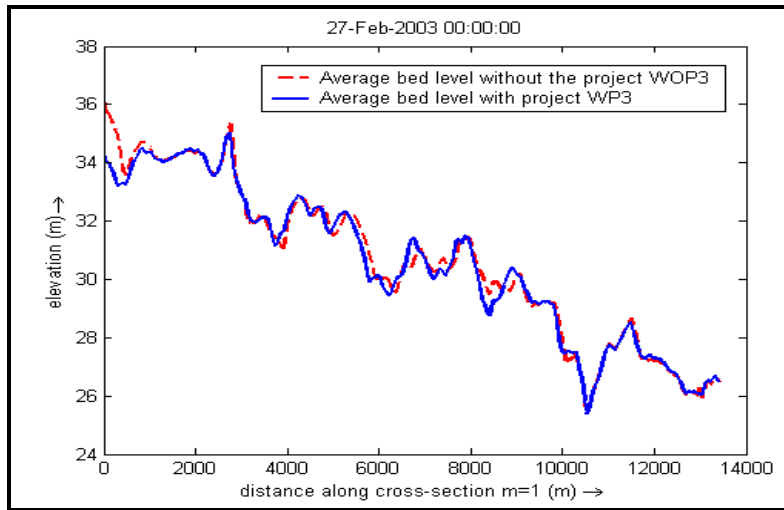


Figure 6.16a: Width averaged bed level along longitudinal profile of the river at the end of simulation ($Q \approx 0.0 \text{ m}^3 / \text{s}$) (zero value is located at km 44.0 of the river).

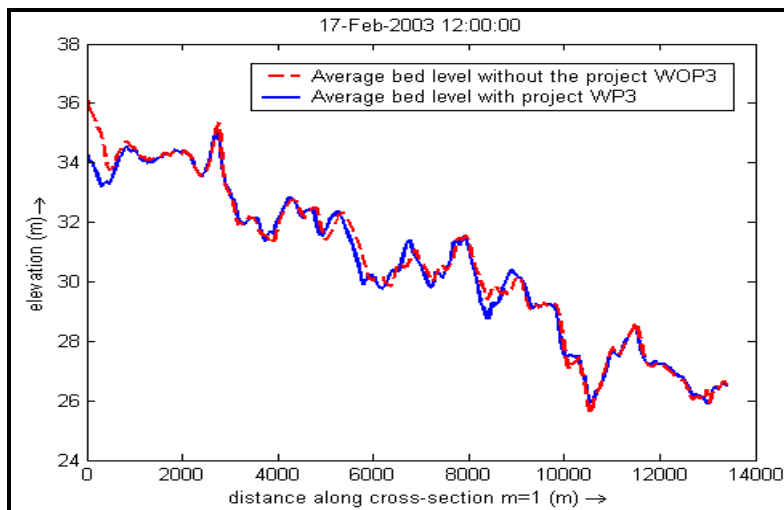


Figure 6.16b: Width averaged bed level along longitudinal profile of the river at peak flow condition ($Q \approx 2800 \text{ m}^3 / \text{s}$) (zero value is located at km 44.0 of the river).

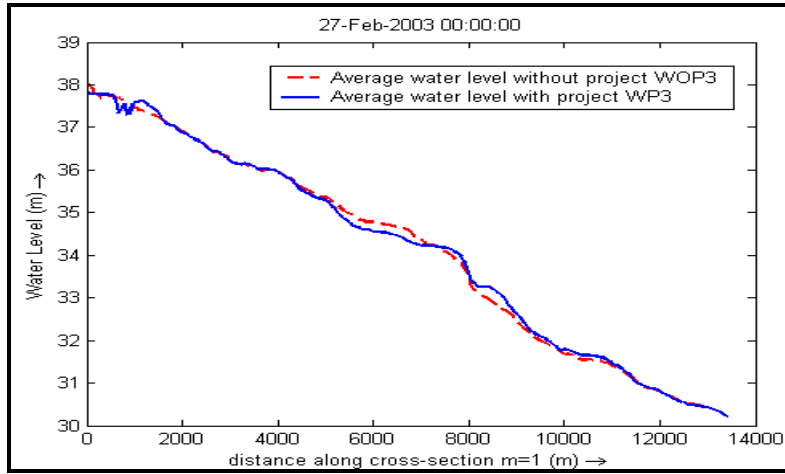


Figure 6.11a: Width averaged water level along longitudinal profile of the river at the end of simulation ($Q \approx 0.0 \text{ m}^3 / \text{s}$) (zero value is located at km 4.0 of the river).

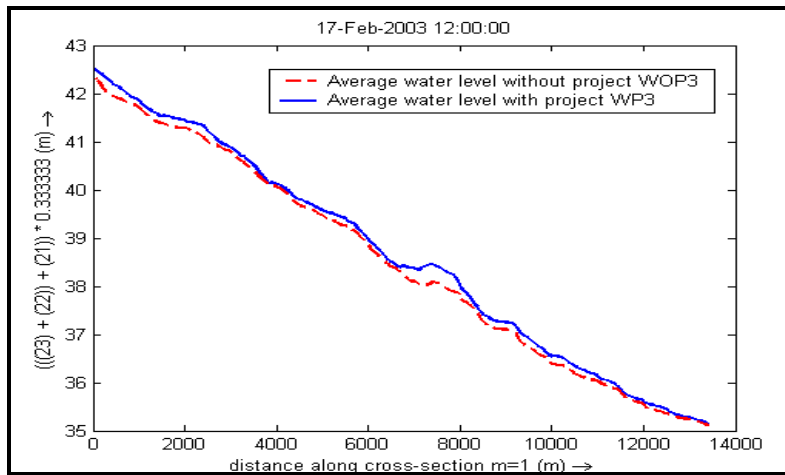


Figure 6.11b: Width averaged water level along longitudinal profile of the river at peak flow condition ($Q \approx 2800 \text{ m}^3 / \text{s}$) (zero value is located at km 4.0 of the river).

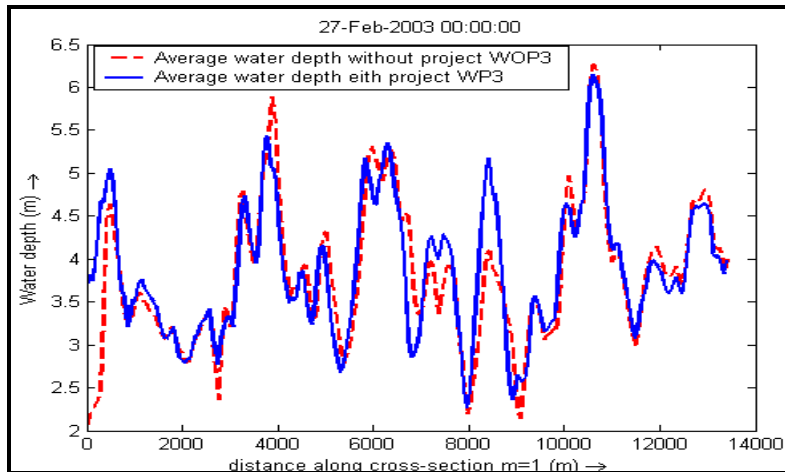


Figure 6.11a: Width averaged water depth along longitudinal profile of the river at the end of simulation ($Q \approx 0.0 \text{ m}^3 / \text{s}$) (zero value is located at km 4.0 of the river).

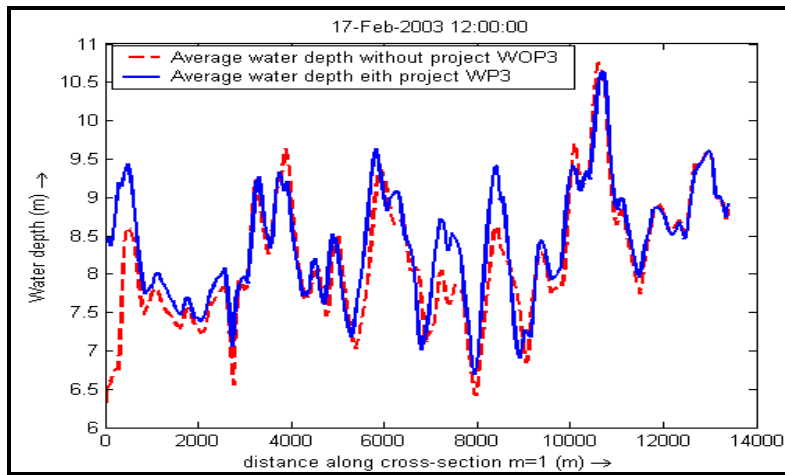


Figure 6.18b: Width averaged water depth along longitudinal profile of the river at peak flow condition ($Q \approx 2800 \text{ m}^3 / \text{s}$) (zero value is located at km 4.0 of the river).

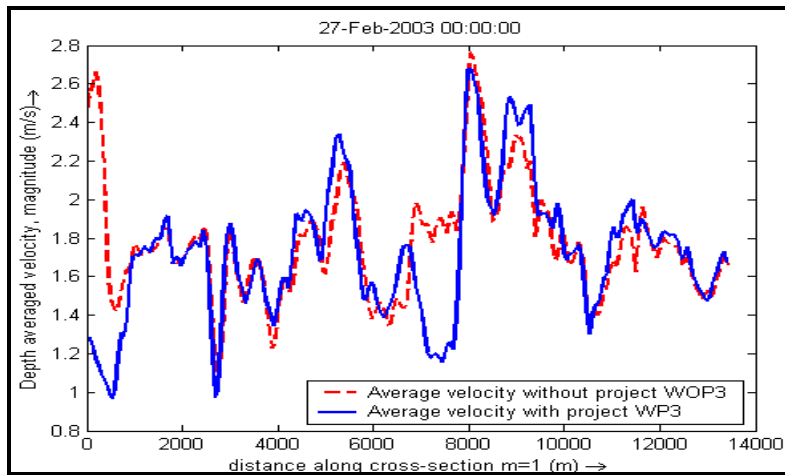


Figure 6.19a: Width averaged velocity along longitudinal profile of the river at the end of simulation ($Q \approx 2000 \text{ m}^3 / \text{s}$) (zero value is located at km 4.0 of the river).

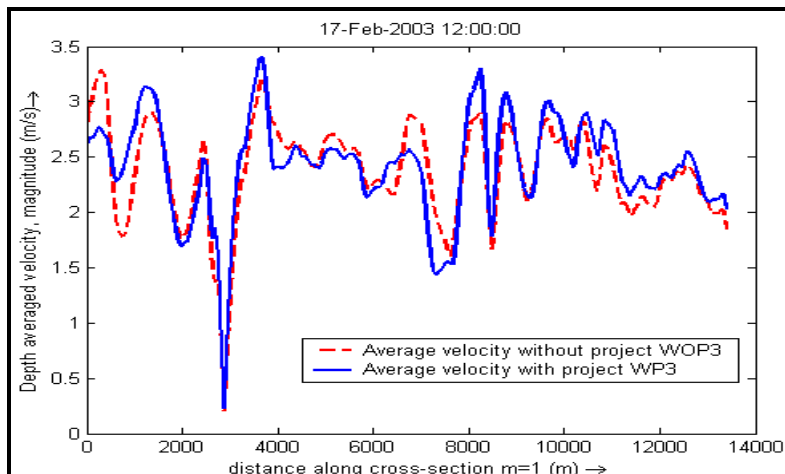


Figure 6.19b: Width averaged velocity along longitudinal profile of the river at peak flow condition ($Q \approx 2800 \text{ m}^3 / \text{s}$) (zero value is located at km 4.0 of the river).

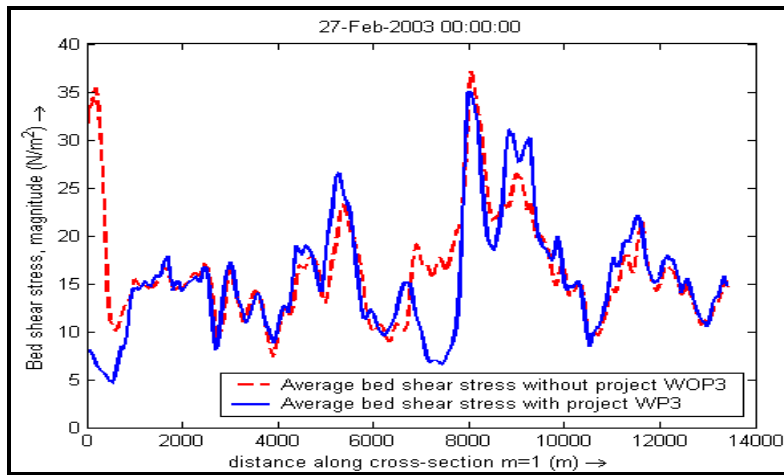


Figure 6.20a: Width averaged bed shear stress along longitudinal profile of the river at the end of simulation ($Q \approx 0.0 \text{ m}^3/\text{s}$) (zero value is located at km 44.0 of the river).

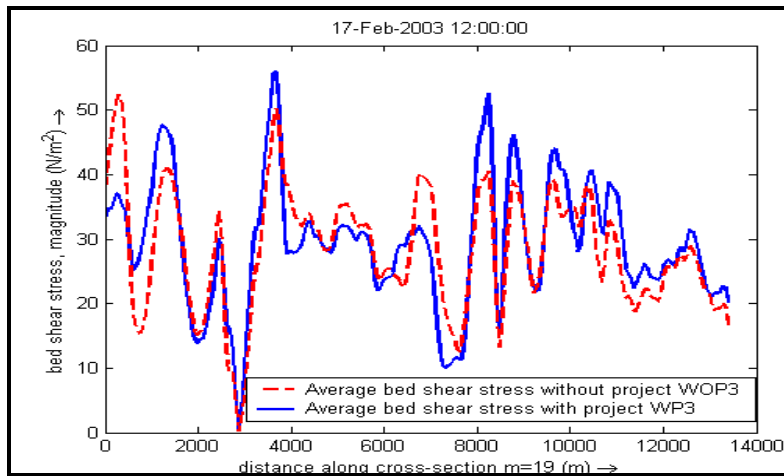


Figure 6.20b: Width averaged bed shear stress along longitudinal profile of the river at peak flow condition ($Q \approx 2800 \text{ m}^3/\text{s}$) (zero value is located at km 44.0 of the river).

From these Figures 6.19a through 6.20b the difference the between situation with and without the project for different important parameters are presented, while the average of them is computed throughout the river width for different discharge conditions.

It is clear from the Figures that the pattern of sedimentation and erosion is reasonable, because for example at the location of sedimentation the velocities and the bed shear stresses are reduces in the case of the with project situation and vice versa for the location of erosion. However the exact differences are not presented due to the average value, because these parameters for both situations are different for each grid lines of the schematization and when the width average values are taken, some differences will adjust themselves with the neighbouring grid lines.

For that it is better to look in detail to some individual points also for some parameters such as bed shear stress as shown in the Figures 6.21 – 6.26.

The situation in the Figure 6.17b might be due temporal dumping of the excavated soil near to the project location. The dumped soil leads in raising the water level in the river and it hides the effect of the project locally. In reality the situation is somewhat different and the consequences can be seen easily in the Pilot Project Meers.

Figures 6.21 and 6.22 are presenting the bed shear stresses for the cases with and without project situation along the main channel including on grid lines of the banks in both sides.

Some differences can be noted in the magnitude of the bed shear stresses, but not very clear for that reason we will look to the points indicated on Figure 6.22. The location of these points can be observed from the previous explanatory Figures that attached to the cumulative erosion and sedimentation in the river (see Figures 6.14, 6.15, 6.16, and 6.17).

There is large variation in bed shear stress, in some location it reaches to around 100 N/m^2 (red parts).

According to Shields, the Shields parameter θ is given by:

$$\theta_{cr} = \frac{\tau_{cr}}{(\rho_s - \rho)gD} = \left(\frac{hi}{\Delta D} \right)_{cr} \Rightarrow D_{cr} = \frac{hi}{\Delta \theta_{cr}}$$

where θ_{cr} is critical dimensionless particle mobility parameter, h is the water depth (m), i is the bed slope, $\Delta = \left(\frac{\rho_s}{\rho} - 1 \right)$, and D_{cr} is the critical particle diameter (m).

Assume that $\theta_{cr} \approx 0.03$, water depth $h \approx 11 \text{ m}$, bed slope $i \approx 0.0004$, and finally $\Delta \approx 1.6$. Then the mean particle diameter that can be moved by this flow can be determined as follows:

$$D_{cr} = \frac{hi}{\Delta \theta_{cr}} = \frac{11 * 0.0004}{1.6 * 0.03} \cong 0.1 \text{ m} \cong 100 \text{ mm}$$

From this result we can conclude that the sediment particle smaller than 100 mm will be transported during some period of the flood and in some specific locations where the larger amount of shear stresses are induced by the flow. Whereas, the particle sizes larger than 100 mm mostly remain stable during such floods. According to the Figure 3.10 there are no particles in the bed larger than 100 mm . This implies that during the peak of the 2002-2003 floods at some locations all the bed materials was in movement. The project has caused a substantial increase of the bed shear stresses and hence substantially mobilized the bed material of the Meuse River.

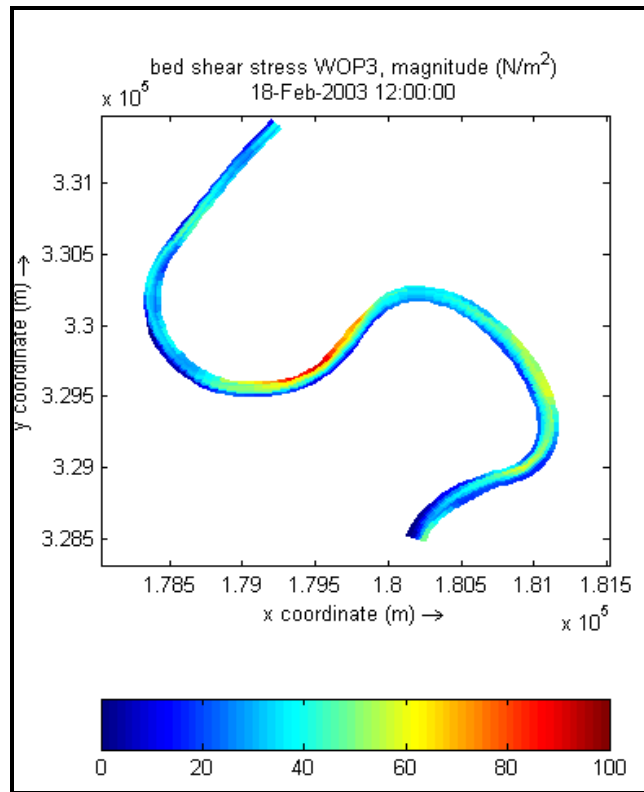


Figure 6.21: Bed shear stress along the river (Without project).

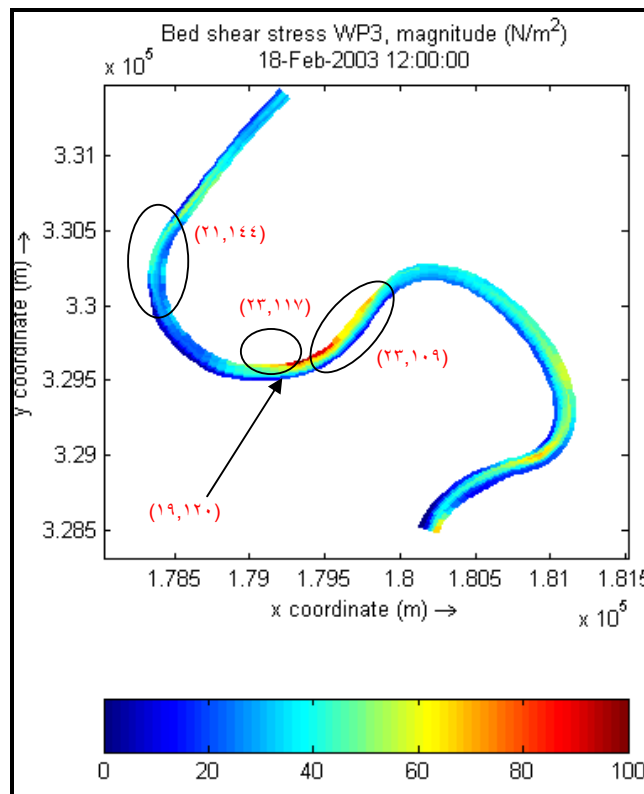


Figure 6.22: Bed shear stress along the river (With project).

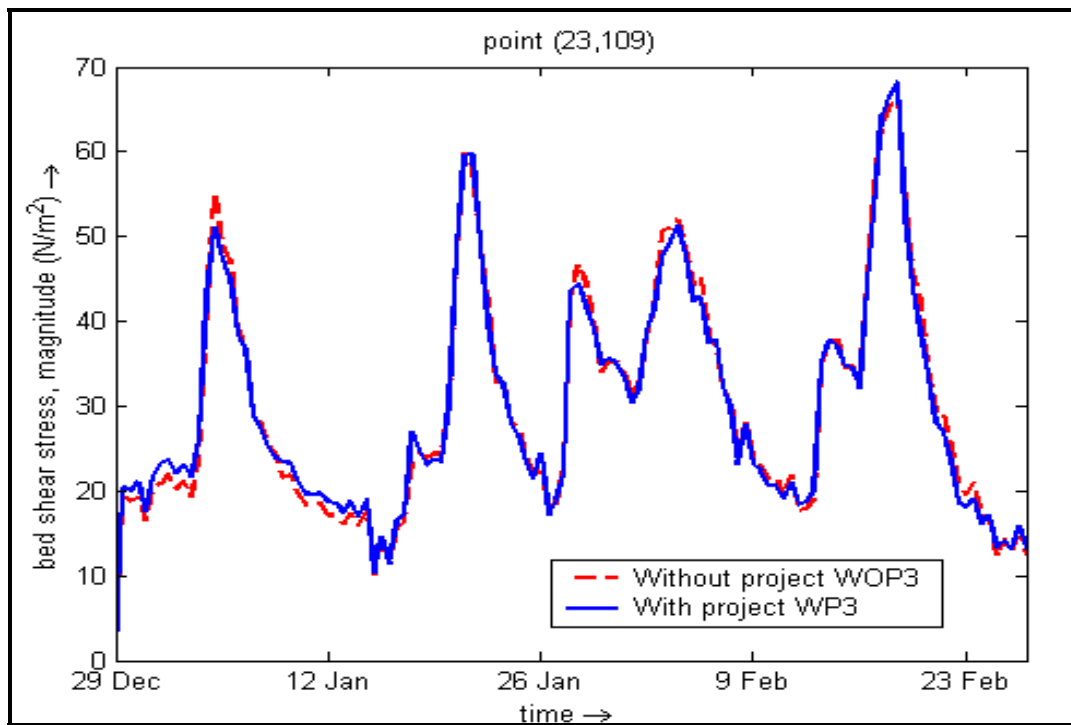


Figure 6.23: Time varying bed shear stress at specific point (23,109) in the river for both of (with project) and (without project) cases.

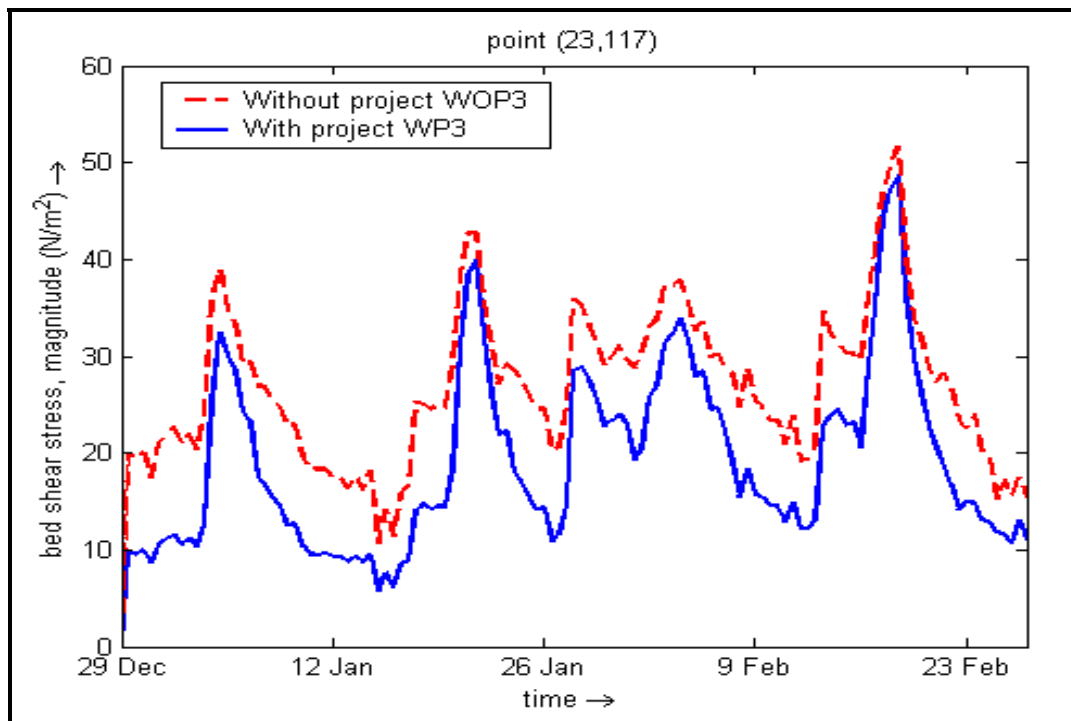


Figure 6.24: Time varying bed shear stress at specific point (23,117) in the river for both of (with project) and (without project) cases.

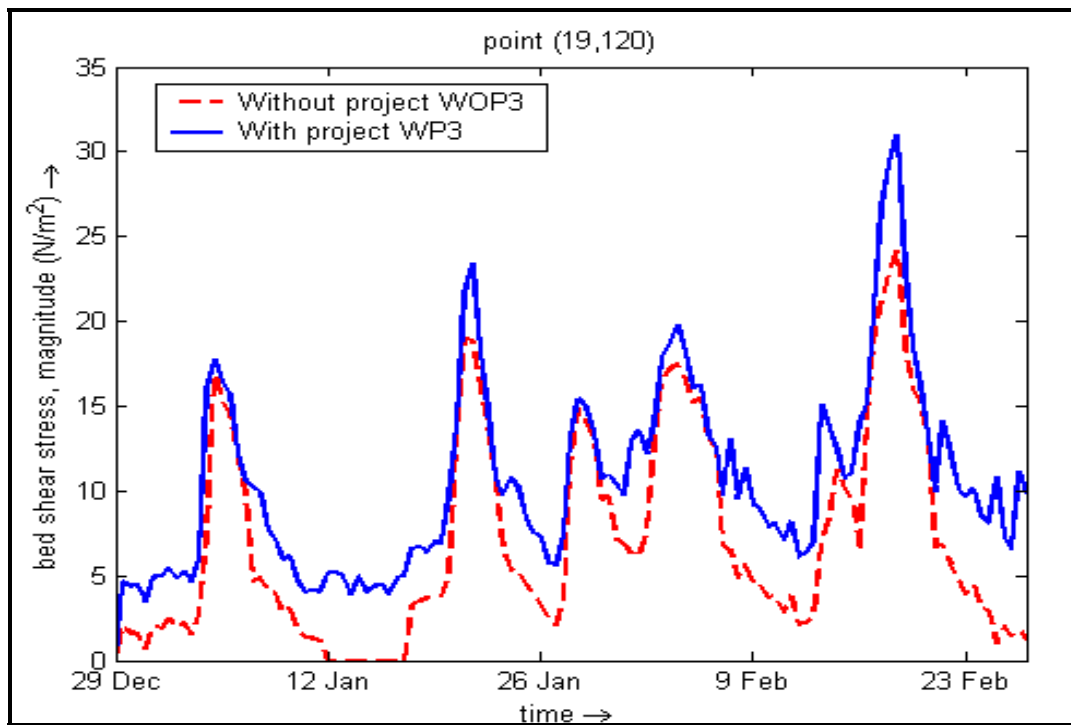


Figure 6.20: Time varying bed shear stress at specific point (19,120) in the river for both of (with project) and (without project) cases.

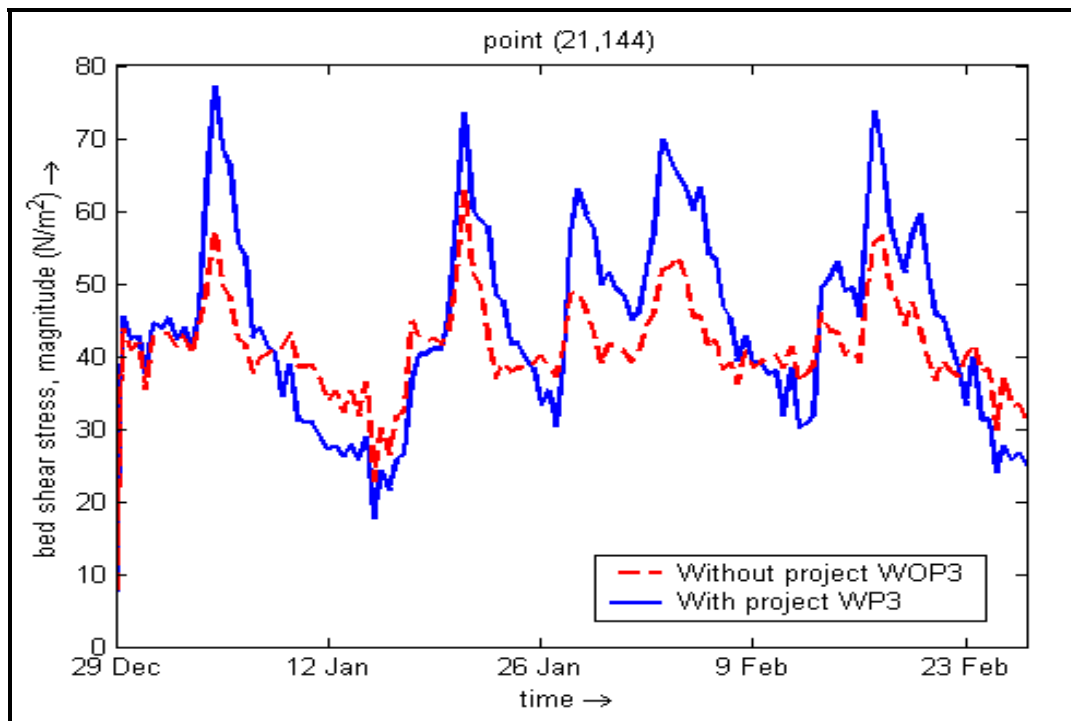


Figure 6.21: Time varying bed shear stress at specific point (21,144) in the river for both of (with project) and (without project) cases.

In the Figures 6.23 through 6.26, the dashed red lines represent the time varying bed shear stresses for the without project situation and the solid blue lines for with project situations. The locations of the different points can be noted from the explanatory Figures different points upstream, at location and downstream of excavation respectively for with project and the blue lines are the same for without project situation. From Figure 6.23, which is the point upstream of excavation (see Figure 6.22), the bed shear stress for with project is almost same as of without project, while the bed shear stress for without project case is much higher at location of excavation than with project (see Figure 6.24). Figure 6.25 shows the bed shear stresses at the outer bend near to the location of erosion of Belgium bank, and it can be concluded that the erosion was due to the project implementation because the bed shear stress is increased in that location. The difference between both cases in the Figure 6.26 is very large at the point downstream of excavation, which probably the erosion will be more in the with project situation.

6.5. Comparison between with project situation (according to Delft2D simulation) and field measurements

It is very important to compare the real situation (field measurements) with the simulation results with Delft2D, because the ability of the model can be tested in simulating the complex phenomena of morphological condition with graded sediment in a bends like Meers of the Meuse River with armoured bed which make the situation more complex, and it can be decided whether or not the above results obtained for both cases is reliable, especially when its important to determining the effect of the project on that location.

The final results of Delft2D of the morphological simulation studied in section 6.3.2 which was the case of studying 60 days morphology will be compared with the field measurements obtained from the input file of the WAQUA model for 2002 – 2003 schematization as shown in Figures 6.27 and 6.28.

From these two Figures it is not easy to decide whether the Delft2D model is good enough or not, because it is difficult to recognize the differences between the existing situation (WAQUA input file Figure 6.27 and the reproduced situation by Delft2D package Figure 6.28. For more detail it is better to zoom in the interested area (excavation area that indicated above) and then compare different bed topographies, as shown in Figure 6.29. Figures 6.30 and 6.31 are shows the relative difference between the cases with and without the project for both field measurements and Delft2D simulation results, respectively. The differences between the result of Delft2D and the existing situation are more clear in the Figure 6.32, it can be noted that they are not identical the pattern are mostly the same in the main channel and most parts of the flood plain. Most of the differences between the floodplains return to that the floodplain of field measurements 2002 – 2003 is combined with the main channel 1998 and used as input file to Delft2D and after the computation with the model some changes happen in the floodplain caused by sedimentation and erosion.

For more accurate results it is important to use the exact field situation of 2001 after the implementation of the project and before the flood of 2002 – 2003. Also in these computations all morphological changes between 1998 till 2001 are neglected because of non availability of data in that period.

The differences could not be neglected if a quantitative or precise results were necessary, but also they are not significant, while a qualitative results are important, and it can be

said its good for having a first idea about the phenomena that taken place in that location.

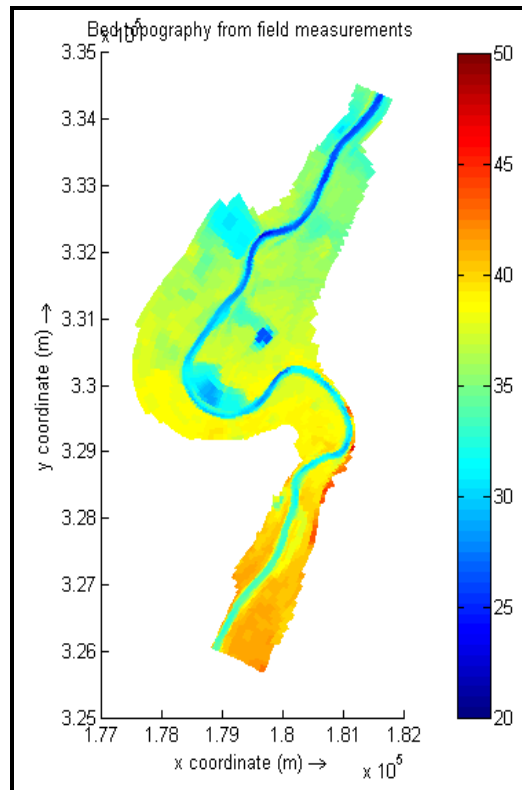


Figure 6.17: Bed topography of the river reach from field measurements (WAQUA model input file).

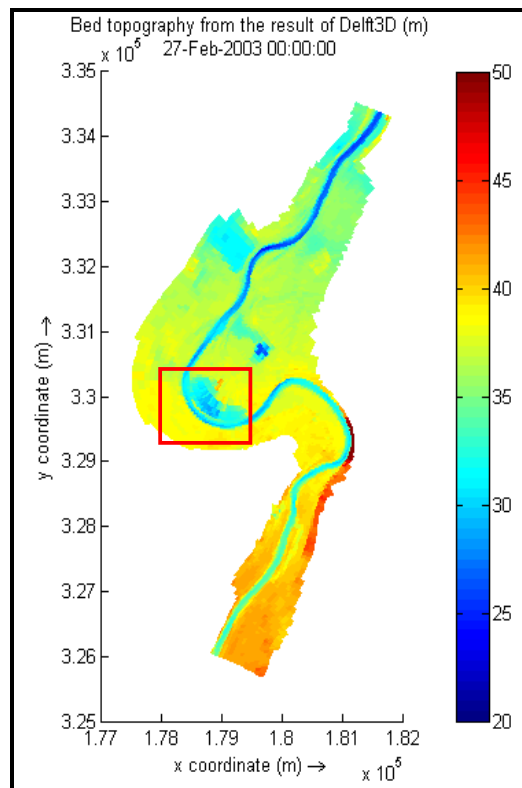


Figure 6.18: Bed topography of the river reaches (Delft3D result of 10 days morphological time).

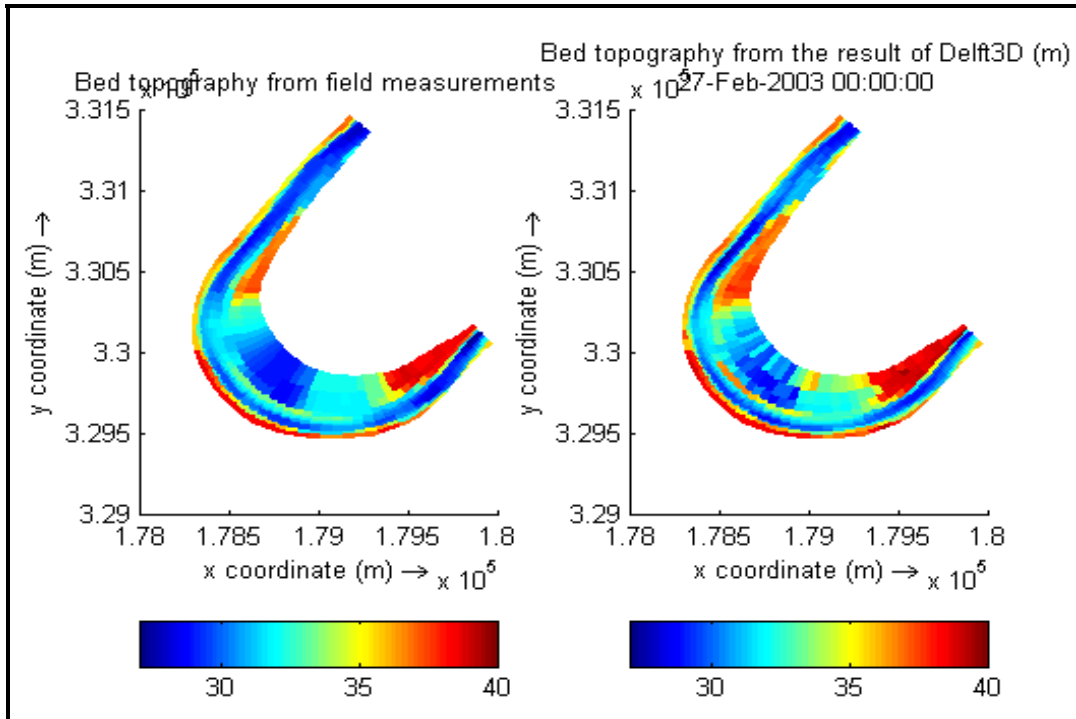


Figure 6.19: Bed topography of the river reaches for both Delft3D result and field measurements.

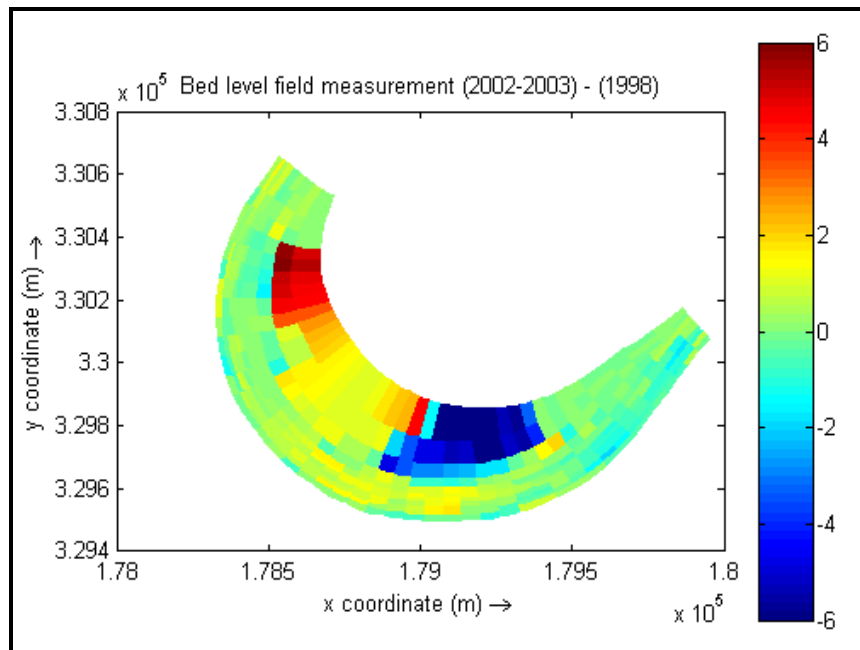


Figure 6.20: Bed level difference between 1998 (before the project) and 2002-2003 (after the flood) from field measurements.

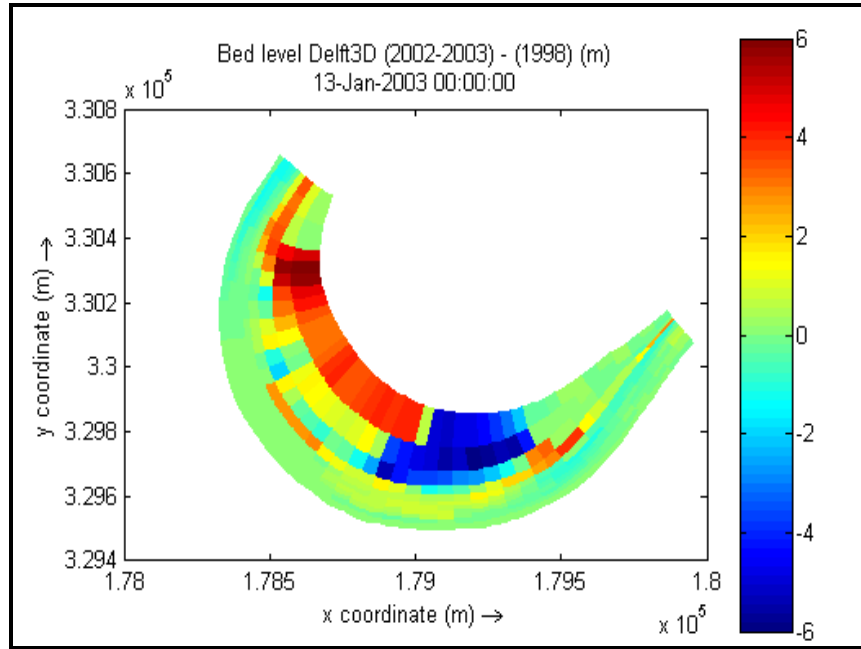


Figure 6.31: Bed level difference between 1998 (before the project) and 2003 (after the flood) Delft3D simulations (cases WOP and WP).

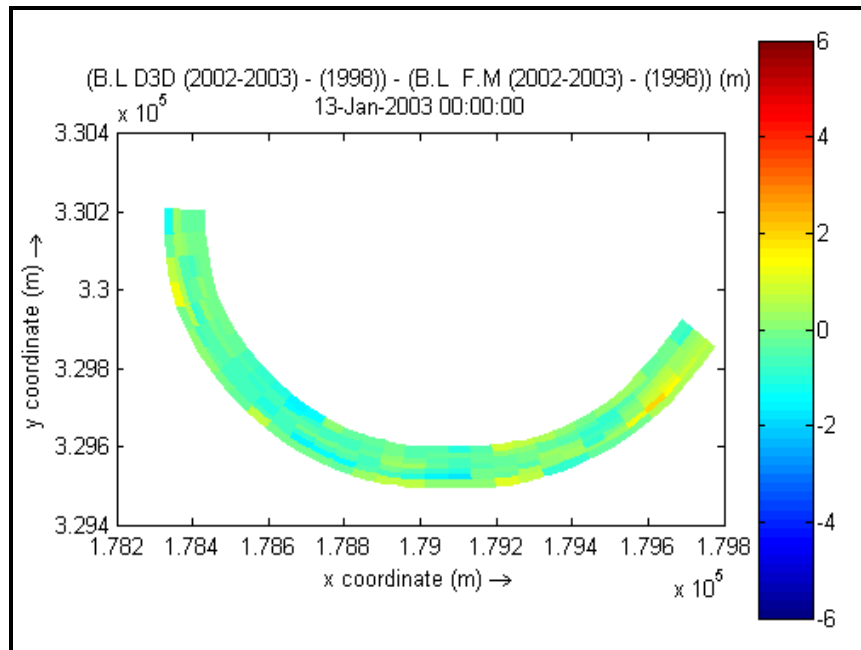


Figure 6.32: Difference between bed level of the river reaches for both Delft3D result and field measurements.

Figure 6.32 shows the difference between the bed topography after the flood resulting from computations with Delft3D and the field measurements, and if we note to the Figure we can see easily some differences which mostly caused by the reasons mentioned above and also some uncertainty of the model, because all required calibrations and verification tests were not done for the model.

6.6. Bed material sorting

Bed material sorting is one of the important result that it can be showed in the numerical computations, but unfortunately there are not any data to compare with the results which obtained from the model, and the Figures which are shown below, are not represent the exact sorting in the reality but they are interpretations of the model.

It was not possible (at this time) to collect the sorting of all sediment fractions that inputted to the model in vertical direction, but the percentage of each fraction can be shown for each layers (top layer, sub-layer 1 and sub-layer 2) for the case with project at the end of the simulation as shown in the figures 6.33a-6.33e.

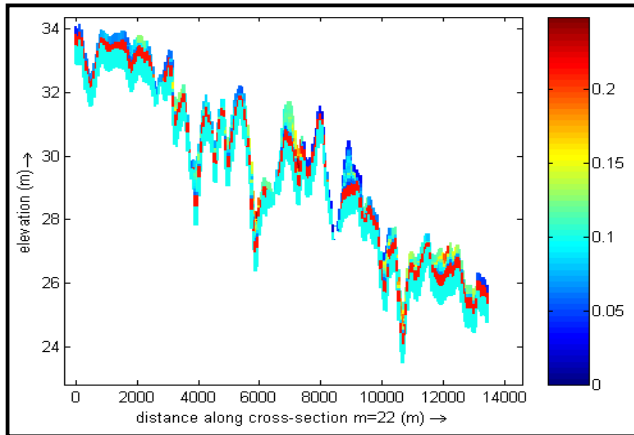


Figure 6.33a: Percentage of fraction ϕ (0.5mm – 2mm) in the longitudinal section of the river.

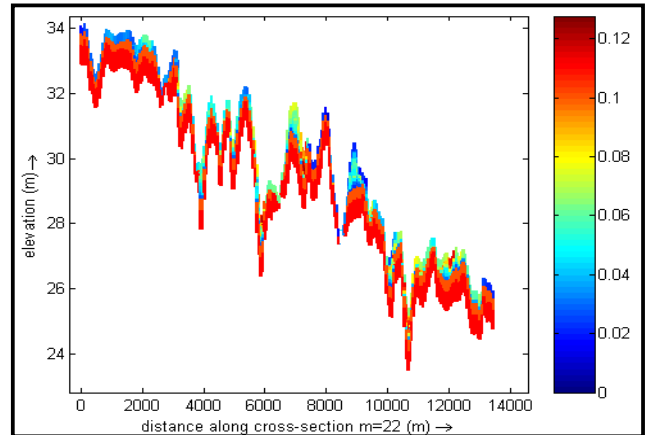


Figure 6.33b: Percentage of fraction ψ (2mm – 4mm) in the longitudinal section of the river.

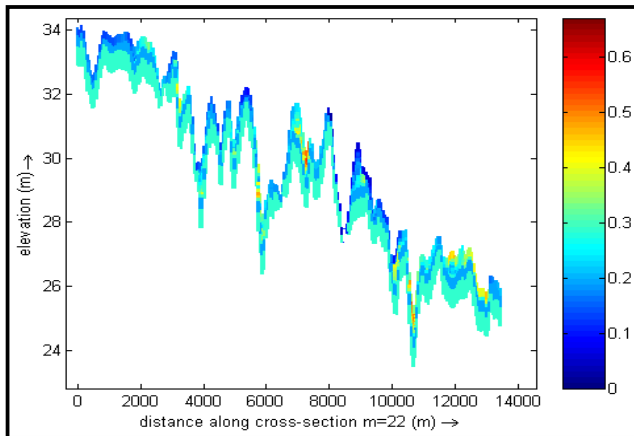


Figure 6.33c: Percentage of fraction χ (4mm – 8mm) in the longitudinal section of the river.

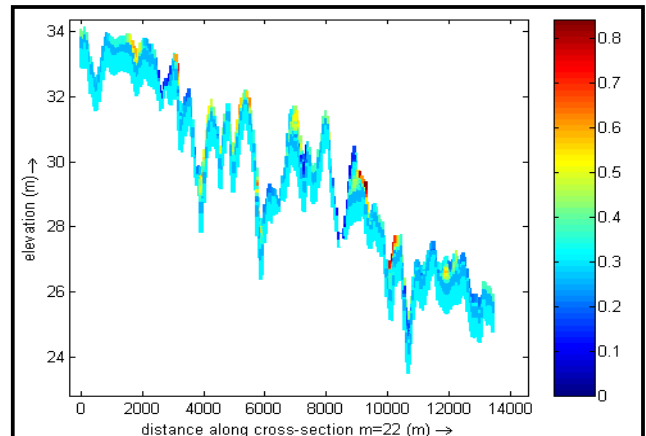


Figure 6.33d: Percentage of fraction ξ (8mm – 16mm) in the longitudinal section of the river

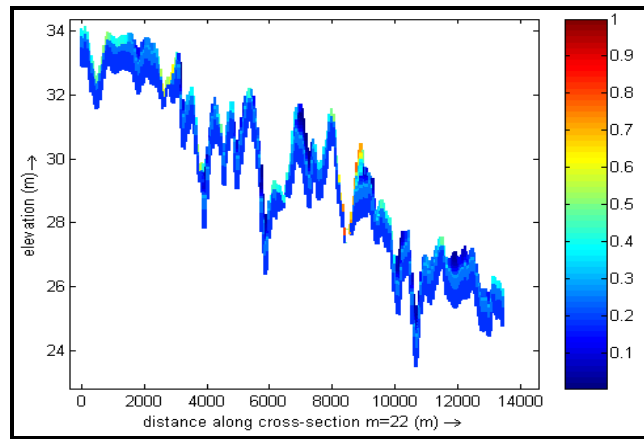


Figure 6.33e: Percentage of fraction ϕ (4.75 mm – 11.0 mm) in the longitudinal section of the river.

The sorting of material in the longitudinal direction of the river is shown in the Figures above almost at centre of the river, it will not be relevant to show Figures for all longitudinal and transverse cross-sections of the river.

The horizontal sorting of bed material can be determined as the arithmetic mean of the transport layer (active layer), as shown in the Figure 6.33 and 6.34 for the cases with and without project, respectively.

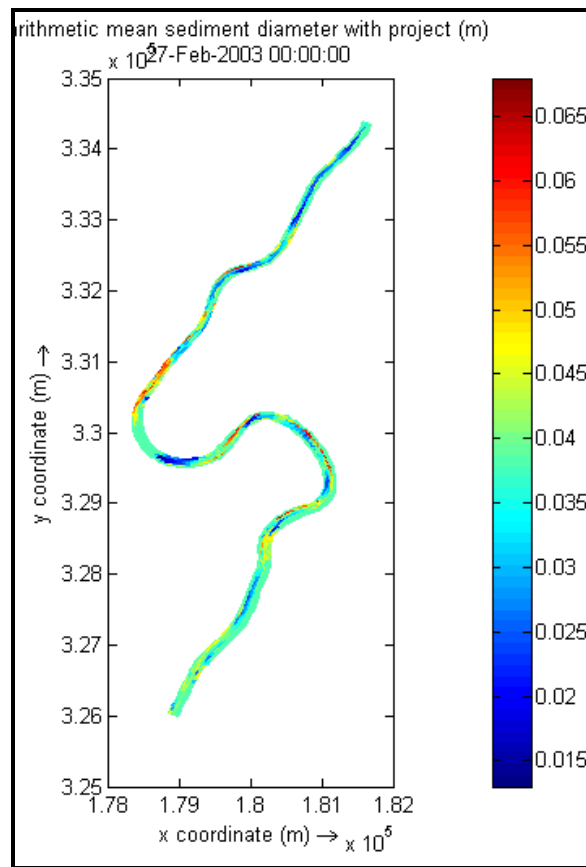


Figure 6.34: Arithmetic mean of bed material (transport layer) for the main channel and banks of the river for with project situation.

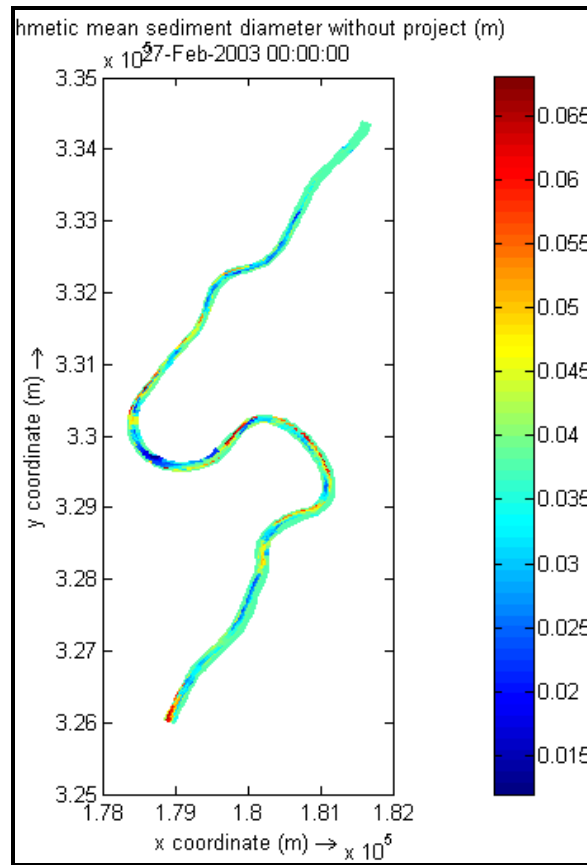


Figure 6.30: Arithmetic mean of bed material (transport layer) for the main channel and banks of the river for without project situation.

v. Discussion

v.1. General

This thesis addresses the morphological processes in the Meuse River near the Pilot Project Meers during 2002 – 2003 floods. The main purpose of the study was to reproduce the phenomena observed during and after these floods by applying numerical modelling (software package Delft2D Graded), for determining the ability of the software in designing floodplain lowering along Common Meuse. In addition, and only if time allowed, it was intended to investigate preventive and/or remedial measures.

The Common Meuse River is characterised by complex morphological phenomena due to the extreme gradation of the bed material and bed armouring in combination with sharp bends creating strong 2D effects. Sometimes it is not easy to figure out what are the possible effects of any project or measures in the river and/or in the floodplain close to the main channel by simple calculations using some sort of empirical relations. Then it is important to go one step further by using numerical or scale models.

As mentioned above in this thesis Delft2D was used for reproducing the existing situation (qualitatively) in the Meuse River at Meers, which caused after implementing the Pilot Project Meers in the floodplain area near to the main channel (floodplain lowering) as a part of the re-naturalization of the Common Meuse (in combination with flood control and sediment mining).

The methodology adopted in this thesis was simulating the situations with and without the project and later comparing the results for determining the effect of the project implemented at this specific location. Next to compare the results of the case with the project with the situation in the river after the floods for investigating the performance of the model.

In this Chapter the results which were presented in Chapter 4 are discussed in some detail. In addition some more general issues related to this project are raised. The following aspects are included in the discussion:

- model setup
- Comparison between uniform and graded sediment simulations
- model calibration and verification
- impact of the Pilot Project Meers
- comparison of results of simulations with field observations
- Proposed future data collection
- preventive and remedial measures
- Future study

4.2. Model setup

In developing the model setup a number of steps have to be taken which have a direct effect on the results. Therefore it is very important to study the effect of each of them carefully before using them. This holds for items like the grid generation, the selection of the time steps and initial and boundary conditions.

In this study the grid generation was not an easy task at all, because the area of interest consists of two sharp consecutive bends with opposite curvature which limited the possibility to refine the grids, when taking into consideration some important parameters in this respect like orthogonality and smoothness of the grid cells. The grid generation has a direct effect on the stability of the computations and on the accuracy of the results. However, refining the grids too much needs more computational time. Computational time was also critical in this particular study. Whereas coarsening them leads to less accurate results, because if there will be some changes in a small area of the model either its effect will not be apparent or it will be overestimated by taking larger area within the model.

The time step usually affects the computational stability of the model, and it has to be checked carefully in order to get reasonable results. Time steps can be checked according to the Courant number and it first should be tested for hydrodynamic condition. As shown in Chapter 5, the hydrodynamic restriction is that the Courant number should be smaller than 1. The size of grid cells has a large effect on the Courant number and time step, but sometimes (like in this research) the minimum grid dimensions are located far from the area of interest which allowed us to increase the time step and to reduce the overall computational time of the different simulations.

Initial conditions should be treated very carefully, because they consist of different items which affect the result of the model in different ways, such as the initial bed topography and the roughness. In this type of steep gravel-bed river it is important to include the armouring phenomena and bed composition in the initial condition, if possible. In principle the model should initially run for some time allow for armour development. The simulations of the morphological phenomena without and with the project could then have been done by using the output of initial computation as an input file of next ones. This however requires a user which is intimately familiar with the model. It is not easy for new users of the model, and this approach was not adopted in this study, mostly due to time limitations.

Also the applied boundary conditions might have a large effect on the overall results obtained from the model, because in this part of the model setup some important elements will be defined, such as the upstream and downstream boundary conditions. Under this study some sensitivity analysis was carried out regarding the upstream boundary conditions (see Appendix A^o) and from the results it could be concluded that the inflow hydrograph has a large effect on the model outcomes. Hence it should be

selected carefully according to the requirements, especially in the case of studying the design alternatives for floodplain lowering.

4.3. Comparison between uniform and graded sediment simulations

It is important to study the behaviour of both uniform and graded sediment with Delft2D and their effect on morphological condition of the river. For that reason we will compare the case of WOP1 (without project for 10 days hydrograph), with the other simulation using uniform sediment with $D_{50}=26$ mm for the same hydrograph. Some of the results are shown in the figures 4.1 and 4.2.

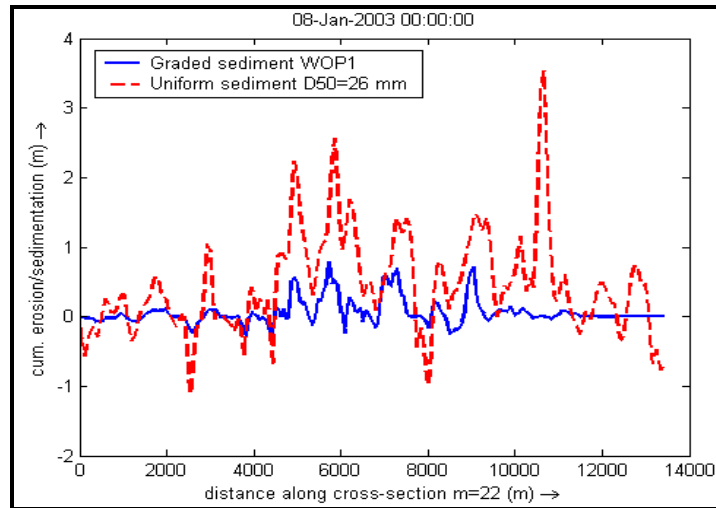


Figure 4.1: Cumulative erosion and sedimentation along the longitudinal profile of the river at centre of the main channel (zero value is located at km 14.0 of the river).

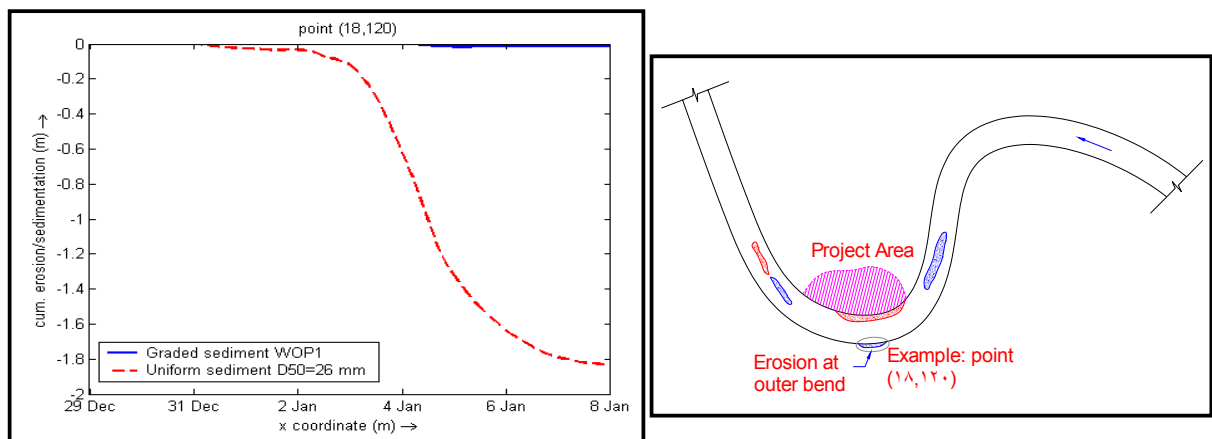


Figure 4.2: Cumulative erosion and sedimentation at outer bend (Belgium bank) for a point (18,120).

It can be easily concluded from the above results that there are large differences between the results of graded and uniform sediment; the quantities are much larger for the case of using uniform sediment in the river. Then it is important and more logic to focus on graded sediment in the Common Meuse because it is the major character of this river reach.

The overall computational time needed for the case of uniform sediment is almost one third compared with the computational time for graded sediment.

5.4. Model calibration and verification:

Calibration and verification of the numerical model can be considered as the key factor determining the accuracy of the model, because in this phase the model behaviour can be studied in a comprehensive way. The accuracy of the results can be controlled by varying the value of some important parameters and by studying the sensitivity of the model for each parameter for obtaining a proper choice for these parameters when using the model.

An **ideal model** needs different kinds of calibration tests, starting from an assessment of the flow condition, continuing with calibrating the transport formula, and finally ending up by calibrating some important parameters that have direct effect on morphological conditions.

Calibrating the flow is generally done by calibrating the roughness of the main channel and the floodplain together. This can be done in a straightforward but not correct and accurate way by specifying a constant value for the roughness coefficient for both the main channel and the floodplain. A more accurate calibration of the roughness coefficient can be applied to the model by defining different values for the roughness of each grid cell within the model, but the preparation of such a roughness file needs substantially more time. Moreover it requires a detailed insight in the flow field during different stages and usually such detailed information is not available.

Every transport formula contains some parameters that have a direct effect on the results. A Meyer-Peter & Müller (MPM) type of formula is used in this specific study, because the objective of the model was focused on bed material load and graded sediments. The first parameter to be selected in a MPM type of sediment transport predictor is the overall calibration factor (TRF). With this factor the transport rates can be controlled between the measured and the computed ones. This factor will directly affect the sediment transport magnitude. This has one-to-one effect on the time-scale of morphological development. The second parameter is the ripple factor (μ) which represents the percentage of the total shear stress that due to the particle roughness. The other contribution to the roughness is caused by the bed forms (dunes). The relative contribution of the particle roughness to the total roughness decreases as the dunes become larger. A smaller ripple factor will lead to less sediment transport and smaller morphological changes. The third and last parameter is the critical Shields parameter θ_{cr} which determines the hydraulic conditions at which sediment is entrained. A lower critical Shields value will increase the total sediment transport.

It is important to mention here that for the Common Meuse only the calibration of TRF was done, because the others two coefficients are less suitable to vary: the critical Shields parameter θ_{cr} is an experimentally determined value and the ripple factor μ

should not be of any influence in the Common Meuse because of the supposed lack of dunes in this river reach.

In principle also a calibration of morphological parameters should be carried out and the value of the different parameters (e.g. for the value of A which determines the lateral slope) should be selected. Another parameter to determine is the active layer thickness. This parameter influences the rate at which the composition of the transport layer adjusts to the conditions in the river. Therefore, it also influences the rate at which morphological changes move further downstream. A thin layer will be able to coarsen much faster than a thick layer. This difference in time influences the magnitude of the morphological effects, and some other parameters. Another important parameter to fix is the morphological time scale factor (MORFAC), which speeds up the morphological changes.

In this particular study a full calibration was not done due to a combination of limitations in the availability time and in adequate data. But some exploring tests were done for some parameters as is explained hereafter.

A rough calibration was made for Chézy coefficient for the main channel (see section 2.2 for more detail). In this calibration the Chézy coefficient for the main channel is changed from $40 \text{ m}^{1/3}/\text{s}$ to $45 \text{ m}^{1/3}/\text{s}$, while a value of $36 \text{ m}^{1/3}/\text{s}$ was applied for the floodplain. Changing the roughness of the main channel has a significant effect on the water levels in the main channel which lowered about 0.2 m at peak flow condition. The problem is however that no measurements were available for a complete calibration. Therefore the results were compared with the results of WAQUA flow model, and in the end $40 \text{ m}^{1/3}/\text{s}$ for main channel and $36 \text{ m}^{1/3}/\text{s}$ for floodplain were selected.

As mentioned before a MPM type of sediment transport formula was used in this study. Earlier some calibration tests were made before for Meuse River by WL/Delft Hydraulics), the MPM predictor was found to be the best for our conditions with the overall calibration factor (TRF) of 0.5 , because it was realized that this formula (but with $\text{TRF} = 1$, no correction) gives twice higher sediment transport rates than observed with measurements.

Some sensitivity analysis was carried out to select the morphological time scale factor using different values for this factor (1 , 2 , and 4); although according to the Delft 2D manual the maximum value of this factor can be as high as about 1000 . But this was not the case in this study, because significant differences were noted when using $\text{MORFAC} = 4$. This is mostly due to the fact that while the inflow hydrograph is squeezed, it affects the hydrodynamic condition of the model (a distorted hydrodynamic condition) and the interpretation of this effect is not easy. Also when $\text{MORFAC} = 2$ is used some small differences were noted, and they are mostly caused by speeding up the morphological changes. The changes in the case of using factor 2 were not significant but they are not negligible either when quantitative results are expected from the model. As mentioned several times before in this study in particular qualitative results were

required rather than quantitative ones. Moreover the collection of data required for the model took more time than expected which limited the time available for the actual simulations. So it became a matter of balancing some inaccuracy of the results versus the computational time of the simulations. Finally MORFAC = ξ was used.

Appendix (A^v) is an example of an input file for the model and the value of the different parameters is specified in this file.

4.5. Impact of the Pilot Project Meers

In Chapter 4 most of the results are presented for the two situations considered notably the case with and the case without the project. Comparisons were made of the morphological changes (results presented in the Sections 4.2.2 & 4.3.2) using the results of 30 days hydrograph. First the comparison was made between the cases with and without the project (for more detail see Section 4.4), and as shown in the Figures (4.10 through 4.26) there are indeed **some** differences between the situations with and without the project. These differences are small in some area and large in the others.

In the without project situation there are some morphological changes which were unexpected, but the major cause for that is that in this model the composition of the bed was not varied spatially. The likely variation could not be introduced, because no information on armour layers in the river bed was available and hence this could not be defined as an initial condition of the model. Also the model does not have enough time to develop this armour layer because of the restriction in time for the simulations.

From the above explanation we can conclude that probably the differences between the cases with and without project situation results from the model is underestimated in some parts of the river. If all required information and sufficient time had been available, these differences could have been much large due to reduction in changes for the without project situation.

Nevertheless still some significant effects of the project on the river morphology can be noted from the results. These effects if some measures had been implemented before the project, such as a protection of the river bed upstream of the project and at the location where the water flows back to the river to reduce erosion. By reducing erosion at upstream of the project the sedimentation at the inner bend near to the project area could have been reduced.

4.6. Comparison of results of simulations with field observations

It is important to test how good the model is able to simulate the actual conditions in the field. For that purpose a comparison between the outcome of Delft2D and the field measurements (determined from the WAQUA model input file implemented after the flood occurrence) was made (see Section 4.5). In this comparison it can be noted that

although the results are not identical, they are quite close to each other as far as the pattern is concerned. That it can be easily judge the model for qualitative results.

The major cause of these differences between Delft2D results and the observed morphological changes can be brought back to the fact that the floodplain area determined by field measurements after the flood 2002 - 2003 in combination with the main channel configuration of 1998 was used as input file for the model to represent the case after the project and before the flood, because the bed topography data for the case after the project and before the flood was not available. But in reality probably both the floodplain and the main channel are not completely alike the ones used. There are large uncertainties in this choice, because in the input file the morphological changes between 1998 till 2001 are neglected in the main channel while there are some floods peaks reaching to more than 2000 m³/s in that period (see appendix A¹). Also the floodplain used is in fact corresponding to the conditions after the flood. This means that some sedimentation is already included before the simulation with the model was started. Any other sedimentation in that area will be appearing as a change between the result of the model and the field measurements bed topography.

The bed material sorting is one of the more interesting results from the simulations with the model. There are some Figures presented in Section 6.6 representing the vertical sorting for different sediment fraction in the different layers defined in the model. Moreover some other Figures shows the horizontal distribution of D₅₀ of the transport layer. Unfortunately however in the case of vertical sorting it was not possible to combine all fractions together, because this option is not implemented yet in the Delft2D quick plot. Furthermore there were no field data to compare with these results. *Finally it can be said these results are just the interpretation of the model for bed material sorting.*

Some others sensitivity analysis was carried out for studying the effect of inflowing hydrograph which mostly important for the case of studying alternative design cases for future flood plain lowering. It can be noted from the result which are shown in Appendix A² that the inflow hydrograph has a significant effect on the morphological changes, and some careful decisions are required for selecting what type of hydrograph should be implemented in the model for studying the effect of the future design of floodplain lowering.

4.4. Proposed future data collection

In order to prepare a good model it is important here to hit the data which are necessary to be available for the purpose of setup, calibration, verification and comparing the model with the real situation. An overview of these data is shown in table 4.1.

Situation	Data to be collected
Before the flood	<ol style="list-style-type: none"> 1. Bed topography 2. Bed and bank material compositions, preferable to have some boreholes for investigating the soil layers. 3. Thickness of armour layer (in gravel bed rivers). 4. Roughness coefficient and information on vegetation in the floodplain area. 5. Location of protection works implemented (if before also) in the selected reach. 6. Other discharges inter to the selected river reach.
After the flood	<ol style="list-style-type: none"> 1. Bed topography, considering natural morphological changes and human interventions 2. Information on vertical and horizontal sorting. 3. Sediment rating curve.
During flood	<ol style="list-style-type: none"> 1. Sediment transport measurement inside the river reach and also from upstream. 2. Water level close and inside the interested area. 3. Time varying morphological changes, (for indicating the effect of each individual discharge on morphology).

Table V.1: Necessary data to be collected for the study at different time intervals

V.A. Preventive and remedial measures

Based on the understanding of the cause of the problems experienced during and after the floods in 2002-2003, it is possible to propose some preventive and/or remedial measures. These measures are listed in the below Table V.1, together with an indication of their working principle and advantages and/or disadvantages.

Possible preventive or remedial measures	Working principle	Advantage	Disadvantage
Bed protection of channel upstream of Pilot Project	Eliminate erosion of the bed, thus causing that less or no sediment is available downstream and hence no bar can be formed downstream	Permanent solution	(1) Creation of a hard point in the river (2) Reduced sediment dynamics, loss of ecological values
Reduction of inflow into Pilot Project Meers area via guide wall on right bank	Reduce reduction of transport capacity in main channel due to smaller flow through the floodplain	(1) Reduced sedimentation and hence smaller bar in inner bend (2) Substantial sediment dynamics in the river	(1) Reduced flow towards the Pilot Project: loss of ecological values?
Bank protection works	Prevent that the	Permanent solution,	None?

along Belgian border, preferably in form of revetment and falling apron	Belgian bank will be undermined	which still allows for some flexibility	
Excavation or dredging of bar along inner bank after major floods and dumping of spoil along Belgian bank	Removal of bar and use of spoil on the other side moves the current during lower flows away from the Belgian bank	Substantial sediment dynamics in the river	Has to be done regularly; needs attention

Table ∇.∇: Possible preventive and/or remedial measures for the Pilot Project Meers

∇.∇. Future studies

Due to the necessity of collecting and improving our knowledge about the phenomena and the problems in the in the Pilot Project Meers, in futures there are several studies are important such as:

- Studying the implementation of the measures and comparing the with the field measurements.
- Studying morphological changes for longer period of time.
- Studying design alternatives for the Pilot Project Meers and expanding them to the other locations along Common Meuse.

8. Conclusions and Recommendations

8.1. Conclusions

In the present study it was attempted to simulate the morphological changes in the Meuse River due the Pilot Project Meers during a number of floods in the period 2002-2003. The simulations were carried out with the modelling package Delft2D Graded, which implies that 2D flow, but including spiral flow via a quasi-3D approach, and 2D morphological phenomena could be simulated, whereas also sorting (vertically and in longitudinal and lateral direction) is included in the model. Based on the present study a number of conclusions can be drawn.

On the morphological changes in the Meuse River near Meers

- The simulations with a real 60-days hydrograph confirm the observations in the field after the 2002-2003 floods (including the emergence of a bar on the inner bank near the Pilot Project, the erosion in the outer bend and the deep scour where the flow over the floodplain enters again into the channel again).
- Hence, the overall results of the model can be considered as reasonable to good when related to the requirements of the study, where in particular qualitative results were required.
- Some of the differences between the model simulations and the conditions in the field after the 2002-2003 floods might be explained by the procedure used for obtaining representative input data for the model. Especially for the case with the project exact data after the project implementation and before the flood were not available. In this case a combination between the main channel of 1998 WAQUA schematization and the floodplain configuration of 2003 was made, thus ignoring all morphological changes between 1998 till 2001. This might have had some effects on the results.
- Another reason for differences might be the fact that probably the simulation without the project was not corresponding to an equilibrium condition. As a consequence morphological changes are a combination of the effect of the non-equilibrium initial conditions and the effect of the Pilot Project. The applied method of subtracting the without case from the case of with project case is formally only allowed when dealing with linear phenomena. Morphological changes, however, are notoriously non-linear.
- Nevertheless, the present model seems to be good enough for getting a first idea about the consequences of projects and/or measures similar to the Pilot Project Meers which might be implemented along the Common Meuse River.
- The model can also be used to test the effect of any preventive or remedial measures.

On the modelling with Delft 2D Graded:

- A morphological factor is introduced in the model, which allows speeding up the morphological simulations. The morphological factor, however, has an effect on the simulated morphological changes in the river, when selected too large. This holds especially when a hydrograph is used as upstream boundary

condition. Hence a careful decision on the value of the morphological factor to be used is required.

- Inflow hydrograph has a large effect on the morphological changes in the river. For better results longer periods with realistic hydrographs should be studied.
- Because of the absence of sufficient field data it was not possible to calibrate the model properly. A proper calibration should separately consider the flow pattern, the sediment transport and the morphological phenomena. Each of these processes has their own calibration coefficients. In this case without detailed field data these coefficients were set an optimal combination of values. Preferably a verification run should be carried out.
- A better calibration might be affect the outcome of the modelling study and might give more accurate results. In this particular study neither the required data nor sufficient time was available. Consequently some of the comparisons were made with another model (WAQUA), which might have induced additional uncertainty and inaccuracy.

On preventive and remedial measures

- In this study preventive and remedial measures could not be explored via model simulations due to time limitations. However, because the cause of the experienced problems was identified via the simulations carried out, it is possible to propose preventive and/or remedial measures.
- The emergence of a bar in the inner bend of the river can be counteracted by giving the river channel a better guidance between km (30) and km (33), which will limit the reduction in transport capacity. This should be balanced against the loss of ecological values.
- The dimensions of the emerging bar in the inner bend near the Pilot Project are determined by the sediment generated in the narrow reach upstream of the project. Provision of a bed protection in this reach will stop the erosion upstream and hence prevent the emergence of the bar.
- Dredging the bar in the inner bend and dumping the dredged spoil along the Belgian bank (after a flood) will reduce the erosion near the Belgian bank. If selected, this method may have to be repeated after future major floods.
- The Belgian bank, which potentially may or can be undermined, can be strengthened by placing additional revetments, if needed in combination with a falling apron.

4.2. Recommendations

Based on the results of the present study a number of recommendations can be formulated.

- If the results of the present study were to be used for the design of preventive or remedial methods for the problems experienced along the Belgian bank, the model should be improved via better calibration and additional simulations under different conditions.
- It might be considered to protect the location of possible erosion with particles which can not be moved by higher flow, in order to reduce erosion in the main channel and this will reduce also the sedimentation quantities.

- The results already available presently allow for the development of better designs of the next projects along the Meuse River.
- Additional field data are needed, in particular data on the composition of the bed material (notably its composition and the thickness of transport layer), because these are of great importance for proper simulations and good comparisons between model and reality in this study area.
- Further investigations for specifying a design case scenario for floodplain lowering considering different flowing hydrographs are needed, because both the floodplain lowering and the flow hydrographs have a significant effect on the morphological phenomena in the river.
- The necessary calibration tests should be done for the model and the updating the calibration parameters should be carried out before using the model for designs. Moreover the model results should be compared with actual field measurements.
- Sediment transport rates computed in the present simulations should be compared with sediment transport measurements by Duizendstra et al (1997)
- In this study no attention was paid to the forming of two cut-off channels downstream of the project area as occurred during the 2002-2003 floods. It is recommended to make a separate study into the occurrence of these channels to arrive at guidelines for the minimum distance between deeper lakes and the main channel.
- It could be considered to verify Delft2D Graded on the basis of the physical model of a part of the Common Meuse River, which was operated at WL/Delft Hydraulics in the period 1994-1996.
- Some 2D computation should be made for determining the accuracy of 2D modelling applied in this study, and for identifying the major deficits of the 2D model.
- Some morphological simulations should be done for longer duration also to study sediment transport phenomena in the Meuse River during and after floods.
- It might be considered to implement an exchange layer in Delft2D package, and doing some simulations with and without this layer to identifying the effect of it on the long and/or short term morphological study.
- Sediment transport should be measured near to the project area in order to better calibrating the model with more reliable data and gives more reasonable results,
- Preparing and including all necessary information in to the model such as (real roughness map, effect of ground water, all geometric features in the floodplain, additional discharged that enter to the river in different locations, which might have some effect on the results.

References:

Ackers, P. and White, W.R. (1973) "Sediment transport, new approach and analysis", Proc. ASCE, JHD, HY11.

Aguirre-Pe, J., and Fuentes, R. (1990). "Resistance to flow in steep rough streams", Journal of Hydraulic Engineering. 116 (1), P.1374-1387.

Andrews, E. D. (1984) "Bed material entrainment and hydraulic geometry of gravel bed rivers in Colorado", Geological Society of America in Bulletin. 90, p. 371 - 378.

Ashida, K., and M. Michiue (1972). "Study on hydraulic resistance and bed load transport rate in alluvial streams". Trans. Jpn. Soc. Civ. Eng. 26, p. 69 - 79.

Bathurst, J. C., Graf, W. H., and Cao, H. H. (1987). "Bed load discharge equations for steep mountain rivers." Sediment transport in gravel bed rivers, C. R. Thorne, J. C. Bathurst, and R. D. Hey, eds., Wiley, New York, Chap. 10, 403-491.

Berkhout, W. A. (2003) "Modelling of large-scale morphological processes in sand - Gravel Rivers", MSc. Thesis, University of Twente.

Bettess, R. and White, W.R. (1981) "Mathematical simulation of sediment movement in streams", Proc. Instn. Civ. Engrs., part 2, 71, Sept.

Chiew, Y., and Parker, G. (1994) "Incipient sediment motion on non-horizontal slopes." J. Hydraulic Res., 32-01, 649-660.

Day, T.J. (1980) "A study of the transport of graded sediments", HRS Wallingford Report No. IT 190, April.

Deigraad, R. (1980) "Longitudinal and transverse sorting of grain sizes in alluvial rivers". Technical University of Denmark, Lyngby.

Dey S., (2003). "Threshold of sediment motion on combined transverse and longitudinal sloping beds" Journal of Hydraulic Research Vol. 41(4), p. 400-410

Di Silvio G. and Peviani M.A. (1989), "Modelling short - and long term evolution of mountain rivers: an application to the Torrent Mallero (Italy)". International workshop on Fluvial Hydraulics of Mountain Regions.

Engelund F., (1974). "Flow and bed topography in channel bends". Journal of hydraulic division, ASCE, 100 (HY11), p. 1631 - 1648.

Einstein, H. A. and Ning Chein (1953). "Transport of sediment mixture with large ranges of grain sizes". University of California, Miss. Riv. Div., Sediment series No. 7.

Egiazaroff, I. (1960) "Calculation of non-uniform sediment concentrations". ASCE, JHD, HY 8, July.

Ferguson, H.A., Hoey, T. B., Wathen, S., Werritty, A. (1996) "Field evidence for rapid downstream fining of river gravels through selective transport". *Geology* 24(7), pp. 179 – 182.

Hirano, M. (1970) "On phenomena of river bed lowering and armouring below reservoirs". 14th proc. of Hydr. Lect. Meeting, Hatsumei, Kaikan, Febr.

Jervis, G. (2003), "Modelling of graded sediment transport". MSc. thesis, UNESCO – IHE Delft.

Karim, M.F., Holly, F.M. Jr. and Kennedy, J.F. (1983) "Bed armouring processes in I-ALLUVIAL and application to Missouri River, IIHR Rep. No. 269, Univ. of Iowa, Dec.

Kikkawa, H., S., Ikeda, and A., Kitagawa, (1996). "Flow and bed topography in curved open channel". *Journal of hydraulic division, ASCE*, 102 (HY 9), p. 1327 – 1342.

Klaassen, G. J. (1981) "Morphological phenomena Common Meuse River". Waterloopkundig Laboratorium, verslag R863 (in dutch).

Klaassen, G. J. (1987) "Armoured river beds during floods". *Eurmech* 210, Genova, Italy

Klaassen, G. J., Lambeek, J, Mosselman, E., Duizendstra, H.D., Nieuwenhuijzen, M.E. (1998). "Re-naturalization of the Meuse River in the Netherlands". Chapter 28 in: *Gravel-bed rivers in the environment*, Eds. P.C. Klingeman, R.L. Beschta, P.D Komar & J.B. Bradley, Water Resources Publications, LLC, Highlands Ranch, Colorado, USA, pp. 660-674

Lambeek, J. J. (1996), "Hydraulic and morphological investigation, Natural rehabilitation project Grensmaas", Delft Hydraulics.

Lesser G.R, Roelvink J.A., Van Kester J.A.T.M., and Stelling G.S., 2004. "Development and validation of a three-dimensional morphological model" *Costal Engineering* 01, pp (883-910).

Lyn, A. D. (1987). "Unsteady sediment transport modelling", *Journal of Hydraulic Engineering*. ASCE, 113 (1). P. 1 – 10.

Meyer-Peter, E., and Muller, R. (1948) "Formulations of the bed-load transport." 2nd Int. Congress, IAHR, Stockholm, Sweden, 39-64.

Middelkoop, H. (red), 1998. "Two rivers Rijn and Meuse in Netherlands". RIZA report 98. 41

Murillo – Munoz, R. E., (1998), "Downstream fining of sediments in the Meuse River". MSc thesis, UNESCO – IHE Delft.

Murillo – Munoz, R. E. and Klaassen G. J. (2003), "Downstream fining of sediments in the Meuse River". Proc. River flow 2003.

Paintal, A.S. (1971) "A stochastic model of bed-load transport", J. of Hydr. Res., 9, No. 4.

Parker, G. (2002). "Transport of gravel and sediment mixture". Sedimentation Engineering Manual Draft, chapter three, ASCE.

Parker, G. (1984). Discussion of "Lateral bed load on side slopes". Journal of hydraulic division, ASCE, 110 (HY2), p. 197 – 199.

Parker, G., and Andrews E., D., (1980). "Sorting of bed load sediment by flow in meander bends". Water Resource Research, 16 (1), p. 1361 – 1373.

Parker, G., and P., C., Klingeman (1982). "On why gravel bed streams are paved". Water Resource Research, 18, p. 1409 – 1423.

Powell, D. M. (1998). "Pattern and processes of sediment sorting in gravel bed rivers." Progress in Physical Geography, 22(1), p. 1 – 32.

Profitt, G.T. and Sutherland, A.J. (1983) "Transport on non-uniform sediment", Journal of Hydraulic Research, 21, No. 1.

Ribberink J. S., (1997). "Mathematical modelling of one dimensional morphological changes in rivers with non-uniform sediment". Delft university of technology, Faculty of civil engineering.

Rouse, H. (1939). "An analysis of sediment transport in the light of fluid turbulence." Soil Conservation Service, Rep. SCS-TP-20, U.S. Department of Agriculture, Washington, D.C.

Shields, A. (1936). "Anwendung der Aehnlichkeitsmechanik der Turbulenzforschung auf die geschiebebewegung", Mitt der Preuss. Versuchsanstalt für Wasserbau und Schiffbau, Berlin, Germany.

Sloff, C.J. Jagers, H.R.A., Kitamura, Y. and Kitamura, P. (2001) “2D morpho-dynamic modelling with graded sediment”. Proc. of 2nd IAHR Symp. on River, Coastal and Estuarine Morpho-dynamics 10 – 14 Sept., Obihiro, Japan

Swamee, P. K. and Ojha, C. S. (1991). “Bed load and suspended load transport in non-uniform sediments.” Journal of Hydraulic Engineering. ASCE, 117 (7). P. 774 – 787.

Taylor, B. D., and Vanoni, V. A. (1991). “Temperature effects in low transport flat-bed flows.” Journal of Hydraulic. Division, ASCE, 97, 1477–1480.

Thomas, W.A. (1977) “HEC-2 Scour and deposition in rivers and reservoirs”. Users manual, Hydrol. Eng. Center, US Army Corps of Engineers.

Weming, W., Sam, S. Y., Wang and Yafei, J. (2000) “Non-uniform sediment transport in alluvial rivers.” Journal of Hydraulic Research. Vol. 38 (7). P. 427 – 434.

Wilcock, P. R. (1993). “Critical shear stress of natural sediments.” Journal of Hydraulic Engineering, 119 (4), P. 491–500.

Yeh, K. C., Li, S. J. and Chen, W. L. (1990). “Modelling of non-uniform sediment fluvial process by characteristics method.” Journal of Hydraulic Engineering. ASCE, 116 (2). P. 109 – 114.

Appendixes

Appendix A

Case WOP: Using 10 days hydrograph

In this simulation we looked to the short term morphological changes due to the peak flow of 2002-2003 floods. The used hydrograph is shown in Figure A.1, and the results of this simulation are shown in Figures A.2 and A.3, which represent the cumulative erosion and sedimentation in the study area.

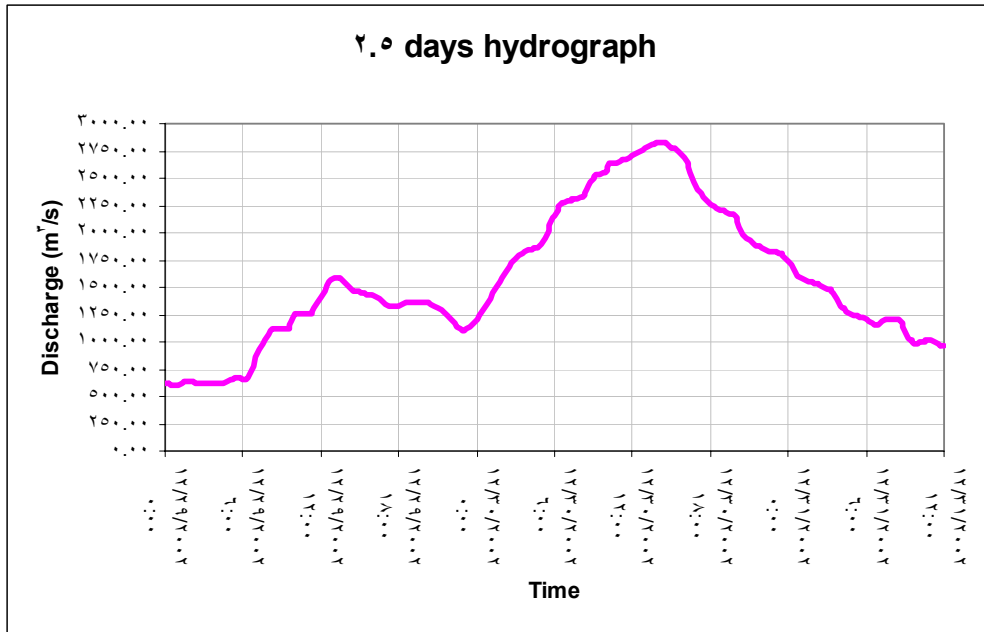


Figure A.1: Squeezed hydrograph of 2002-2003 floods by factor 10.

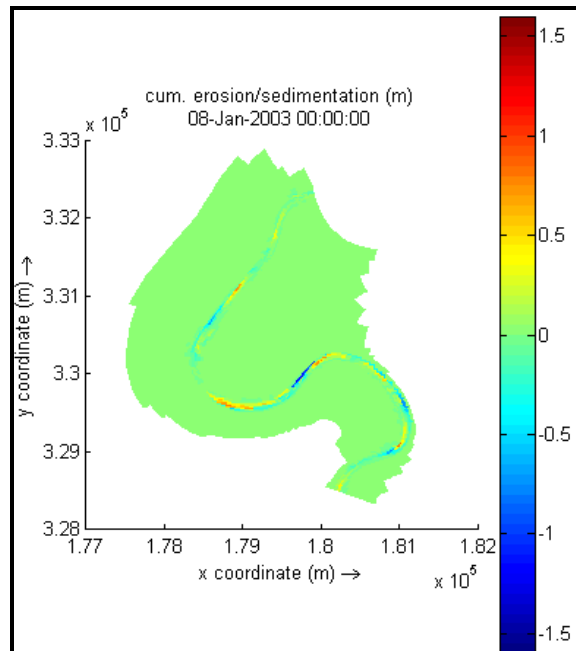


Figure A.2: Cumulative erosion and sedimentation for 10 days morphological study.

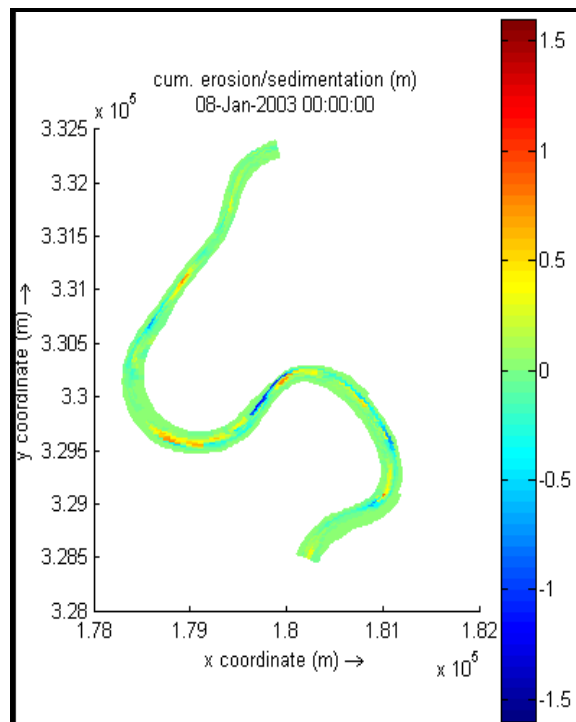


Figure A\'.5: Cumulative erosion and sedimentation for study in the main channel \'.5 days hydrograph.

In the Figures A\'.5 and A\'.5 we can note some patterns of sedimentation and erosion in different locations of the main channel (outer and inner bends). This might be because the initial condition of the bed material that introduced to the model is contain all fractions, and due to time limitation the model was not run with constant low discharge for obtaining the armouring phenomena.

Appendix A

Case WOP: Using 3 days hydrograph (with repeated hydrograph)

The idea of using this hydrograph came from the original hydrograph of 2002-2003, which is shown in Figure 6.1. There are some other peak flows at the beginning of 2002. Some of them are close to the maximum peak which occurred during 2002 and the beginning of 2003. As a trial we wanted to study the effect of these three peaks and put in two other peaks with the same magnitude with maximum peak. This gives a hydrograph with a repetition of the B flood (end 2002 – beginning 2003) with three similar peaks as shown in the Figure A2.1 below.

The results of this simulation are shown in Figure A2.2, which represent the cumulative sedimentation and erosion pattern after the repeated flood depicted in Figure A2.2.

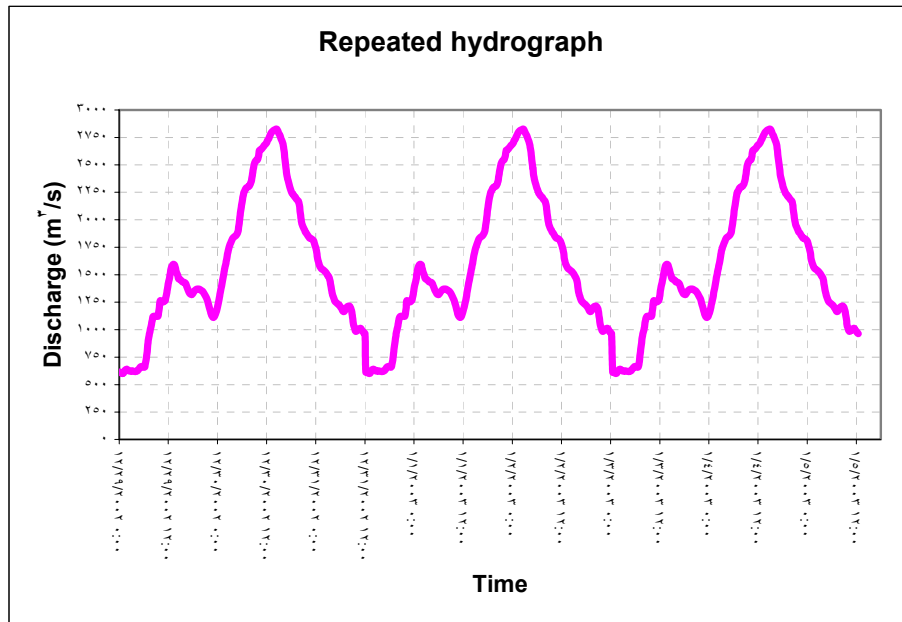


Figure A2.1: Repeated hydrograph of 2002-2003 floods.

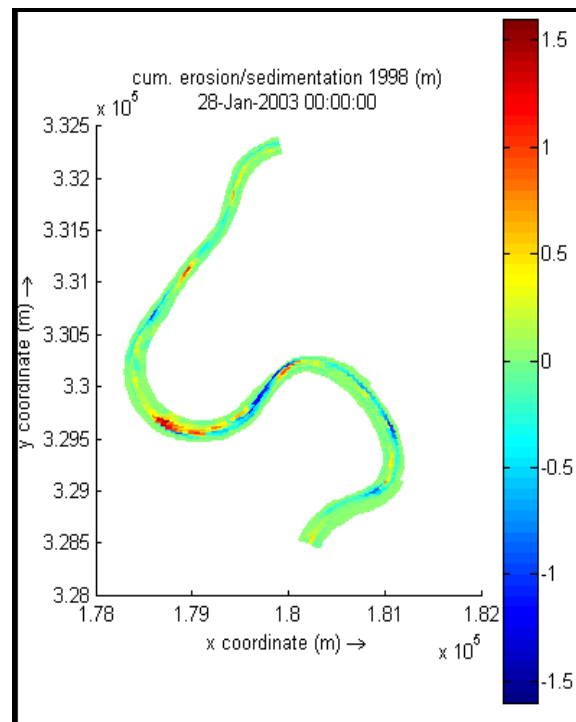


Figure A2.2: Cumulative erosion and sedimentation study in the main channel for 10 days repeated hydrograph.

By comparing the erosion and sedimentation pattern in Figure A2.2 with Figure A1.3 it can be concluded that the pattern of sedimentation and erosion is similar to the case WOP1 with a single peak, but here the magnitude of the changes are larger for both sedimentation and erosion cases.

Appendix A3

Case WP1: Using 10 days hydrograph

In this case same hydrograph of appendix A1 was used (see Figure A1.1 above), for studying 10 days of morphological changes in the river for the case with the project implemented to have an idea about the difference between situation with and without the project and to try to Figure out the effect of the project at that location.

From Figures A3.1 & A3.2, some sedimentation and erosion can be noted within the main channel of the river. The pattern is close to the pattern formed in appendix A1 but the magnitude might be larger than without the project. This will be discussed later when comparing the two situations with and without the project.

The sedimentation and erosion pattern near to the project is similar to what was explained in the explanatory Figure 6.6 in Section 6.3.1. They are very logic results, because when the project is implemented the width of the river above some level will be larger, and then the velocity will decrease in the main channel. Hence the sediment transport capacity of the river will decrease also, and as a consequence sedimentation will take place at the beginning of the project in the main channel near to the inner bend.

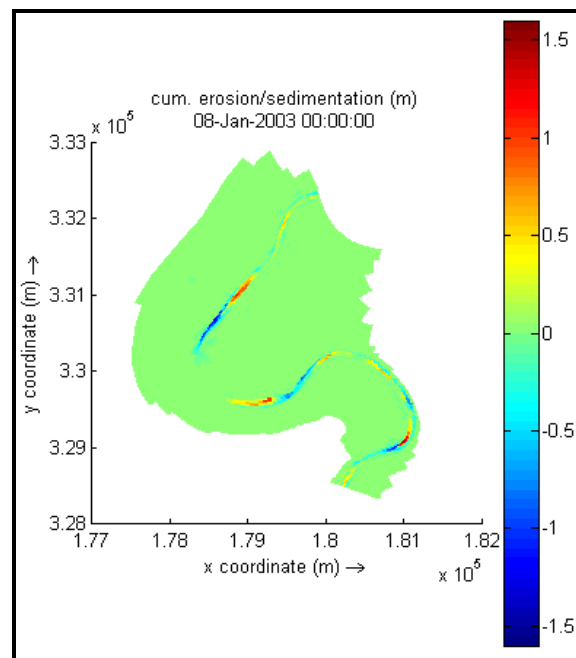


Figure A3.1: Cumulative erosion and sedimentation for 10 days morphological study.

Due the drawdown curve the water depth in the river will decrease somewhere upstream of the project area. Also the velocity will increase because the width is not changes and there is same discharge, and as a result some erosion should take place in the main channel, which can be seen from the Figure A3.1.

When the water returns from the floodplain to the main channel at the end of excavation, and most of the sediments were deposited (bed load), it has the tendency to erode the main channel at that particular location, and after some distance this flow will return to

its natural conditions and some part of the sediments will deposited again in the main channel.

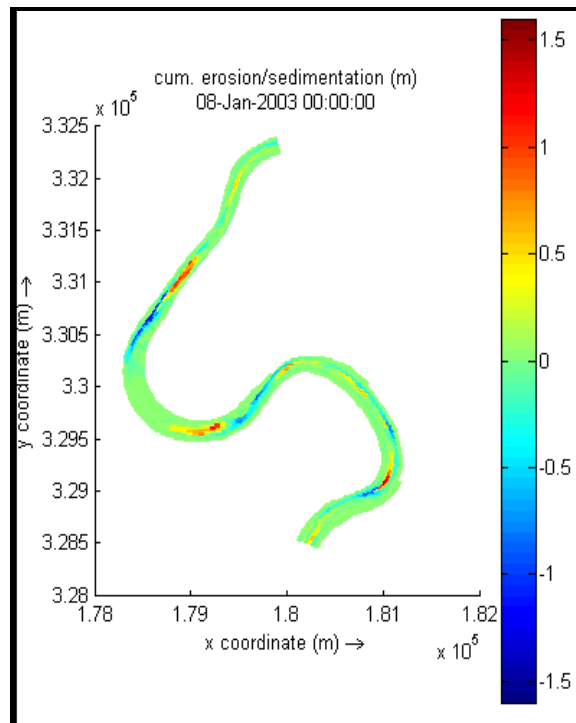


Figure A^{2.1}: Cumulative erosion and sedimentation study in the main channel for 1st days hydrograph.

Appendix A ξ

Case WP γ : Using γ days hydrograph (with repeated hydrograph)

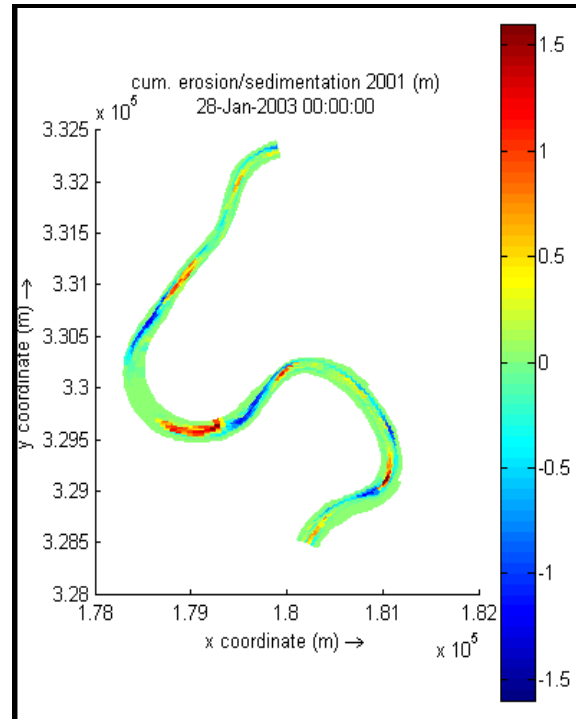


Figure A ξ . γ : Cumulative erosion and sedimentation study in the main channel for γ days repeated hydrograph.

The same pattern of sedimentation and erosion can be noted as the previous simulation, but here the quantities appear to be more than that of Appendix A γ (see Figure A γ . γ).

Appendix A^o

Additional computation for the case with project situation for 3 · days hydrograph

Two other simulations were made (only for the case of with project case) for determining the sensitivity of the model for the input hydrograph and its effect on the outputs. The first hydrograph comes from the normal 1 · days hydrograph and multiplying each discharges duration with 1.5^o (for obtaining 1.5^o days hydrograph), and the other is a 3 · days real hydrograph squeezed by factor 3 (also for obtaining 1.5^o days hydrograph), as shown below:

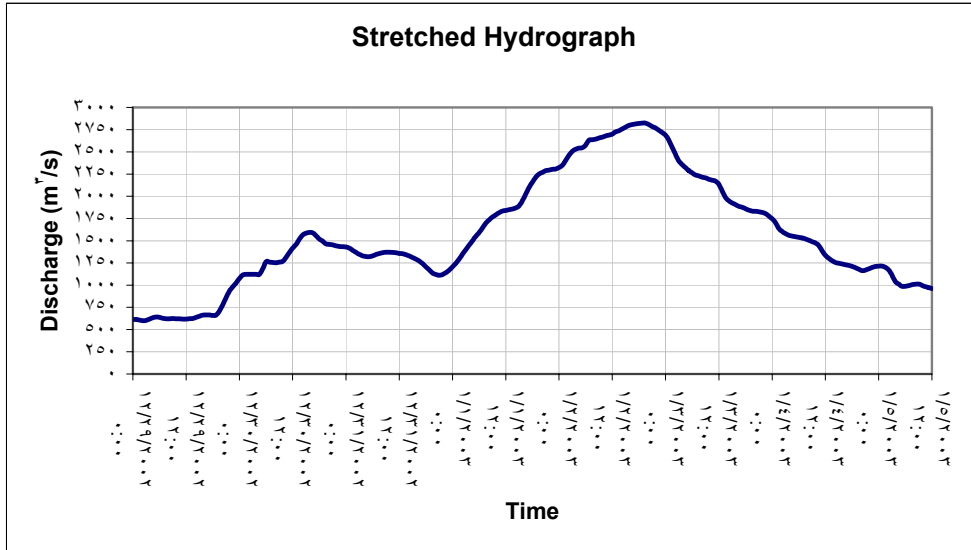


Figure A^{o.1}: Stretched hydrograph (1 · days Normal hydrograph multiplied by factor 1.5^o and used in simulation with MORFAC 3).

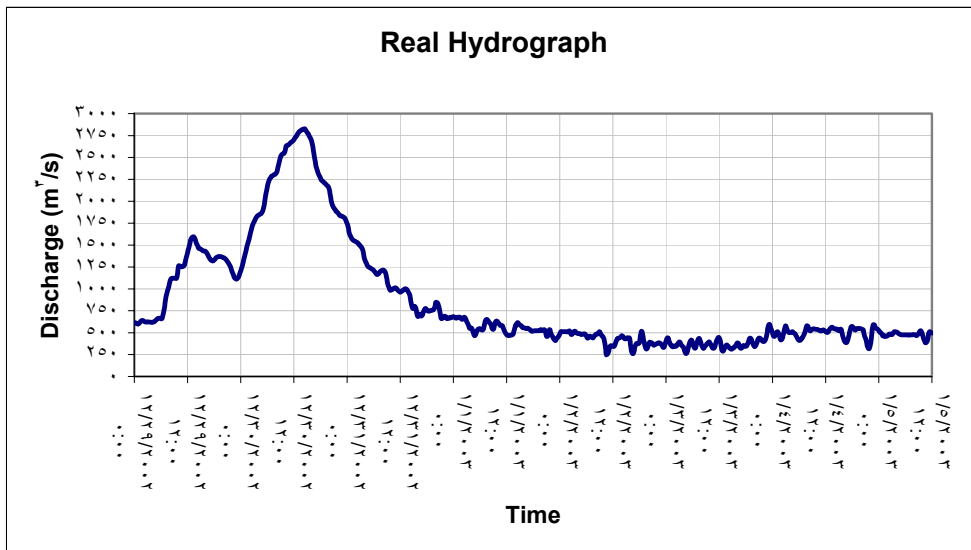


Figure A^{o.2}: Real hydrograph (3 · days Normal hydrograph Squeezed by factor 3 and used in simulation with MORFAC 3).

For case of with project the morphological changes studied also with these two different hydrographs with a morphological factor ξ (morphological time of $\tau \cdot$ days). The main purpose of these tow simulations was to study the effect of the input hydrograph on the outcomes.

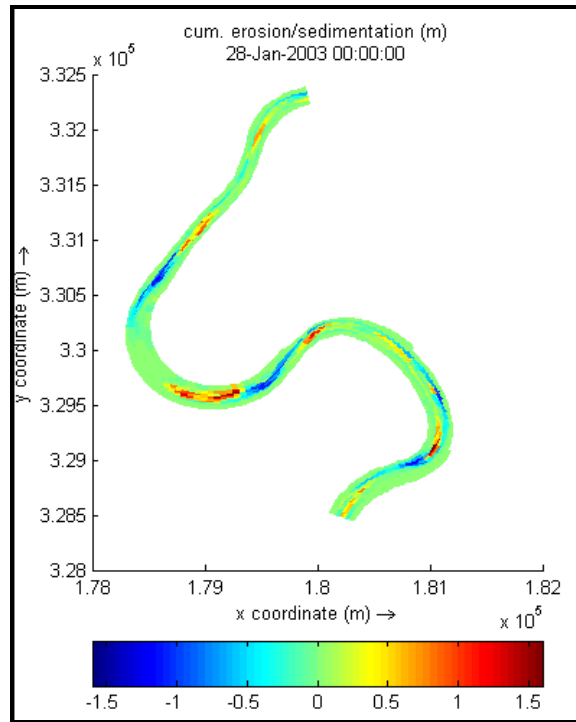


Figure A^{0.τ}: Cumulative erosion and deposition in the main channel for $\tau \cdot$ days hydrograph and morph. factor ξ for with project case (stretched hydrograph).

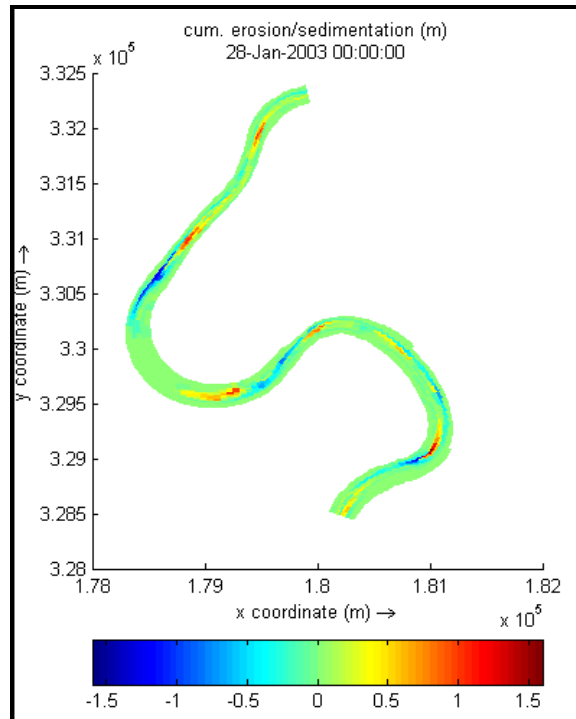


Figure A^{0.ξ}: Cumulative erosion and deposition in the main channel for $\tau \cdot$ days hydrograph and morph. factor ξ for with project case (real hydrograph).

If these two results are compared with the Figure 6.1 (repeated hydrograph), it can be seen that there are some differences between them in term of magnitude of erosion and sedimentation.

The results of the simulation with the real hydrograph is seems to be less compared with the others, this because in this simulation there is only one single peak, while in the repeated hydrograph simulation (Figure 6.3) there are three peaks with same magnitude of discharges. However, the case of stretched hydrograph is also consisting of one peak but for longer duration (3 times longer than real hydrograph).

It's easier to understand the difference between them by showing the result of each case in a specific location as shown in the Figure below:

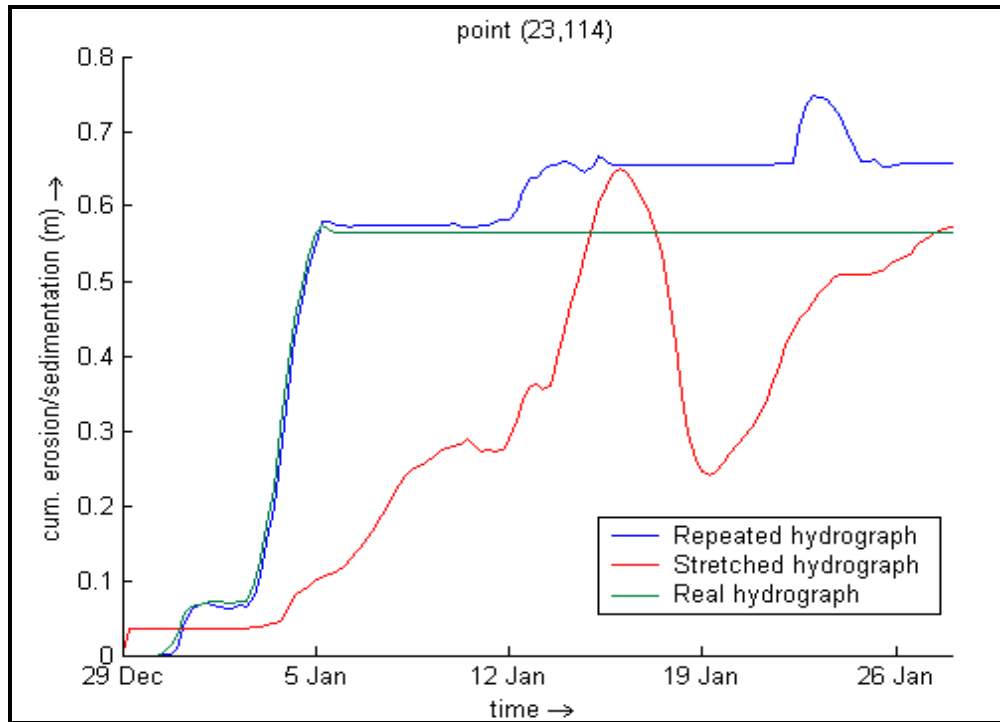


Figure A6.2: Time dependent cumulative erosion and sedimentation at a point where sedimentation was taken place for same morphological time.

This Figure very clearly indicated the difference between the effects of mentioned different hydrograph, the behaviour of the blue and green line are almost the same until the flow reaches the peak (only peak for green line and first peak for blue line) . Later on a large difference can be noted between them, because in the case of blue line after the recession two other peaks were came and the effect of each of them can be easily noted. While in the case of green line after the peak the recession was came and it seems to be after the flood peak there is no large effect on the morphology.

The red line had totally different behaviour, because in this case the peak is delayed by stretching the hydrograph, but at the end it matches with green line.

Now we can conclude that the input hydrograph has a large impact and effect on the outcome results from the model, and the selection of it needs a careful decision because might give totally different result.

Appendix A¹

Relation between grid lines in N direction and the river chainage

Grid lines N direction	River chainage (km)	Model chainage (m)	Comment
1	24.0	.	Beginning of model boundary (upstream boundary)
0	24.1	300	
10	25.1	600	
15	25.4	900	
20	25.7	1200	
25	26.0	1500	
30	26.3	1800	
35	26.6	2100	
40	26.9	2400	
45	27.2	2700	
50	27.5	3000	
55	27.8	3300	
60	28.1	3600	
65	28.4	3900	
70	28.7	4200	
75	29.0	4500	
80	29.3	4800	
85	29.6	5100	
90	29.9	5400	
95	30.2	5700	
100	30.5	6000	
105	30.8	6300	
110	31.1	6600	The project area is lied between the grid lines (110 and 145) in (N direction), which corresponds to the river chainage of (30.2 to 33.5), and model chainage of (5700 to 9000).
115	31.4	6900	
120	31.7	7200	
125	32.0	7500	
130	32.3	7800	
135	32.6	8100	
140	32.9	8400	
145	33.2	8700	
150	33.5	9000	
155	33.8	9300	
160	34.1	9600	
165	34.4	9900	
170	34.7	10200	
175	35.0	10500	
180	35.3	10800	
185	35.6	11100	

Grid lines N direction	River chainage (km)	Model chainage (m)	Comment
190	30.9	11400	
195	36.2	11700	
200	36.0	12000	
205	36.8	12300	
210	37.1	12600	
215	37.4	12900	
220	37.7	13200	
226	38.0	13500	End of model boundary (downstream boundary)

Table A 7.1: relation between the grid lines in (N direction) of the model with the chainage of the river and the chainage of the model.

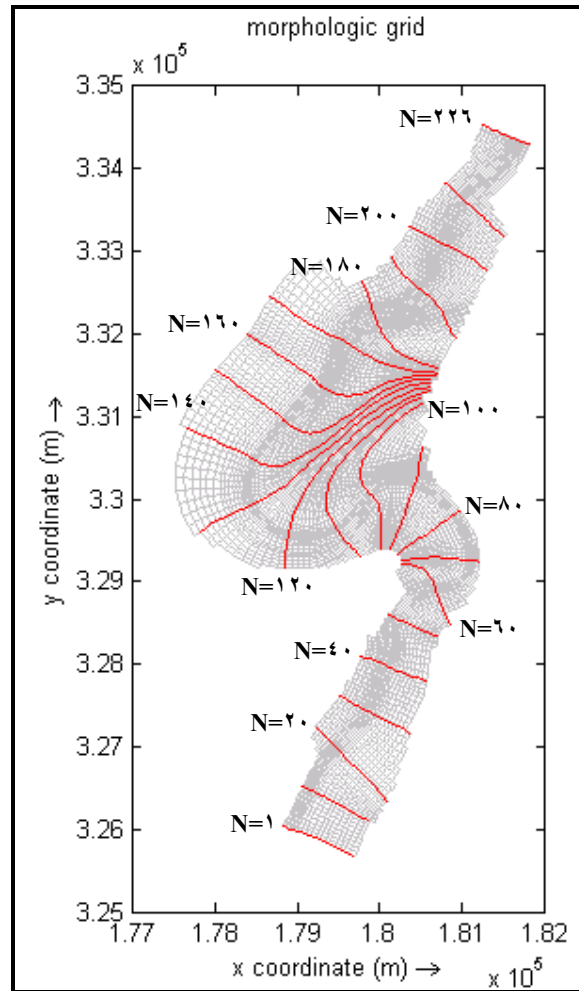


Figure A 7.1: Explanatory figure showing the grid system of the model and indicating some grid lined in N direction.

Appendix A

Model input files

A.1. MDF file

In this file most of the files can be found that defined to the model and an example of MDF file is shown in below, the most important parameters and files are indicated in bold. These files are for the case WP.

```

Ident = #Delft2D-FLOW 2012.02.29.12.03#
Runid = #tw\#
Commnt=
Runtxt= #New test: tw\o MEAN      #
      #Changing the location of D/S #
      #Boundary Condition and      #
      #changing bathymetry file    #
      #changing numerical parameter #
      #to the last option 2002     #
Filcco= #Cuted Active.grd#
Fmtcco= #FR#
Anglat= 0.20000000e+001
Grdang= 0.00000000e+000
Filgrd= #Cuted Active.enc#
Fmtgrd= #FR#
MNKmax= 0.92371
Thick = 1.00000000e+002
Fildep= #MC^FP.2.dep#
Fmtdep= #FR#
Commnt=
Fildry= ##
Fmtdry= #FR#
FiltD = ##
Fmttd = #FR#
Nambar= #          #
MNbar = [ ] [ ] ##
MNwlos= [ ] [ ]
Commnt=
Itdate= #2012-12-29#
Tunit = #M#
Tstart= 0.00000000e+000
Tstop = 2.16000000e+004
Dt = 1.00000000e-001
Tzone = .
Commnt=
Sub\ = # I#
Sub^ = # #
Name\ = #          #
Name^ = #          #
Name^ = #          #
    
```

```

Nameξ = #          #
Nameο = #          #
Wnsvwp= #N#
Filwnd= ##
Fmtwnd= #FR#
Wdint= #Y#
Commnt=
Restid= #tw\ .\ . . . . \ . . . . . \ . . . . . #
Commnt=
Filbnd= #tw\ ο . bnd#
Fmtbnd= #FR#
FilbcH= ##
FmtbcH= #FR#
FilbcT= #tw\ ο . bct#
FmtbcT= #FR#
FilbcQ= #tw\ ο . bcq#
FmtbcQ= #FR#
Filana= ##
Filcor= ##
FilbcC= ##
FmtbcC= #FR#
Rettis= . . . . . e+ . . .
        . . . . . e+ . . .
Rettib= . . . . . e+ . . .
        . . . . . e+ . . .
Commnt=
Ag = 9.8\ . . . . . ξ e+ . . .
Rhow = \ . . . . . e+ . . . 2
Alph = [.]
Tempw = \ . . . . . e+ . . . 1
Salw = 2.1\ . . . . . e+ . . . 1
Rouwav= # #
Wstres= 6.3\ . . . . . 2 e- . . . 2 \ . . . . . e+ . . . 2 \ . . . . . 1 e- . . . 2 \ . . . . . e+ . . . 2
Rhoa = \ . . . . . e+ . . .
Betac = ο . . . . . e- . . . 1
Equili= #N#
Tkemod= #          #
Ktemp = .
Fclou = . . . . . e+ . . .
Sarea = . . . . . e+ . . .
Filtmp= ##
Fmttmp= #FR#
Temint= #Y#
Tstmp = [.] [.]
Commnt=
Roumet= #C#
Filrgh= #Roghness.rgh#
Fmtrgh= #FR#
Xlo = . . . . . e+ . . .
Htur\ d= #N#
Filed= ##

```



```

PHderiv= #YYY#
PHproc= #YYYYYYYYYYY#
PHflux= #YYYY#
Commnt=          attribute file fourier analyzed
Filfou= ##
Online= #Y#
Prmap = [.]
Prhis = [.] [.] [.]
Flmap = .....e+... 1.8.....e+... 2.16.....e+... 4
Flhis = .....e+... 1.....e+... 1 2.16.....e+... 4
Flpp = .....e+... .....e+... .....e+...
Flrst = 1.44.....e+... 3
Commnt=
FilYdw= #w.Ydw#
ThetaW= . . .
Commnt=
Filsed= #GS.sed#
Filmor= #GS.mor#
TraFrm= #GS.tra#
Commnt=
    
```

A.5. Boundary condition files

- Upstream boundary condition: the upstream boundary condition is consisting of a hydrograph, an example is shown in Figure A.5 below.

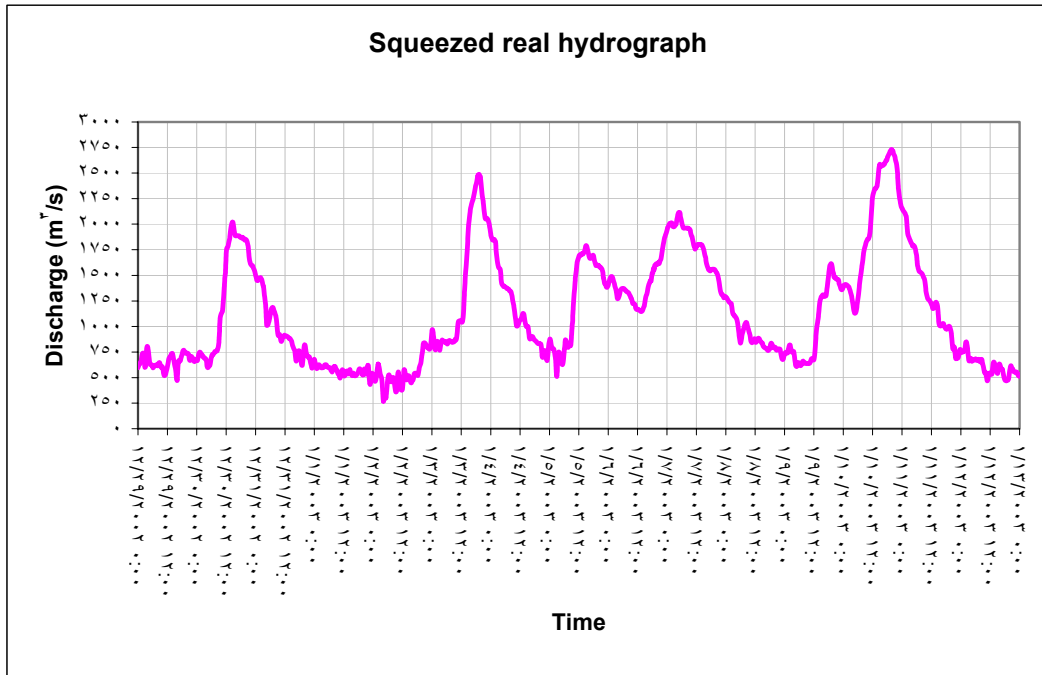


Figure A.5: In put hydrograph as upstream boundary condition

- Downstream boundary condition: the downstream boundary condition is consisting of a rating curve situated at km 38 of the river, an example is shown in Figure A4.5 below.

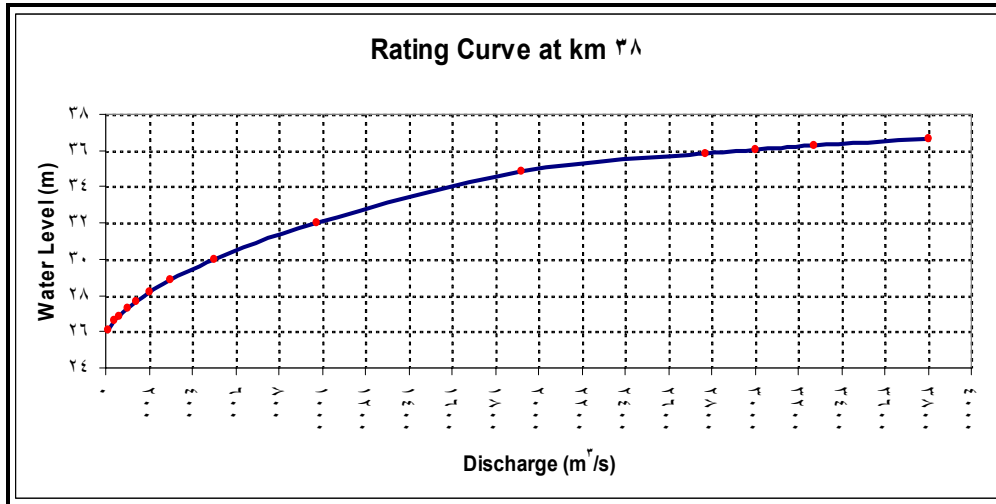


Figure A4.5: Rating curve for the river at km 38 used as a downstream boundary condition

A4.5. Sediment files

This file contains all information about the sediment particle and the fractions used in the model, an example is shown below.

Sediment File Information]

File Created By = Delft2D-FLOW-GUI, Version: 3.18.4
 File Creation Date = 19-12-2003, 1:00:40
 File Version = 02.00

[Sediment Overall]

Cref = 1600.0 [kg/m³] = CSoil Reference density for hindered settling calculations
 IopSus = 0 [-] \: Suspended sediment size is calculated dependent on d₀

[Sediment]

Name = #0.2-3mm# [-] Name as specified in NamC in md-file
 SedTyp = bedload [-] Must be "sand" or "mud" (or "bedload" for non-constituent fractions)
 RhoSol = 2600.0 [kg/m³] Density
 SedMinDia = 0.0002 [m] Sand only: Minimum sediment diameter
 SedMaxDia = 0.003 [m] Sand only: Minimum sediment diameter
 CDryB = 1600.0 [kg/m³] Dry bed density
 SdBUi = #GS_mass.dep# [kg/m³] Initial sediment mass at bed per unit area (uniform value or file name)
 FacDss = 1.0

[Sediment]

Name = # γ - \wedge mm# [-] Name as specified in NamC in md-file
 SedTyp = bedload [-] Must be "sand" or "mud" (or "bedload" for non-constituent fractions)
 RhoSol = $\gamma\gamma\gamma\gamma$ [kg/m γ] Density
 SedMinDia = $\gamma\gamma\gamma$ [m] Sand only: Minimum sediment diameter
 SedMaxDia = $\gamma\gamma\gamma$ [m] Sand only: Minimum sediment diameter
 CDryB = $\gamma\gamma\gamma\gamma$ [kg/m γ] Dry bed density
 SdBUni = #GS_mass.dep# [kg/m γ] Initial sediment mass at bed per unit area (uniform value or file name)
 FacDss = $\gamma\gamma$

[Sediment]
 Name = # \wedge - $\gamma\gamma$ mm# [-] Name as specified in NamC in md-file
 SedTyp = bedload [-] Must be "sand" or "mud" (or "bedload" for non-constituent fractions)
 RhoSol = $\gamma\gamma\gamma\gamma$ [kg/m γ] Density
 SedMinDia = $\gamma\gamma\gamma$ [m] Sand only: Minimum sediment diameter
 SedMaxDia = $\gamma\gamma\gamma$ [m] Sand only: Minimum sediment diameter
 CDryB = $\gamma\gamma\gamma\gamma$ [kg/m γ] Dry bed density
 SdBUni = #GS_mass.dep# [kg/m γ] Initial sediment mass at bed per unit area (uniform value or file name)
 FacDss = $\gamma\gamma$

[Sediment]
 Name = # $\gamma\gamma$ - $\xi\gamma$ mm# [-] Name as specified in NamC in md-file
 SedTyp = bedload [-] Must be "sand" or "mud" (or "bedload" for non-constituent fractions)
 RhoSol = $\gamma\gamma\gamma\gamma$ [kg/m γ] Density
 SedMinDia = $\gamma\gamma\gamma\gamma$ [m] Sand only: Minimum sediment diameter
 SedMaxDia = $\gamma\gamma\gamma\gamma$ [m] Sand only: Minimum sediment diameter
 CDryB = $\gamma\gamma\gamma\gamma$ [kg/m γ] Dry bed density
 SdBUni = #GS_mass.dep# [kg/m γ] Initial sediment mass at bed per unit area (uniform value or file name)
 FacDss = $\gamma\gamma$

[Sediment]
 Name = # $\xi\gamma$ - $\gamma\gamma\gamma$ mm# [-] Name as specified in NamC in md-file
 SedTyp = bedload [-] Must be "sand" or "mud" (or "bedload" for non-constituent fractions)
 RhoSol = $\gamma\gamma\gamma\gamma$ [kg/m γ] Density
 SedMinDia = $\gamma\gamma\gamma\gamma$ [m] Sand only: Minimum sediment diameter
 SedMaxDia = $\gamma\gamma\gamma$ [m] Sand only: Minimum sediment diameter
 CDryB = $\gamma\gamma\gamma\gamma$ [kg/m γ] Dry bed density
 SdBUni = #GS_mass.dep# [kg/m γ] Initial sediment mass at bed per unit area (uniform value or file name)
 FacDss = $\gamma\gamma$

A_{1.4}. Transport files

This file contains the type of transport formula used in the model and the important parameters and factors that should be indicated, in this study MPM type of formula is used with an overall calibration factor of 0.9, as shown below.

```
2 IFORM
#2 MEYER-PETER MULLER
0.9
```

A_{1.5}. Morphology files

All parameters and factors related to morphology can be defined in this file and introduced to the model, as shown below.

```
[MorphologyFileInformation]
```

```
FileCreatedBy = Delft2D-FLOW-GUI, Version: 3.18.4
FileCreationDate = 19-12-2013, 1:00:40
FileVersion = 0.2.0
```

```
[Morphology]
```

```
MorFac = 1.0 [-] Morphological scale factor
MorStt = 0.0 [-] First time step relative to ITDATE for updating
Thresh = 0.1 [m] Threshold sediment thickness for reducing sediment exchange
BedUpd = true [T/F] Update bed level during flow run
CmpUpd = true [T/F] Update bed composition during flow run
EqmBc = true [T/F] Equilibrium concentration at inflow boundaries
DensIn = true [T/F] Include effect of sediment on density gradient
AksFac = 1.0 [-] Van Rijn's reference height = AKSFAC * KS
RWave = 2.0 [-] Wave related roughness = RWAVE * estimated ripple height.
Van Rijn Recommends range 1-3
Rouse = true [T/F] Set equilibrium sediment concentration values to standard
Rouse profiles
AlfaBs = 0.0 [-] Longitudinal bed gradient factor for bed load transport
AlfaBn = 1.0 [-] Transverse bed gradient factor for bed load transport
Sus = 1.0 [-] Multiplication factor for suspended sediment reference
concentration
Bed = 1.0 [-] Multiplication factor for bed load transport vector magnitude
SusW = 0.0 [-] Wave-related suspended sed. transport factor
BedW = 0.0 [-] Wave-related bed-load sed. transport factor
SedThr = 0.001 [m] Minimum threshold depth for sediment computations
ThetSD = 0.0 [-] Fraction of erosion to assign to adjacent dry cells
HMaxTH = 0.0 [m] Max depth for variable THETSD. Set < SEDTHR to use
global value only
FWFac = 0.0 [-] Tuning parameter for wave streaming
EpsPar = false [T/F] Only for waves in combination with k-epsilon turbulence
model
```

TRUE : Van Rijn's parabolic-linear mixing distribution for current-related mixing
 FALSE: Vertical sediment mixing values from K-epsilon turbulence model

IopKCW = 1 [-] Flag for determining Rc and Rw
 1 (default): Rc from flow, Rw=RWAVE*1.1*1.0
 2 : Rc=RDC and Rw=RDW as read from this file
 3 : Rc=Rw determined from mobility

RDC = 1.1 [-] Rc in case IopKCW = 2
 RDW = 1.1 [-] Rw in case IopKCW = 2

Espir = 1.1 [-] Calibration factor spiral flow

ISlope = 2 [-] Flag for bed slope effect
 1 : None
 2 (default): Bagnold
 3 : Koch & Flokstra

AShld = 1.1 [-] Bed slope parameter Koch & Flokstra
 BShld = 1.0 [-] Bed slope parameter Koch & Flokstra

IHidExp= 3 [-] Flag for hiding & exposure
 1 (default): none
 2 : Egiazaroff
 3 : Ashida & Michiue, modified Egiazaroff
 4 : Soehngen, Kellermann, Loy
 5 : Wu, Wang, Jia

[Underlayer]
 IUnderLyr = 2 [-] Flag for underlayer concept
 1 (default): one fully mixed layer
 2 : graded sediment underlayers

ExchLyr = false [T/F] Switch for exchange layer

TTLForm = 1 [-] Transport layer thickness formulation
 1 (default): constant (user-specified) thickness

ThTrLyr = 1.1 [-] Thickness of the transport layer

MxNULyr = 2 [-] Number of underlayers (excluding final well mixed layer)

ThUnLyr = 1.1 [-] Thickness of each underlayer

IniComp = morlyr.ini

[Output]
 Dm = true
 Dg = true
 Percentiles = 1 6 5 8 9
 HidExp = false
 WithPores = true

A.7. Initial compositions file (morlyr.ini)

In this file there are possibility to define different layers for the bed composition to the model, the percentage of each fractions defined in the sediment file can be specified here for the different layers, as shown in below.

[BedCompositionFileInformation]

FileVersion = 0.1.00

[Layer]

Type = mass fraction

Fraction \ = 0.00

Fraction \ = 0.00

Fraction \ = 0.22

Fraction \ = 0.40

Fraction \ = 0.38

Thick = 0.20

[Layer]

Type = mass fraction

Fraction \ = 0.21

Fraction \ = 0.10

Fraction \ = 0.19

Fraction \ = 0.26

Fraction \ = 0.24

Thick = 0.00

[Layer]

Type = mass fraction

Fraction \ = 0.10

Fraction \ = 0.11

Fraction \ = 0.29

Fraction \ = 0.31

Fraction \ = 0.19

Thick = 0.70

Appendix A¹

In the Figure A.1 the 1998-2001 hydrograph is shown for indicating the high value of discharges that might have some effect on the morphological conditions on the Meuse River. The effect of these discharges is neglected in the simulations made in this particular study due to non availability of adequate data representing the exact field situation.

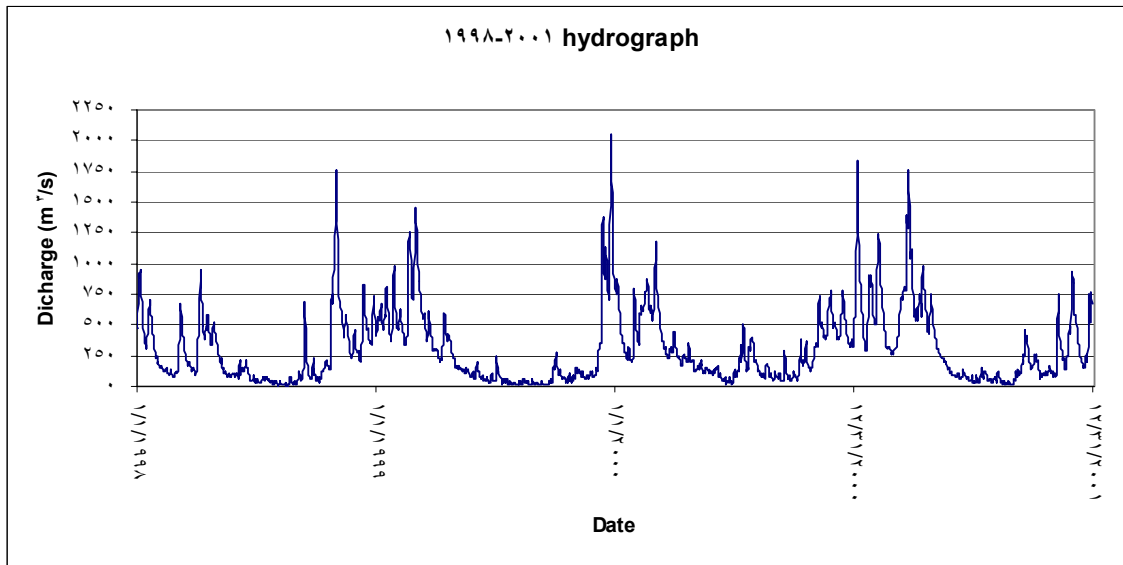


Figure A.1: 1998-2001 hydrograph

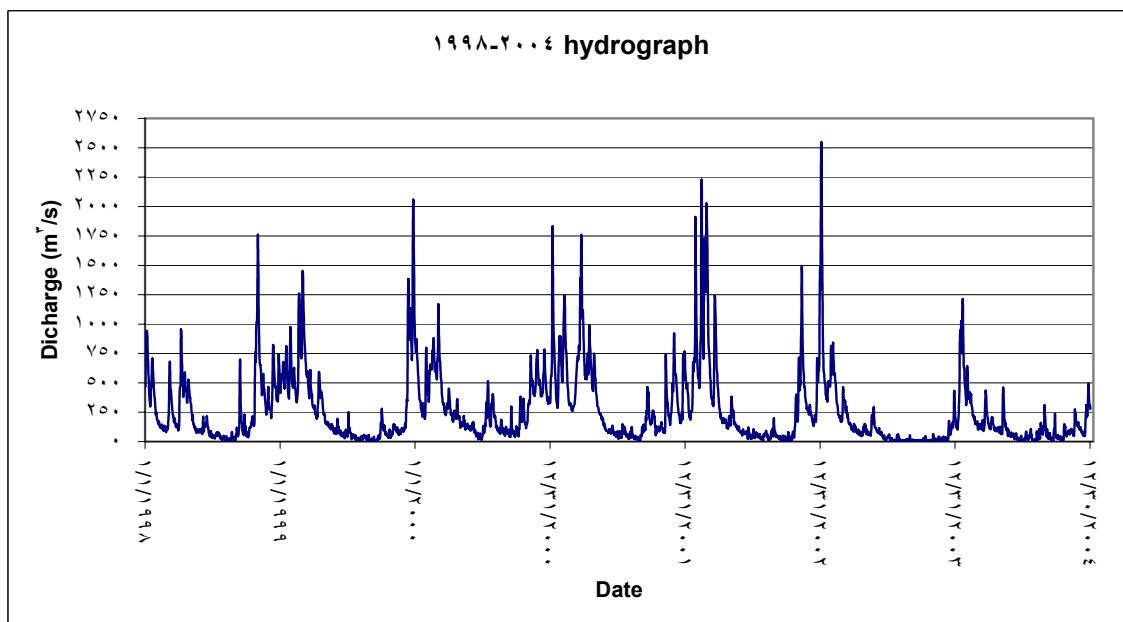


Figure A.2: 1998-2002 hydrograph

